

The Pennsylvania State University

The Graduate School

College of Engineering

**TRAJECTORY DESIGN USING APPROXIMATE
ANALYTIC SOLUTIONS OF THE N-BODY PROBLEM**

A Dissertation in

Aerospace Engineering

by

Julio César Benavides

© 2010 Julio César Benavides

Submitted in Partial Fulfillment
of the Requirements
for the Degree of

Doctor of Philosophy

December 2010

The dissertation of Julio César Benavides was reviewed and approved* by the following:

David B. Spencer

Associate Professor of Aerospace Engineering
Dissertation Advisor
Chair of Committee

Robert G. Melton

Professor of Aerospace Engineering

Dennis K. McLaughlin

Professor of Aerospace Engineering

Richard W. Robinett

Professor of Physics

George A. Lesieutre

Professor of Aerospace Engineering
Head of the Department of Aerospace Engineering

*Signatures are on file in the Graduate School.

ABSTRACT

The N-body problem as formulated by Sir Isaac Newton in the seventeenth century has been a rich source of mathematical and scientific discovery. Continuous attempts invested into the solution of this problem over the years have resulted in a host of remarkable theories that have changed the way the world is viewed and analyzed. A final solution in terms of an infinite time-dependent power series was finally discovered in the latter part of the twentieth century. However, the slow convergence of this result makes its implementation impractical in every day spacecraft trajectory design and optimization. The only feasible way to solve the N-body problem reliably is to numerically integrate the equations of motion.

This dissertation derives two new variable time step algorithms using time dependent power series solutions developed for the two-body problem. These power series solutions allow the space-dependent N-body problem to be transformed into a time-dependent system of equations that can be solved analytically. The analytic results do not yield global solutions, but rather approximate outcomes whose order of accuracy can be controlled by the user.

The two algorithms are used to investigate scenarios corresponding to a highly elliptical orbit in the two-body problem; periodic, central configuration scenarios in the three-body problem; and a non-periodic scenario in the restricted three-body problem. The results obtained are compared to the outcomes returned by a variable time step fourth-order, fifth-order Runge-Kutta numerical integration algorithm. The outcomes derived for each situation demonstrate that the two new variable time step algorithms are both more accurate and much more efficient than their Runge-Kutta counterpart.

TABLE OF CONTENTS

LIST OF FIGURES	vi
ACKNOWLEDGEMENTS.....	viii
DEDICATION.....	xi
CHAPTER 1: INTRODUCTION.....	1
CHAPTER 2: THE HISTORY OF THE N-BODY PROBLEM.....	6
Aristotle.....	6
Ptolemy.....	7
Copernicus.....	8
Galileo.....	10
Brahe.....	10
Kepler.....	11
Newton.....	13
Euler.....	14
Lagrange.....	15
Poincare.....	18
Sundman.....	18
Wang.....	19
Suggested Reading.....	20
CHAPTER 3: THE TWO-BODY PROBLEM.....	22
Equations of Motion.....	22
The Orbit Equation.....	24
Circular Orbit Solutions.....	27
Classical Orbital Element Solutions.....	29
Power Series Solutions.....	35
<i>Fundamental Invariant Characteristics</i>	37
<i>Lagrange Coefficients and Recursion Relationships</i>	38
<i>Radius of Convergence</i>	41
<i>Using Power Series Iteratively</i>	43
Numerical Integration Solutions.....	46
<i>Runge-Kutta 4</i>	47
<i>Runge-Kutta 5</i>	49
<i>A Variable Time Step Runge-Kutta Algorithm</i>	52
Discussion.....	55

CHAPTER 4: NEW SOLUTIONS OF THE TWO-BODY PROBLEM	56
A New Time Transformation.....	56
A Fourth-Order Solution of the Two-Body Problem.....	57
A Fifth-Order Solution for Parabolic Orbits.....	61
Higher-Order Solutions of the Two-Body Problem.....	65
<i>The Modified Power Series Approach</i>	65
<i>The Gamma Polynomial Approach</i>	67
New Variable Time Step Propagators.....	70
<i>The 47 Variable Time Step Propagator</i>	70
<i>The 67 Variable Time Step Propagator</i>	73
Discussion	75
 CHAPTER 5: NEW SOLUTIONS OF THE N-BODY PROBLEM.....	77
Power Series Solutions	77
Fourth-Order Solutions	80
Higher-Order Solutions.....	81
Variable Time Step Algorithm for the N-Body Problem.....	82
Central Configuration Trajectories	84
A Hohmann Transfer in the Restricted Three-Body Problem	93
Discussion	99
 CHAPTER 6: CONCLUSIONS AND FUTURE WORK.....	101
Summary	101
Conclusions.....	102
Relevance	103
Future Work	104
<i>Higher Order Solutions</i>	104
<i>Linear Orbit Theory</i>	105
<i>Thrust Applications</i>	105
<i>Perturbations Dependent on Position and Velocity</i>	106
 REFERENCES	107

LIST OF FIGURES

Figure 2.1: Aristotle's Geocentric Universe	7
Figure 2.2: Deferent-Epicycle System.....	8
Figure 2.3: Geocentrism vs. Heliocentrism	9
Figure 2.4: The Inner Planets in the Platonic Solid Model.....	12
Figure 2.5: The Outer Planets in the Platonic Solid Model	13
Figure 2.6: Homothetic Solution of the Three-Body Problem	15
Figure 2.7: Lagrange Points in the Circular Restricted Three-Body Problem.....	16
Figure 2.8: Equal Mass Central Configuration Solution of the Three-Body Problem	17
Figure 2.9: Unequal Mass Central Configuration Solution of the Three-Body Problem ..	17
Figure 3.1: Two-Body Problem Coordinate System.....	23
Figure 3.2: Restricted Two-Body Problem Coordinate System	24
Figure 3.3: Geometry of an Elliptical Orbit.....	26
Figure 3.4: Effect of Eccentricity on Orbital Geometry	27
Figure 3.5: Classical Orbital Elements	30
Figure 3.6: Perifocal Coordinate System	34
Figure 3.7: An Elliptical Orbit with Respect to the Earth.....	45
Figure 3.8: Absolute Error Results Using a Seventh-Order Iterative Power Series	46
Figure 3.9: Absolute Error Results Using RK4	49
Figure 3.10: Absolute Error Results Using RK5	52
Figure 3.11: Absolute Error Results Using RK45 with a 10^{-6} Tolerance	54
Figure 3.12: Absolute Error Results Using RK45 with a 10^{-7} Tolerance	54
Figure 4.1: Absolute Error Results Using 47P with a 10^{-3} Tolerance	72
Figure 4.2: Absolute Error Results Using 47P with a 10^{-4} Tolerance	72
Figure 4.3: Absolute Error Results Using 67P with a 10^{-7} Tolerance	74
Figure 4.4: Absolute Error Results Using 67P with a 10^{-8} Tolerance	75
Figure 5.1: Three-Body Equal Mass Central Configuration.....	88
Figure 5.2: Equal Mass Central Configuration Using RK45 with a 10^{-7} Tolerance.....	89
Figure 5.3: Equal Mass Central Configuration Using 47P with a 10^{-4} Tolerance	89
Figure 5.4: Equal Mass Central Configuration Using 67P with a 10^{-8} Tolerance	90

Figure 5.5: Three-Body Unequal Mass Central Configuration	91
Figure 5.6: Unequal Mass Central Configuration Using RK45 with a 10^{-7} Tolerance.....	92
Figure 5.7: Unequal Mass Central Configuration Using RK45 with a 10^{-4} Tolerance.....	92
Figure 5.8: Unequal Mass Central Configuration Using 67P with a 10^{-8} Tolerance.....	93
Figure 5.9: Hohmann Transfer in the Restricted Three-Body Problem.....	94
Figure 5.10: Hohmann Transfer in the Earth-Moon System	96
Figure 5.11: Satellite Transit through Lunar Sphere of Influence	97
Figure 5.12: Three-Body Hohmann Transfer Using RK45 with a 10^{-8} Tolerance	98
Figure 5.13: Three-Body Hohmann Transfer Using 47P with a 10^{-5} Tolerance	98
Figure 5.14: Three-Body Hohmann Transfer Using 67P with a 10^{-9} Tolerance	99

ACKNOWLEDGEMENTS

I thank my Lord and Savior, Jesus Christ, for His Eternal, unconditional Love and Power. His Footsteps were always visible in the sand, even when mine seemed to fade away from time to time. Without His blessings, this dissertation would have never seen the light of day.

Special thanks go out to my mentor, Dr. David Spencer, for his guidance and patience in this research endeavor and throughout my graduate school experience. Thank you for believing in me and inviting me to become a member of the Space Flight Dynamics Laboratory (a.k.a. “Team Spencer”) at Penn State. Dr. Spencer will always have a special place in my heart. I would also like to thank Dr. Robert Melton, Dr. Dennis McLaughlin, and Dr. Richard Robinett for their guidance both in and out of class and for taking the time to be a part of my doctoral dissertation committee.

I would like to thank the Bill Gates Millennium Scholars Program for funding my college experience. Their dedicated support opened the doors to a great undergraduate and graduate education and has allowed me to travel along a path where mastery is defined as a trajectory of endless learning.

I would like to thank my mother, Mary Benavides, my brother, Daniel Galeana, and my sister-in-law, Sofia Galeana, for their love and support throughout my life. A special “I love you,” goes out to my two precious nieces, Tabitha and Angela Galeana. It is my hope that the knowledge and experience I have gained throughout the years will allow me to be an asset in their respective walks of life.

I would like to thank my dear friend, Robin Waltz, for all the support she’s given me throughout the years with classrooms, books, websites, schedules, rides, movies, and

food. I would also like to thank my friend, Oly Longoria, for all the love and support she's given me since my tutoring days at South Texas Community College. I look forward to having many more dinners with her full of wine, bread, cheese, and plenty of good stories. I would like to thank my friend, Margaret Rodriguez, for her unwavering support, endless smile, positive attitude, and steadfast belief that I can accomplish any task I set my mind to.

I started my college days in 1999 at South Texas Community College (STCC) after not being in school for over six years. During my three years at the college, I had the honor and privilege of being mentored by four wonderful professors: Dr. Michael Bagley ("The Bridge"), Dr. Mahmoud Fathelden, Dr. Mohamed Werfelli, and Dr. Mahmoud Gasseem. These instructors planted the seeds of the strong foundation in mathematics, physics, and engineering that enabled me to complete this dissertation. I would also like to thank Alicia Elizondo and Leonor Suarez, who were the program assistants of the Science and Mathematics Departments, respectively, at STCC. Without their guidance and efforts, my community college experience would not have been as extraordinary as it was. I would like to thank Marcelo Suarez for being my best friend during that period.

In the three years that I attended Embry-Riddle Aeronautical University, I had the honor of being mentored by Dr. Karl Seibold, Dr. Phillip Anz-Meador, and Dr. Ronald Madler. From these professors, I learned the art of being a polyhistor engineer who doesn't limit his knowledge to one specific field of math and science. I would like to thank Dr. David Viger and Mr. David Brandstein, the Director and Coordinator, respectively, of the McNair Scholars Program for all their academic support and friend

ship during my time at the university. I would also like to thank James Wulff, Brian Bullers, Dalia Guízar, Carmen Catacora, and Homero Horacio Ruiz Pérez for being my dear friends and for all the great times we shared during those years.

Finally, I would like to thank my high school physics teacher, Mr. Cantu, for introducing me to the world of math, physics, and engineering so many years ago. Mr. Cantu was tough; anyone who took either of his two physics classes would agree with me about that. The “B” that I earned in his class was actually one of my proudest achievements in high school; along with the “A” he gave me after taking his infamous “Light Test.” Despite all this, it was obvious from the first day of that class that he had a great interest in the education of his students and a great passion for the subject he taught. Mr. Cantu was the teacher who inspired me to pursue a degree in a technical field and to this day, even my teaching style is heavily influenced by him.

DEDICATION

This Dissertation is Dedicated to:

THE ETERNAL FIRE

Deuteronomy 4:24

Hebrews 12:29

...for the life you have given me and for granting me Your Strength and Wisdom.
My Life is Yours.

CHAPTER 1

INTRODUCTION

The N-body problem is the problem of finding the motion of N point particles given their masses and initial states when only their mutual gravitational attraction, as governed by Newton's Laws of Motion and Law of Universal Gravitation, are taken into account. This problem forms the foundation of Celestial Mechanics and more specific to this research, Astrodynamics. Celestial Mechanics is defined as the study of the dynamic motion of celestial bodies, such as planets and asteroids. Astrodynamics, on the other hand, is defined as the study of the motion of man-made objects in space, subject to both naturally and artificially induced forces. Natural forces include gravitational attraction and solar radiation pressure effects. Artificially induced forces include the various forms of propulsion that currently exist [1-2].

The equations of motion that govern the N-body problem are a function of their positions with respect to each other and their respective gravitational parameters. The gravitational parameter of a celestial body is defined as the product of its mass and the universal gravitational constant. In compact form, the N-body problem equations of motion with respect to the system's barycenter (center of mass) are

$$\ddot{\bar{\mathbf{r}}}_i = \sum_{\substack{j=1 \\ j \neq i}}^N \frac{\mu_j (\bar{\mathbf{r}}_j - \bar{\mathbf{r}}_i)}{\|\bar{\mathbf{r}}_j - \bar{\mathbf{r}}_i\|^3} = \sum_{\substack{j=1 \\ j \neq i}}^N \frac{\mu_j \Delta \bar{\mathbf{r}}_{ji}}{\Delta r_{ji}^3} \quad (1.1)$$

In this expression, i is the index of the current body, j is an index that represents the effect of other bodies on the current object, $\ddot{\bar{\mathbf{r}}}$ and $\bar{\mathbf{r}}$ are the current body's acceleration and position vectors, respectively;

$$\ddot{\bar{r}} = \{\ddot{x} \quad \ddot{y} \quad \ddot{z}\}^T \quad (1.2)$$

$$\bar{r} = \{x \quad y \quad z\}^T \quad (1.3)$$

μ_j is the gravitational parameter of each respective body, and N represents the number of bodies being analyzed. The problem described by equation 1.1 is a second-order, nonlinear, coupled, space dependent, variable coefficient, homogeneous system of $3N$ ordinary differential equations that in general has no practical time dependent, analytic solution and can only be solved through the use of numerical integration.

The N -body problem has been studied since the time man first looked up into the night sky and started developing models that described the motion of celestial bodies observable to the naked eye. Through the work of many mathematicians, physicists, and astronomers; these models steadily increased in accuracy throughout the years. Much of the knowledge that has been developed pertains to the two-body and relative two-body problems, for which complete solutions have been derived. A large amount of literature also exists for the three-body problem, which includes a global, time dependent power series solution. Moreover, many solutions have also been derived for special cases of systems with more than three bodies. A final solution in terms of an infinite time series was finally proposed at the end of the twentieth century. However, the implementation of this solution is rendered unfeasible by the number of terms required to obtain a reliable outcome, even when small time intervals are examined.

Numerical integration is a useful alternative that is capable of solving any version of the N -body problem in a reasonable amount of time. However, high-accuracy numerical integrators, while efficient, also require a significant number of steps to implement. Moreover, time step sizes must be managed appropriately to minimize the

amount of round-off error that is inherent in the numerical process. For the case of numerical integrators such as the fourth-order and fifth-order Runge-Kutta algorithms, the first error comes from the fact that an infinite power series is truncated and the second arises from the small numerical round-off errors that occur at each step in the computation. Both of these errors can be minimized by implementing an algorithm that continuously monitors the solution's precision during the course of the computation and adaptively changes the step size to maintain a consistent level of accuracy. As a result, the step size may change many times during the course of the computation. Larger time steps are used where the solution is varying slowly, and smaller steps are used where the solution varies rapidly. A variable time step numerical integration algorithm is usually much faster than its constant time step counterpart, because it concentrates its computational effort on time intervals that need it most and takes large strides over portions that don't need small time steps.

This work proposes a new solution to the N-body problem using methods that were originally developed for the two-body problem in the late 1950's as a foundation. The techniques introduced in this dissertation do not produce global solutions, but rather approximate, analytic outcomes whose order of accuracy can be controlled by the user. As will be demonstrated, these analytic expressions can also be used recursively to design spacecraft trajectories in a manner that is both more accurate and more efficient than a variable time step Runge-Kutta 4-5 numerical integration algorithm. The remaining chapters in this dissertation can be summarized as follows:

- * Chapter 2 presents a brief history of the N-body problem and outlines a suggested reading list that introduces the reader to both the basic and advanced technical concepts of the N-body problem.
- * Chapter 3 presents and discusses the equations of motion of the two-body problem. An analytic, time dependent solution for the case of circular orbits is derived. The classical orbital element method used to determine future states for elliptical, parabolic, and hyperbolic orbits is outlined and discussed. Time dependent, power series solutions of the relative two-body problem are presented and used recursively to analyze a highly elliptical orbit scenario. The fourth-order and fifth-order Runge-Kutta numerical integration algorithms are introduced and used to investigate the same scenario analyzed by the power series solution. A variable time step algorithm that incorporates these two numerical integrators is also derived. Discussion on the absolute error and simulation time results returned by the four numerical experiments conclude the chapter.
- * Chapter 4 transforms the relative two-body problem into a time dependent system using the power series solutions derived in Chapter 3. A fourth-order, analytic solution is derived for the transformed system and the result is shown to be a useful alternative to the universal form of Kepler's equation when working in any coordinate system. A fifth order solution is derived for the case when a vehicle is initially located at the periapsis of a parabolic orbit. Two methods are proposed to solve the transformed problem when higher-order coefficients are implemented. Finally, all of these results are used to develop two new variable time step

propagators that are more accurate and more efficient than the variable time step Runge-Kutta numerical integrator.

- ✱ Chapter 5 derives a new power series solution, a fourth-order solution, and a higher-order solution for the N-body problem. A variable time step numerical integration algorithm that extends the RK45, 47P, and 67P capabilities derived in Chapter 4 to the solution of the N-body problem is introduced. The algorithms are then used to solve periodic central configuration scenarios and a non-periodic scenario in the three-body and restricted three-body problem, respectively.
- ✱ Chapter 6 summarizes this work and draws conclusions from the results obtained in this dissertation. Future work that uses the methods derived by the author is also discussed.

CHAPTER 2

THE HISTORY OF THE N-BODY PROBLEM

This chapter gives a brief history of the N-body problem. This problem is based on the principles of classical mechanics as derived by Isaac Newton in 1687. A more accurate description of gravity was later developed by Albert Einstein in 1915. However, the velocities of all bodies and man-made satellites found in the solar system are relatively small when compared to the speed of light and, consequently, the predictions made by Newton's equations agree extremely well with observational data. As will be seen, the development of models that describe the motion of celestial objects in the night sky and the search for a solution of the N-body problem has led to some of the greatest advancements in mathematics, physics, and astronomy.

ARISTOTLE

The Greek philosopher Aristotle (384 BC-322 BC) proposed that the Earth was located at the center of the Universe and that the Sun and all the planets known at that time (Mercury, Venus, Mars, Jupiter, and Saturn) orbited the Earth. These orbits were assumed to be circular in nature, due to the elegance that the ancient Greeks attributed to circles and spheres. This view of the Universe, known as Geocentrism, was motivated by the fact that all celestial objects observable with the naked eye seemed to revolve around the Earth in the night sky. It was also a common belief that the Earth was a stable, immovable, spherical solid. Aristotle was convinced that since the Earth was made of "Earth-stuff," its nature was not to move in circles, but to always seek the center of the Universe. Due in large part to the advent of the Dark Ages, Geocentrism was the

dominant view of the Universe until the latter part of the 16th century [3-7]. Figure 2.1 shows the geocentric universe envisioned by Aristotle.

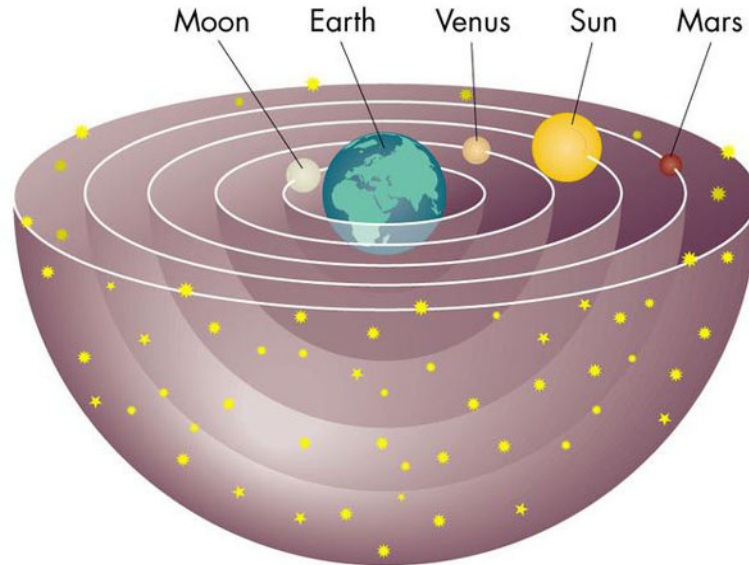


Figure 2.1: Aristotle's Geocentric Universe
<http://www.astro.umass.edu/~myun/teaching/a100/images/geocentric.jpg>

PTOLEMY

The Roman astronomer and mathematician Ptolemy (90-168) continued the work of Aristotle and created the first systematic model of celestial motion called the Geocentric Model of the Universe. In this model, the sun, the moon, planets, and stars were embedded in transparent, rotating crystalline spheres called deferents, which were centered at the Earth. An additional, smaller sphere, called an epicycle, was then embedded in the deferent. Finally, the planet was embedded in the epicycle sphere. The deferent rotated around the Earth while the epicycle rotated within the deferent. This caused the planet to move closer to and farther from the Earth at various points in its orbit. Additional epicycles could also be embedded into the original epicycle, which caused the planet to slow down, stop, and then move backward with respect to the Earth.

These extra epicycles allowed Ptolemy to account for the unusual retrograde motion of some planets that was observed in the night sky. The Geocentric Model of the Universe gave accurate predictions of future positions of celestial objects, but was considered too complex and cumbersome to implement [8-13]. Figure 2.2 shows a typical deferent-epicycle system for the Sun with respect to the Earth.

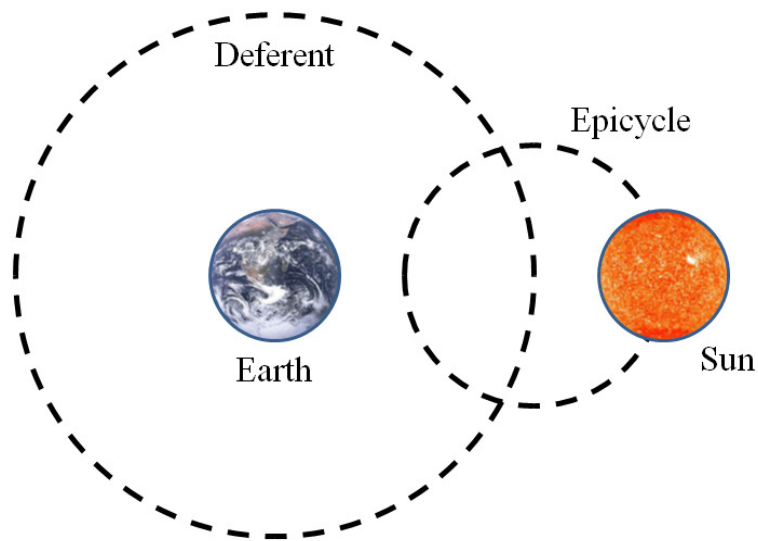


Figure 2.2: Deferent-Epicycle System

COPERNICUS

The Polish astronomer Nicolaus Copernicus (1473-1543) formulated the Heliocentric Model of the Universe. This model places the Sun at the center of the solar system with the Earth and the rest of the planets revolving around it in circular orbits. Copernicus proposed that the Earth experiences three types of motion: daily rotation about an axis, annual tilting of this axis, and an annual revolution around the Sun. These three displacements were used to explain the occasional retrograde motion of the planets with respect to the Earth and allowed him to conclude that the distance from the Earth to the Sun is much smaller than the distance from the Earth to the stars. He also conjectured

that a planet's orbital period (the time it takes to complete one revolution around the Sun) was directly proportional to its distance from the Sun. His work is often regarded as the starting point of modern astronomy and the defining epiphany that began the Scientific Revolution. Although Copernicus' proposal of Heliocentrism would later be proven correct, the assumption of circular orbits caused his numerical results to be less accurate than those predicted by Ptolemy's Geocentric Model when determining the future positions of planets. For this reason, and also for fear of religious persecution, his complete findings were not published until after his death [14-19]. Figure 2.3 gives a visual comparison between Geocentrism and Heliocentrism.

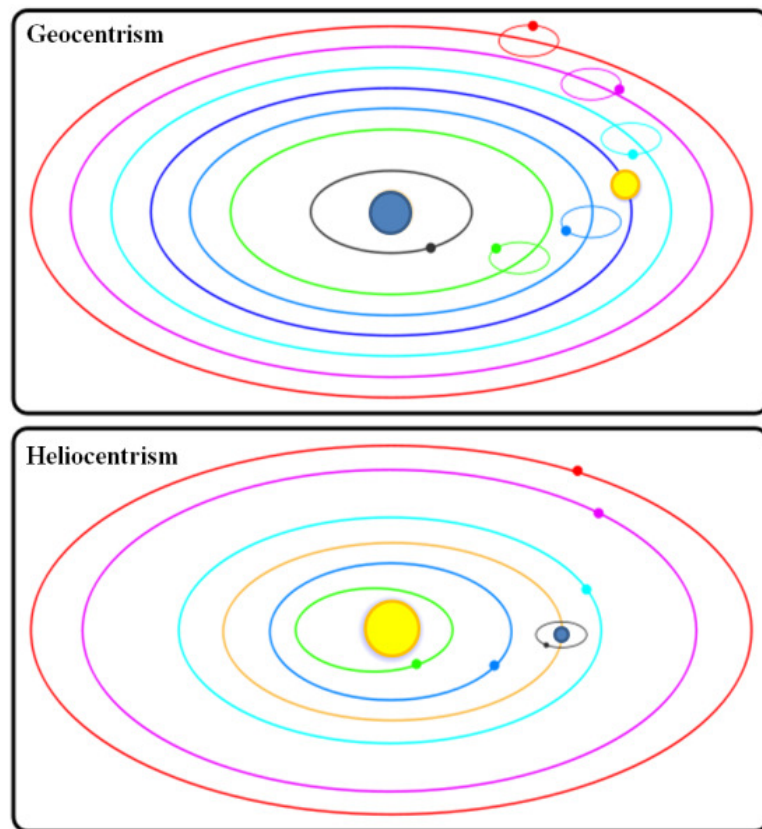


Figure 2.3: Geocentrism vs. Heliocentrism
<http://www.astro.umass.edu/~myun/teaching/a100/images/comparison.jpg>

GALILEO

The Italian astronomer and mathematician Galileo Galilei (1564-1642) made many astronomical observations that supported Copernicus' Heliocentric Model with an improved version of the telescope. Among his many discoveries, he observed that Venus exhibits phases ranging from crescent to full, similar to those seen on the Moon; a phenomenon that was a key prediction of the Heliocentric Model. Moreover, he discovered the four largest moons of Jupiter (Ganymede, Callisto, Io, and Europa) and through subsequent observations, concluded that they orbited the planet and not the Earth. Galileo was also the first astronomer to observe the rings of Saturn. These discoveries were critical, because they could not be explained by the Geocentric Model. Galileo spent the last days of his life under house arrest after the Church concluded that his discoveries supporting Heliocentrism were heretical in nature [20-22].

BRAHE

In 1597, the Danish astronomer Tycho Brahe (1546-1601) was granted the island of Hven where he built one of the finest observatories of the time. He constructed several large instruments that were used to produce the most accurate astronomical observations of his time. This precise and redundant data allowed him to catalogue the positions of the planets with enough accuracy that it finally became possible to determine whether the Geocentric or Heliocentric Models described the Universe more correctly. Instead, he developed his own model of the universe called the Tychonic Model, which combined the mathematical benefits of Heliocentrism with the philosophical benefits of the Geocentric Model. The Tychonic Model assumes that the Earth is located at the center of the universe with the Sun and the Moon revolving around it. The other five planets

known at the time revolved around the Sun. Brahe was able to demonstrate that the motion of the Sun and the planets with respect to the Earth predicted by his new model were equivalent to the predictions given by Heliocentrism. This result was appealing to many astronomers of the time, because it allowed them to pursue the benefits of the Copernican model without the fear of religious persecution [23-26].

KEPLER

The German astronomer and mathematician Johannes Kepler (1571-1630) became Brahe's assistant in 1600 and after his death in 1601 used Brahe's accurate data to develop his own theories of celestial motion. Kepler was a firm believer in Heliocentrism, but he also had a difficult time letting go of the concept of circular orbits. For this reason, he initially developed the Platonic Solid Model of Planetary Motion. In this system, the planets orbited the Sun in circular orbits and the size of their orbital paths was described by inscribing and circumscribing three-dimensional polyhedra within solid spheres. The diameter of the six spheres corresponding to the six planets known at the time was determined by the order of the platonic solids embedded in them. Kepler deduced that the structure of the solar system and the distance relationships between the planets were dictated by ordering the platonic solids in the following manner: octahedron, icosahedron, dodecahedron, tetrahedron, and the cube. Figures 2.4 and 2.5 give a visual representation of Kepler's Platonic Solid Model.

While the theory was mathematically beautiful and successfully explained the diameters of the orbits of the planets, Kepler later abandoned the Platonic Solid Model after observing that the results predicted by it did not match Brahe's accurate data. Still, convinced that the concept of Heliocentrism was correct, he came to the realization that

the idea of circular orbits had to be abandoned. He eventually discovered that the orbit of Mars could be accurately described by an ellipse. Kepler generalized his analysis to include the motions of all planets and subsequently proposed his three Laws of Planetary Motion [27-33]:

- * All the planets move in elliptical orbits with the Sun at one focal point.
- * The radius vector drawn from the Sun to a planet sweeps out equal areas in equal time intervals.
- * The square of the orbital period of any planet is proportional to the cube of the semimajor axis of the elliptical orbit.

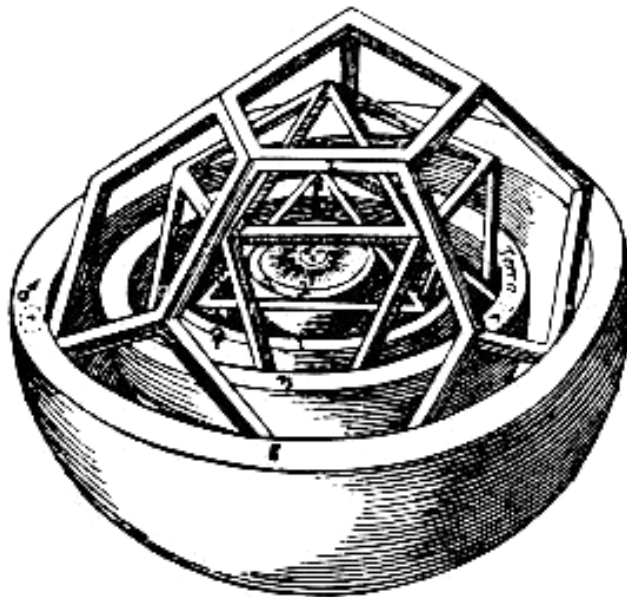


Figure 2.4: The Inner Planets in the Platonic Solid Model
<http://www.uwgb.edu/dutchs/Graphics-Other/histsci/kepsph1.gif>

It is important to note that Kepler derived these laws through empirical observation and did not actually prove their validity mathematically. He was, however, able to derive an expression using geometric constructions that could be used to

determine the future locations of the planets in the night sky. This expression, known today as Kepler's equation, was a crowning achievement for the cause of Heliocentrism. For the first time in the history of the N-body problem, a theory based on Heliocentrism was able to produce results that were far more accurate than the outcomes predicted by the Geocentric Model.

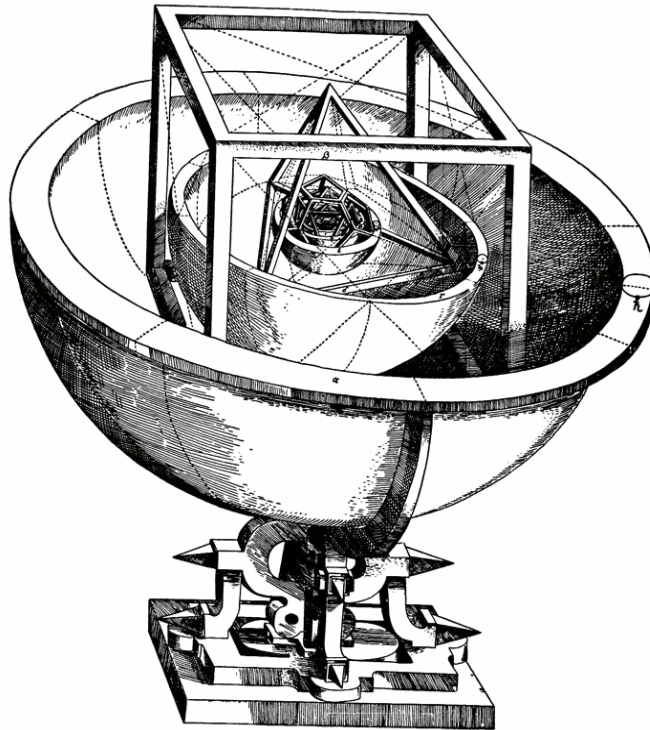


Figure 2.5: The Outer Planets in the Platonic Solid Model
http://ocw.nd.edu/architecture/nature-and-the-built-environment/lecture-5/keplers-crystal/image_preview

NEWTON

The English mathematician and physicist Isaac Newton (1643-1727) developed the Calculus and proposed the Three Laws of Motion, which became the foundation of modern Mechanics. He also proposed the Law of Universal Gravitation, which states that every particle in the Universe attracts every other particle with a force that is directly

proportional to the product of their masses and inversely proportional to the square of the distance between them. This new inverse square force law allowed him to formulate the N-body problem as it is known today. Newton was able to solve the two-body problem, the inverse cube, and the inverse fifth force laws using analytical geometry constructions and his newly developed limit techniques. He also made the first known attempts to solve the three-body problem, although this endeavor soon proved to be much more difficult than the effort invested in solving the two-body problem. From his work, Newton reasoned that the planets don't rotate around the Sun; instead, the Sun and the planets all rotate about their common center of mass. This solution allowed him to conclude that the orbit of a point mass in space with respect to another will take the shape of a conic section (circle, ellipse, parabola, or hyperbola). This result also allowed him to derive all of Kepler's Laws of Planetary Motion analytically and expand Kepler's equation to include all four conic sections [34-38].

EULER

The success of the two-body problem motivated mathematicians to search for solutions for the problem of more than two bodies. The Swiss mathematician Leonhard Euler (1707-1783) introduced the concept of the synodic (rotating) coordinate system in his analysis of the restricted three-body problem. The term "restricted" indicates that the mass of one of the particles being analyzed is negligible, causing it to have no gravitational influence on the motion of the other two particles. The use of this type of coordinate system allowed him to discover a family of periodic orbits with respect to the line connecting the two primary masses. Euler also discovered a family of solutions for the full three-body problem known as homothetic central configuration solutions. A

homothetic central configuration is one in which the positions of the point particles being analyzed by the three-body problem collapse homothetically at their center of mass. The term “homothetically” implies that the particles are released without initial velocities and then eventually dilate without rotation [39-43]. Figure 2.6 shows a homothetic solution in the three-body problem.

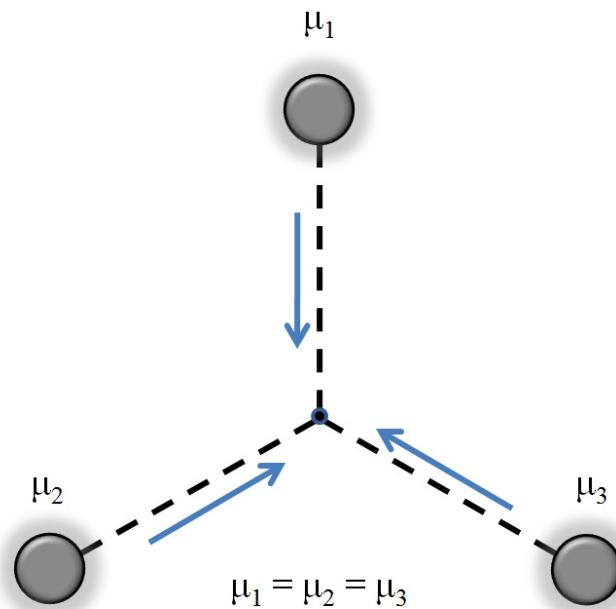


Figure 2.6: Homothetic Solution of the Three-Body Problem

LAGRANGE

The Italian mathematician Joseph Louis Lagrange (1736-1813) continued Euler’s work on the three-body problem and discovered five equilibrium points (known today as the Lagrange points) when analyzing the circular restricted three-body problem. The circular restricted three-body problem assumes that the two primary masses are either fixed in space or move in circular coplanar orbits about their center of mass. As seen in a frame of reference which rotates with the same period as the two co-orbiting bodies, the centrifugal force and gravitational fields of the two principal bodies are in balance at the

Lagrange point, allowing a third object to be stationary with respect to the primary bodies. The first three Lagrange points, L_1 , L_2 , and L_3 , are referred to as the collinear Lagrange points, because they are located on the same axis as the two primary bodies. The fourth and fifth points are referred to as the triangular Lagrange points, because their distances from the two primary bodies form equilateral triangles with sides equal to the distance between the two principal bodies. Figure 2.7 shows the location of the Lagrange points in the circular restricted three-body problem.

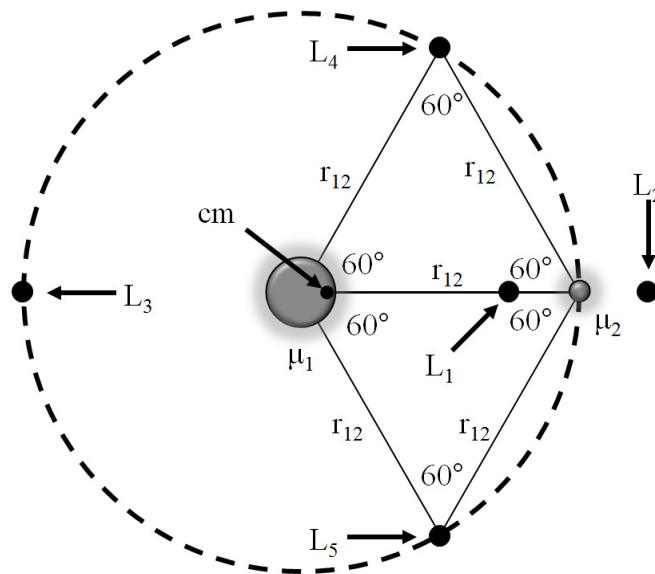


Figure 2.7: Lagrange Points in the Circular Restricted Three-Body Problem

Lagrange also derived solutions for many special cases of the full three-body problem, including a family of homographic, central configuration solutions which lie at the vertices of a rotating equilateral triangle that can shrink and expand periodically. The term “homographic” implies that the configuration formed by the three bodies at any given instant moves in such a way as to remain similar to itself as time varies [44-48]. Two of these central configuration solutions are shown in Figures 2.8 and 2.9.

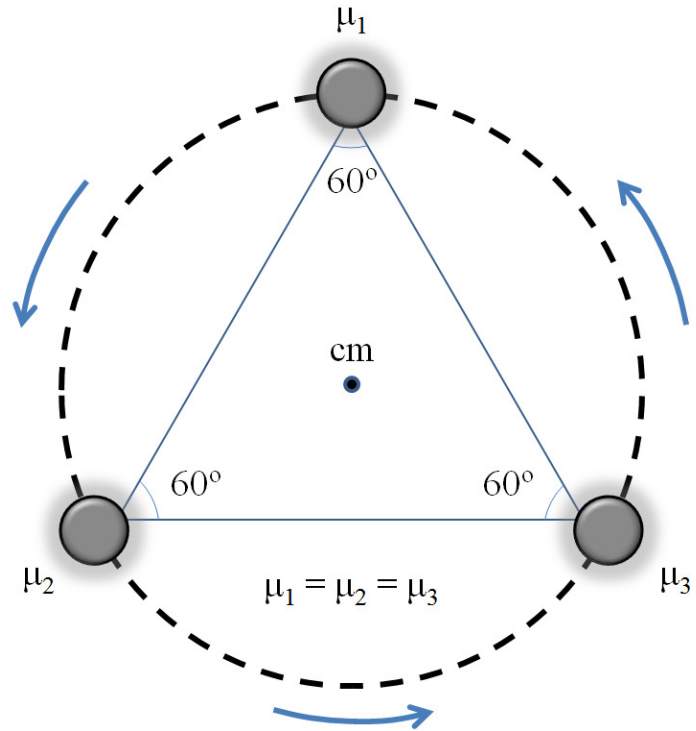


Figure 2.8: Equal Mass Central Configuration Solution of the Three-Body Problem

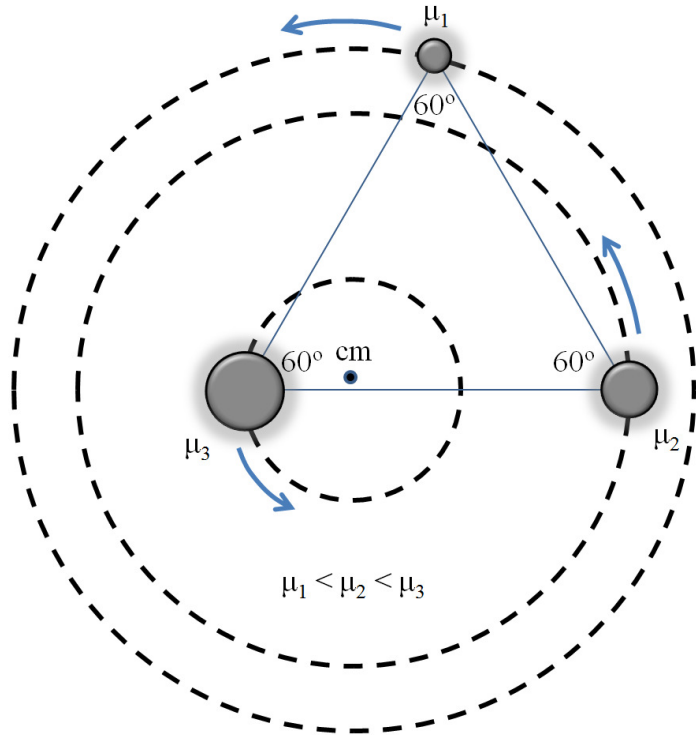


Figure 2.9: Unequal Mass Central Configuration Solution of the Three-Body Problem

POINCARÉ

In 1887, Oscar II, King of Sweden and Norway, initiated a mathematical competition and established a prize for anyone who could find a power series solution of the N-body problem. In the event that a solution could not be derived, the prize would be awarded for an important contribution to classical mechanics. Out of the twelve papers submitted, only five of them tackled the problem of N-bodies. However, the five papers failed to develop the power series solution required by the jury, which consisted of three of the most respected mathematicians of that time and who themselves had tackled the problem of N-bodies in their research: Gösta Mittag-Leffler, Charles Hermite, and Karl Weierstrass. Under these circumstances, the panel decided to award the prize to the French mathematician Jules Henri Poincaré (1854-1912) for his remarkable contribution to the understanding of the equations of dynamics (called Hamiltonian systems today) and for the many new ideas he brought into mathematics and mechanics. Although he did not actually solve the problem, his work demonstrated that certain numerical solutions of the three-body problem result in chaotic motion with no obvious sign of a repetitious path. The evolution of these orbits is so sensitive to minor changes in an object's position and velocity with respect to other gravitating bodies that it is essentially unpredictable. Poincaré's manuscript was important, because it laid the foundation of deterministic chaos theory [49-54].

SUNDMAN

In 1912, the Finnish mathematician Karl Fritiof Sundman introduced a new transformation based on the theory of complex-variable functions that allowed him to derive a power series solution for the three-body problem. He was able to prove that this

series is convergent for all real values of time, except when the initial state (position and velocity) corresponds to an angular momentum of zero. However, Sundman later discovered that although the time series converges uniformly, it does so very slowly. For this reason, calculating the state of a particle to any useful precision at a future time requires so many terms that his solution is of little practical use. It was later discovered that Sundman's transformation could not be extended to the problem of N-bodies and, consequently, seven more decades would pass before a global solution of the N-body problem could be determined [55].

WANG

In 1991, the Chinese mathematician Qiudong Wang developed a global power series solution to the N-body problem by introducing a new “blowing up” transformation that was also based on the theory of complex variables. In order to develop this result, Wang had to omit any consideration of the complicated singularities that can be encountered by the solution of the N-body problem. The implementation of this solution, however, results in the same behavior observed with Sundman's work on the three-body problem: the power series, though convergent on the whole real axis, has a very slow convergence. One would have to sum up millions of terms to determine the motion of the particles involved for insignificantly short intervals of time. Consequently, the round-off errors resulting from its implementation makes the power series unusable in numerical work [56].

SUGGESTED READING

This chapter has briefly discussed the N-body problem from a historical point of view. In the author's opinion, a significant number of volumes would be needed to document or even fully summarize the extensive amount of theoretical literature that has been written over the years about the topic. What follows, however, is a short list of publications recommended by the author that discuss several aspects of the N-body problem. This list is by far not an exhaustive one, but it will allow the reader to develop a strong foundation in the principles of the problem being analyzed in this dissertation.

- * Curtis' *Orbital Mechanics for Engineering Students* is a great undergraduate level text that discusses many of the concepts of the two-body problem and trajectory design. The derivations in this book are outlined in a step-by-step manner and explained very well, making it an excellent resource for both beginning and advanced astrodynamacists [57].
- * Vallado's *Fundamentals of Astrodynamics and Applications* is an excellent text that discusses many aspects of the N-body problem including its history and the formulation of the equations of motion. An emphasis is then placed on the theory of two bodies with detailed derivations. Many real-life algorithms used to implement the analytic results derived are presented and explained in detail [58].
- * Newton's *Mathematical Principles of Natural Philosophy* was the landmark publication that laid the foundation of classical mechanics. This was the first text that discussed the equations of motion pertaining to the N-body problem. The book gives the first solution of the two-body problem and discusses some of the first attempts at solving the three-body problem [59].

- ✧ Lagrange's *Analytical Mechanics* was another landmark publication that reformulated Newton's classical mechanics into a form that emphasized work and energy methods. These new methods are then used to derive many important outcomes from the two-body problem and used to develop many solutions for special cases of the three-body problem [60].
- ✧ Szebehely's *Theory of Orbits: The Restricted Problem of Three Bodies* is an advanced classical text that provides a deep and thorough analysis of the restricted three-body problem [61].
- ✧ Pollard's *Mathematical Introduction to Celestial Mechanics* is an advanced text that gives a complete description of the solution of the two-body problem, an introduction to Hamiltonian equations, and a brief treatment of the restricted N-body problem. It is a great starting point for the study of Hamiltonian systems and celestial mechanics [62].
- ✧ Meyer's *Periodic Solutions of the N-body Problem* provides an excellent, systematic investigation of the special cases pertaining to the N-body problem for which periodic, time dependent solutions can be derived [63].

CHAPTER 3

THE TWO-BODY PROBLEM

This chapter presents and discusses the equations of motion of the two-body problem. An analytic, time dependent solution for the case of circular orbits is derived. The classical orbital element method used to determine future states for elliptical, parabolic, and hyperbolic orbits is outlined and discussed. Time dependent, power series solutions of the relative two-body problem are presented and used recursively to analyze a highly elliptical orbit scenario. The fourth-order and fifth-order Runge-Kutta numerical integration algorithms are introduced and used to investigate the same scenario analyzed by the power series solution. A variable time step algorithm that incorporates these two numerical integrators is also derived. Discussion on the absolute error and simulation time results returned by the four numerical experiments conclude the chapter.

EQUATIONS OF MOTION

The two-body problem is an important model that can be used to analyze the motion of satellites orbiting the Earth or traveling through interplanetary space. Any deviation in real-life applications from the predictions it makes are the result of perturbations caused by other gravitational sources or other forces, both natural and induced. Figure 3.1 shows the coordinate system of the two-body problem. The equations of motion that govern the two-body problem are

$$\ddot{\bar{\mathbf{r}}}_1 = \frac{\mu_2(\bar{\mathbf{r}}_2 - \bar{\mathbf{r}}_1)}{\|\bar{\mathbf{r}}_2 - \bar{\mathbf{r}}_1\|^3} = \frac{\mu_2\Delta\bar{\mathbf{r}}}{\Delta r^3} \quad (3.1)$$

$$\ddot{\bar{\mathbf{r}}}_2 = \frac{\mu_1(\bar{\mathbf{r}}_1 - \bar{\mathbf{r}}_2)}{\|\bar{\mathbf{r}}_1 - \bar{\mathbf{r}}_2\|^3} = -\frac{\mu_1\Delta\bar{\mathbf{r}}}{\Delta r^3} \quad (3.2)$$

where μ_1 and μ_2 are the gravitational parameters of the primary and secondary body, respectively, and $\bar{\mathbf{r}}_1$ and $\bar{\mathbf{r}}_2$ are the position vectors of the primary and secondary body, respectively.

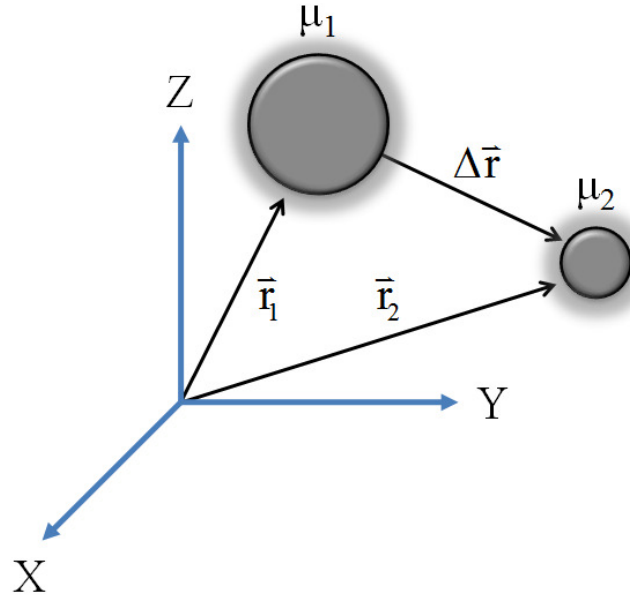


Figure 3.1: Two-Body Problem Coordinate System

Subtracting equation 3.1 from equation 3.2 yields the acceleration vector of the second body with respect to the first (relative acceleration vector),

$$\ddot{\bar{\mathbf{r}}}_2 - \ddot{\bar{\mathbf{r}}}_1 = -\frac{(\mu_1 + \mu_2)(\bar{\mathbf{r}}_2 - \bar{\mathbf{r}}_1)}{\|\bar{\mathbf{r}}_2 - \bar{\mathbf{r}}_1\|^3} \rightarrow \Delta\ddot{\bar{\mathbf{r}}} = -\frac{\mu\Delta\bar{\mathbf{r}}}{\Delta r^3} \quad (3.3)$$

where μ is the sum of the gravitational parameters. This relative motion outcome is the fundamental equation of the two-body problem. Additionally, when the gravitational parameter of the second body, μ_2 , is much smaller than the gravitational parameter of the

first, μ_1 , the relative motion expression given by equation 3.3 becomes the restricted two-body problem. The term “restricted” indicates that the mass of the second body being analyzed is negligible, causing it to have no gravitational influence on the motion of the first as shown in Figure 3.2.

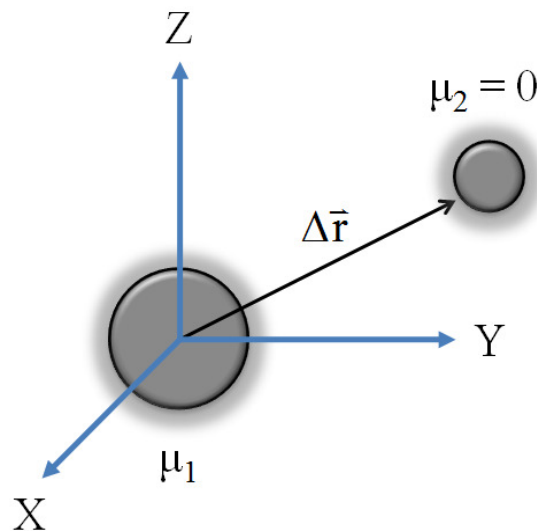


Figure 3.2: Restricted Two-Body Problem Coordinate System

THE ORBIT EQUATION

Johannes Kepler stated in his First Law of Planetary Motion that all the planets move in elliptical orbits with the Sun at one focus. Sir Isaac Newton later expanded this result by determining that the solution of the relative two-body problem would take the form of a conic section: circle, ellipse, parabola, and hyperbola. However, he derived this outcome using analytical geometry constructions and his newly developed concept of the limit. It wasn't until a few years after Newton's death that Daniel Bernoulli solved the relative two-body problem using the methods of calculus which, ironically, had been invented by Isaac Newton himself and Gottfried Leibniz, and further developed by his father and uncle; Johann and Jacob Bernoulli, respectively. Daniel Bernoulli's solution of the relative two-body problem, now commonly referred to as the orbit equation, was

not a time dependent outcome but one based on the geometry of the orbit in question. It is in essence the equation for a conic section in polar coordinates. Three different ways of writing the orbit equation are

$$\Delta r = \frac{p}{1 + e \cos(v)} = \frac{a(1 - e^2)}{1 + e \cos(v)} = \frac{h^2}{\mu} \frac{1}{1 + e \cos(v)} \quad (3.4)$$

where Δr is the magnitude of the relative position vector and the remaining variables are defined as follows:

- * a is the semimajor axis, which determines the size of the orbit;
- * e is the eccentricity, which determines the shape of the orbit;
- * v is the true anomaly, which determines the angular location of the second body relative to the periapse point;
- * p is the semi-parameter, which is equivalent to the magnitude of the relative position vector when the true anomaly is equal to 90° ; and
- * h is the magnitude of the specific angular momentum vector, which is determined by the cross-product of the relative position and velocity vectors,

$$\bar{h} = \Delta \bar{r} \times \Delta \bar{v} \rightarrow h = \|\bar{h}\| = \|\Delta \bar{r} \times \Delta \bar{v}\| \quad (3.5)$$

Figure 3.3 shows the geometry of the variables that form the orbit equation for an elliptical orbit.

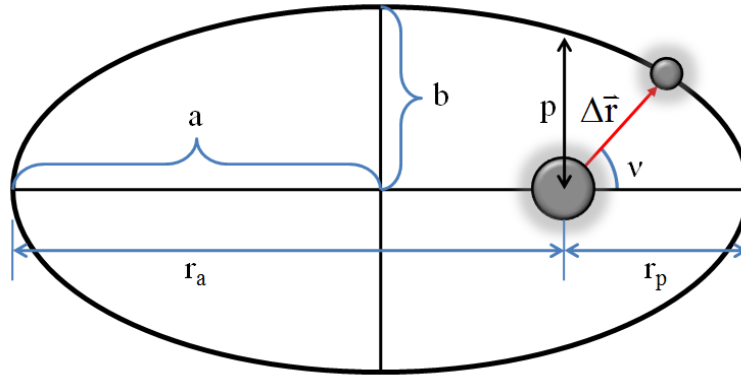


Figure 3.3: Geometry of an Elliptical Orbit

In this figure, b is the semiminor axis, r_p is the radius of periapsis (the point where the second body is closest to the primary body), and r_a is the radius apoapsis (the point where the second body is furthest from the primary body). The magnitude of the relative position vector is equal to the radius of periapsis when the true anomaly is equal to 0° and to the radius of apoapsis when the true anomaly is equal to 180° . In addition to being called the major axis, the line connecting the radius of periapsis with the radius of apoapsis is also known as the line of apsides.

As was mentioned earlier, the orbit's eccentricity determines its shape and can be obtained by finding the magnitude of the eccentricity vector, which always points towards the radius of periapsis,

$$\bar{e} = \frac{1}{\mu} \left[\left(\Delta v^2 - \frac{\mu}{\Delta r} \right) \Delta \bar{r} - (\Delta \bar{r} \cdot \Delta \bar{v}) \Delta \bar{v} \right] \quad (3.6)$$

The four conic section solutions of the relative two-body problem are related to eccentricity in the following manner:

- * If $e = 0$, the orbit is circular.
- * If $0 < e < 1$, the orbit is elliptical.

- * If $e = 1$, the orbit is parabolic.
- * If $e > 1$, the orbit is hyperbolic.

These outcomes can be seen in Figure 3.4.

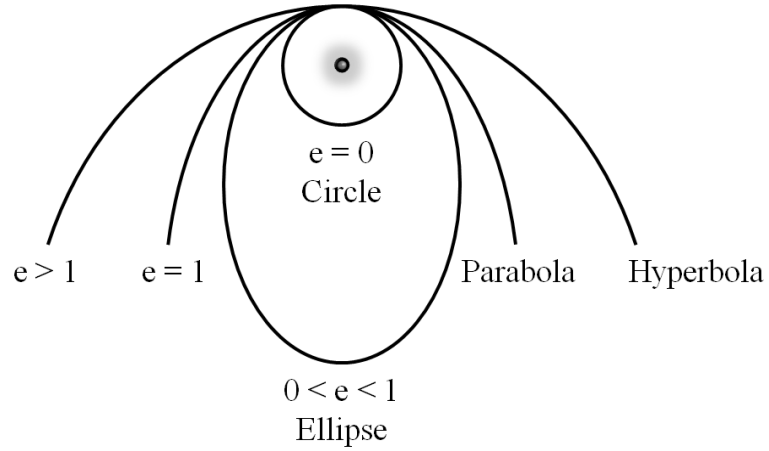


Figure 3.4: Effect of Eccentricity on Orbital Geometry

CIRCULAR ORBIT SOLUTIONS

Equation 3.3 is a second order, non-linear, coupled, space dependent vector differential equation that can be expanded into a first-order matrix equation,

$$\Delta \dot{\bar{s}} = \mathbf{A} \Delta \bar{s} \rightarrow \begin{cases} \Delta \dot{\bar{r}} \\ \Delta \dot{\bar{v}} \end{cases} = \begin{bmatrix} \mathbf{0}_{3 \times 3} & \mathbf{I}_{3 \times 3} \\ -\left(\frac{\mu}{\Delta r^3}\right) \mathbf{I}_{3 \times 3} & \mathbf{0}_{3 \times 3} \end{bmatrix} \begin{cases} \Delta \bar{r} \\ \Delta \bar{v} \end{cases} \quad (3.7)$$

In this expression, $\Delta \dot{\bar{s}}$ and $\Delta \bar{s}$ are the relative rate of change and relative state vectors, respectively, \mathbf{A} is the space dependent coefficient matrix, μ is the sum of the gravitational parameters, $\mathbf{0}_{3 \times 3}$ is a 3x3 zero matrix, $\mathbf{I}_{3 \times 3}$ is a 3x3 identity matrix, $\Delta \bar{r}$ is the relative position vector, and $\Delta \bar{v}$ is the relative velocity vector. The initial conditions for equation 3.7 are

$$\Delta\bar{\mathbf{s}}(t_0) = \Delta\bar{\mathbf{s}}_0 = \begin{Bmatrix} \Delta\bar{\mathbf{r}}_0 \\ \Delta\bar{\mathbf{v}}_0 \end{Bmatrix} \quad (3.8)$$

where $\Delta\bar{\mathbf{s}}_0$ is the relative initial state, and $\Delta\bar{\mathbf{r}}_0$ and $\Delta\bar{\mathbf{v}}_0$ are the initial relative position and velocity vectors, respectively. As stated earlier, there is no practical time dependent, analytic, general solution to this vector differential equation. The only exception to this is the case when the two bodies are in circular orbits with respect to their center of mass. For such a case, the mean angular motion of both bodies is a constant defined as

$$n = \sqrt{\frac{\mu}{\Delta r_0^3}} = \sqrt{\frac{\mu}{a^3}} \quad (3.9)$$

With this definition, the coefficient matrix, \mathbf{A} , becomes a sparse constant matrix,

$$\mathbf{A} = \begin{bmatrix} \mathbf{0}_{3 \times 3} & \mathbf{I}_{3 \times 3} \\ -n^2 \mathbf{I}_{3 \times 3} & \mathbf{0}_{3 \times 3} \end{bmatrix} \quad (3.10)$$

This causes the vector differential equation given by equation 3.7 to become a system of equations with constant coefficients for which an analytic solution can be derived. Using eigenvalue methods [64], the general solution can be stated as

$$\Delta\bar{\mathbf{s}}(t) = \mathbf{M}\Delta\bar{\mathbf{c}} \rightarrow \begin{Bmatrix} \Delta\bar{\mathbf{r}} \\ \Delta\bar{\mathbf{v}} \end{Bmatrix} = \begin{bmatrix} \cos(nt)\mathbf{I}_{3 \times 3} & \sin(nt)\mathbf{I}_{3 \times 3} \\ -n \sin(nt)\mathbf{I}_{3 \times 3} & n \cos(nt)\mathbf{I}_{3 \times 3} \end{bmatrix} \begin{Bmatrix} \Delta\bar{\mathbf{c}}_1 \\ \Delta\bar{\mathbf{c}}_2 \end{Bmatrix} \quad (3.11)$$

where \mathbf{M} is the fundamental eigenvalue matrix, $\Delta\bar{\mathbf{c}}$ is a generic state constant of integration, and $\Delta\bar{\mathbf{c}}_1$ and $\Delta\bar{\mathbf{c}}_2$ are generic vector constants of integration. Using the initial conditions given by equation 3.8, the unique solution of equation 3.7 becomes

$$\Delta\bar{s}(t) = \Phi\Delta\bar{s}_0 \rightarrow \begin{Bmatrix} \Delta\bar{r} \\ \Delta\bar{v} \end{Bmatrix} = \begin{bmatrix} \cos(nt)\mathbf{I}_{3 \times 3} & \frac{1}{n}\sin(nt)\mathbf{I}_{3 \times 3} \\ -n\sin(nt)\mathbf{I}_{3 \times 3} & \cos(nt)\mathbf{I}_{3 \times 3} \end{bmatrix} \begin{Bmatrix} \Delta\bar{r}_0 \\ \Delta\bar{v}_0 \end{Bmatrix} \quad (3.12)$$

where Φ is the relative state transition matrix. The state of each body with respect to the systems' barycenter can then be given by

$$\bar{s}_1(t) = -\frac{\mu_2}{\mu} \Delta\bar{s}(t) \quad (3.13)$$

$$\bar{s}_2(t) = \frac{\mu_1}{\mu} \Delta\bar{s}(t) \quad (3.14)$$

This time dependent, analytic solution applies to circular orbits only and cannot be extended to the case of elliptical, parabolic, and hyperbolic orbits. For these orbit types, a trajectory designer can use the classical orbital element approach to determine future states given a set of initial conditions.

CLASSICAL ORBITAL ELEMENT SOLUTIONS

The orbit equation can be used to determine a future state consisting of a relative position and velocity given a set of initial conditions in inertial space,

$$\{ \Delta t \quad \Delta\bar{r}_0 \quad \Delta\bar{v}_0 \}^T \rightarrow \{ \Delta\bar{r}_f \quad \Delta\bar{v}_f \}^T \quad (3.15)$$

This section will outline the procedure for the case of an elliptical orbit. The reader is referred to Curtis [65] or Vallado [66] for the procedure involving parabolic and hyperbolic orbits. The first step in this process is to determine the classical orbital elements of the orbit being analyzed:

- * Semimajor axis, a ;
- * Eccentricity, e ;
- * Inclination, i ;
- * Right Ascension of the Ascending Node, Ω ;
- * Argument of Periapsis, ω ; and
- * True Anomaly, ν .

The semimajor axis and eccentricity determine the orbit's size and shape, respectively, while the inclination, right ascension of the ascending node, and argument of periapsis determine the orbit's orientation in inertial space. The true anomaly determines the location on the orbit of the second body with respect to the first. A visual description of these elements can be seen in Figure 3.5.

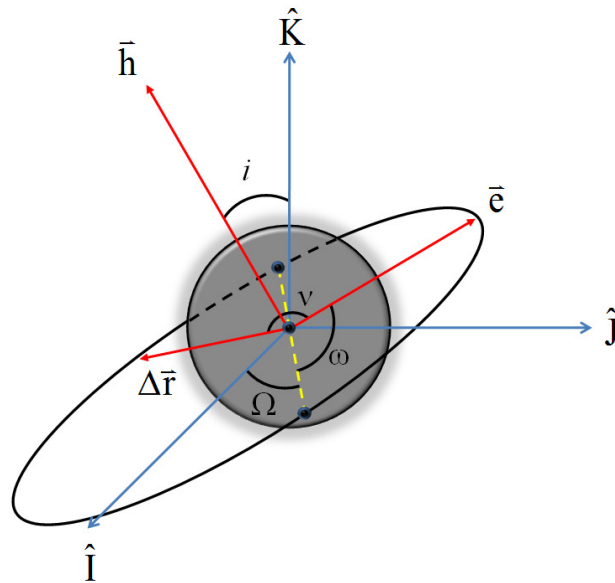


Figure 3.5: Classical Orbital Elements

The relative position and velocity vectors can be used to determine the semimajor axis a through the use of the specific mechanical energy equation,

$$\varepsilon = \frac{\Delta v^2}{2} - \frac{\mu}{\Delta r} = \frac{-\mu}{2a} \rightarrow a = \frac{-\mu \Delta r}{\Delta r \Delta v^2 - 2\mu} \quad (3.16)$$

where ε is the orbit's specific mechanical energy. Eccentricity e is determined by evaluating the magnitude of equation 3.6. The inclination i is determined by first calculating the orbit's specific angular momentum vector given by equation 3.5 and then finding the angle between the specific angular momentum vector and the inertial \hat{K} axis,

$$i = \cos^{-1} \left(\frac{\bar{h} \cdot \hat{K}}{h} \right) \quad (3.17)$$

Inclination is the angle formed by the orbital plane and the inertial $\hat{I}-\hat{J}$ plane. It will always fall between 0° and 180° , so no quadrant check is required by equation 3.17. The right ascension of the ascending node, Ω , is calculated by first determining the ascending node vector $\bar{\eta}$, which is part of the line of nodes. The line of nodes is the line formed by the intersection of the orbital plane and inertial $\hat{I}-\hat{J}$ plane. The ascending node vector is perpendicular to both the inertial \hat{K} axis and the specific angular momentum vector, so it can be determined by

$$\bar{\eta} = \hat{K} \times \bar{h} \quad (3.18)$$

The right ascension of the ascending node is the angle formed by the inertial \hat{I} axis and the line of nodes,

$$\Omega = \cos^{-1} \left(\frac{\hat{I} \cdot \bar{\eta}}{\eta} \right) \quad (3.19)$$

This angle can range between 0° and 360° , so a quadrant check is necessary:

* If $\eta_j \geq 0$ then $0^\circ \leq \Omega \leq 180^\circ$.

* If $\eta_j < 0$ then $180^\circ < \Omega < 360^\circ$.

The argument of periapsis ω is the angle formed by the ascending node vector and the eccentricity vector,

$$\omega = \cos^{-1} \left(\frac{\bar{\eta} \cdot \bar{e}}{\eta e} \right) \quad (3.20)$$

This angle can also range between 0° and 360° , so a quadrant check is necessary:

* If $e_k \geq 0$ then $0^\circ \leq \omega \leq 180^\circ$.

* If $e_k < 0$ then $180^\circ < \omega < 360^\circ$.

Finally, true anomaly is the angle between the eccentricity vector and the relative position vector,

$$\nu = \cos^{-1} \left(\frac{\bar{e} \cdot \Delta \bar{r}}{e \Delta r} \right) \quad (3.21)$$

The quadrant check used to determine the correct angle is:

* If $\Delta \bar{r} \cdot \Delta \bar{v} \geq 0$ then $0^\circ \leq \nu \leq 180^\circ$.

* If $\Delta \bar{r} \cdot \Delta \bar{v} < 0$ then $180^\circ < \nu < 360^\circ$.

Once the orbit's classical orbital elements have been determined, the initial eccentric anomaly E_0 is given by

$$E_0 = 2 \tan^{-1} \left[\sqrt{\frac{1-e}{1+e}} \tan \left(\frac{\nu_0}{2} \right) \right] \quad (3.22)$$

where v_0 is the true anomaly corresponding the initial state. Eccentric anomaly is the angle formed by the eccentricity vector and the line connecting the location of the second body with center of the ellipse. The eccentric anomaly corresponding to the new state E_f is determined by solving Kepler's equation,

$$E_f = E_0 + e[\sin(E_f) - \sin(E_0)] + n\Delta t \quad (3.23)$$

where n is the mean angular motion,

$$n = \sqrt{\frac{\mu}{a^3}} \quad (3.24)$$

and Δt is the time between states,

$$\Delta t = t_f - t_0 \quad (3.25)$$

Kepler's equation is a transcendental expression that can only be solved using an iterative procedure such as Newton's root-finding method. Once the new eccentric anomaly has been determined, the true anomaly corresponding to the new state v_f is found by rearranging equation 3.22,

$$v_f = 2 \tan^{-1} \left[\sqrt{\frac{1+e}{1-e}} \tan\left(\frac{E_f}{2}\right) \right] \quad (3.26)$$

The orbit equation is used to define the relative position vector in the perifocal coordinate system $(\hat{P}, \hat{Q}, \hat{W})$, where the principle direction is parallel to the eccentricity vector, which points towards the periapsis point [67]. This can be seen in Figure 3.6.

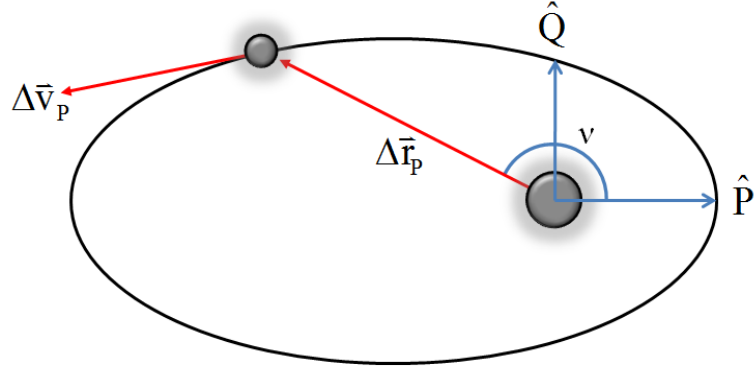


Figure 3.6: Perifocal Coordinate System

Working in the perifocal coordinate system, the relative position and velocity vectors, respectively, corresponding to the new state are given by

$$\Delta \vec{r}_P = \frac{p}{1 + e \cos(v_f)} [\cos(v_f) \hat{P} + \sin(v_f) \hat{Q}] \quad (3.27)$$

$$\Delta \vec{v}_P = \sqrt{\frac{\mu}{p}} \{-\sin(v_f) \hat{P} + [e + \cos(v_f)] \hat{Q}\} \quad (3.28)$$

Finally, the new state can be converted to inertial coordinates using a transformation matrix,

$$\Delta \vec{r}_f = T \Delta \vec{r}_P \quad (3.29)$$

$$\Delta \vec{v}_f = T \Delta \vec{v}_P \quad (3.30)$$

where the transformation matrix (T) is given by

$$T = \begin{bmatrix} c(\Omega)c(\omega) - c(i)s(\Omega)s(\omega) & -c(\Omega)s(\omega) - c(i)s(\Omega)c(\omega) & s(i)s(\Omega) \\ s(\Omega)c(\omega) + c(i)c(\Omega)s(\omega) & -s(\Omega)s(\omega) + c(i)c(\Omega)c(\omega) & -s(i)c(\Omega) \\ s(i)s(\omega) & s(i)c(\omega) & c(i) \end{bmatrix} \quad (3.31)$$

where $c(\) = \cos(\)$ and $s(\) = \sin(\)$.

The classical orbital element method returns exact results when future states are being predicted for all orbit types (with the exception of circular orbits) governed by the relative two-body problem when an initial state and a propagation time are known. However, it quickly becomes apparent that the classical orbital element method requires a substantial number of steps to implement. Moreover, the procedure cannot be extended to cases where the motion of more than two bodies is taken into account. A time dependent, analytic solution that can be applied to the motion of any number of bodies would allow the trajectory designer to determine a future state in just one step. Such a time dependent solution has been developed in the form of a power series for the relative two-body problem and, as will be derived by the author in the next chapters, this power series can be extended to the N-body problem.

POWER SERIES SOLUTIONS

A time dependent solution of the relative two-body problem can be expressed in terms of a Taylor series expansion given the initial relative position and velocity [68-70],

$$\Delta\bar{\mathbf{r}}(t) = \sum_{k=0}^{\infty} \frac{t^k}{k!} \left. \frac{d^k \Delta\bar{\mathbf{r}}}{dt^k} \right|_0 = \Delta\bar{\mathbf{r}}_0 + \frac{t}{1!} \left. \frac{d\Delta\bar{\mathbf{r}}}{dt} \right|_0 + \frac{t^2}{2!} \left. \frac{d^2 \Delta\bar{\mathbf{r}}}{dt^2} \right|_0 + \frac{t^3}{3!} \left. \frac{d^3 \Delta\bar{\mathbf{r}}}{dt^3} \right|_0 + \dots \quad (3.32)$$

where the first and second order derivatives are defined as

$$\left. \frac{d\Delta\bar{\mathbf{r}}}{dt} \right|_0 = \Delta\bar{\mathbf{v}}_0 \quad (3.33)$$

$$\left. \frac{d^2 \Delta \bar{r}}{dt^2} \right|_0 = -\frac{\mu}{\Delta r_0^3} \Delta \bar{r}_0 \quad (3.34)$$

Successive terms in the Taylor series expansion can be found by defining the following quantities:

$$\alpha = \frac{\mu}{\Delta r_0^3} \quad (3.35)$$

$$\beta = \left(\frac{\Delta v_0}{\Delta r_0} \right)^2 \quad (3.36)$$

$$\lambda = \frac{\Delta \bar{r}_0 \cdot \Delta \bar{v}_0}{\Delta r_0^2} \quad (3.37)$$

These three values are known as fundamental invariants because they are independent of the selected coordinate system and they form a closed set under the operation of time differentiation. Consequently, differentiation of the fundamental invariants with respect to time leads to the following outcomes:

$$\frac{d\alpha}{dt} = -3\alpha\lambda \quad (3.38)$$

$$\frac{d\beta}{dt} = -2\lambda(\alpha + \beta) \quad (3.39)$$

$$\frac{d\lambda}{dt} = \beta - \alpha - 2\lambda^2 \quad (3.40)$$

With these definitions, the higher order derivatives in the Taylor series expansion given by equation 3.32 can now be expressed as

$$\Delta\bar{r}(t) = \Delta\bar{r}_0 + t\Delta\bar{v}_0 - \frac{t^2}{2!}\alpha\Delta\bar{r}_0 + \frac{t^3}{3!}(3\alpha\lambda\Delta\bar{r}_0 - \alpha\Delta\bar{v}_0) + \dots \quad (3.41)$$

Fundamental Invariant Characteristics

The fundamental invariant α can be described as the local angular acceleration of the second body with respect to the first. Looking at equation 3.35, it can be concluded that this local angular acceleration approaches zero as the distance between the two bodies approaches infinity. Moreover, the fundamental invariants β and λ can be rewritten in terms of α . Once again working in the perifocal coordinate system shown in Figure 3.6, the magnitude of the relative position vector is the orbit equation. The magnitude of the relative velocity is given by

$$\Delta v_0 = \sqrt{\frac{\mu[1 + e^2 + 2e \cos(v)]}{p}} \quad (3.42)$$

Substituting the orbit equation and equation 3.42 into the definition of the fundamental invariant β given by equation 3.36 and simplifying yields

$$\beta = \left(\frac{\Delta v_0}{\Delta r_0} \right)^2 = \alpha \left[\frac{1 + e^2 + 2e \cos(v)}{1 + e \cos(v)} \right] \quad (3.43)$$

A close scrutiny of equation 3.43 allows us to conclude the following:

- * When $e = 0$ (circular orbit), $\beta = \alpha$.
- * When $e = 1$ (parabolic orbit), $\beta = 2\alpha$.
- * When $v = 0^\circ$, $\beta = \alpha(1 + e)$.
- * When $v = 180^\circ$, $\beta = \alpha(1 - e)$.
- * When $v = 90^\circ$ or 270° , $\beta = \alpha(1 + e^2)$.

Likewise, substituting the orbit equation and equation 3.42 into the definition of the fundamental invariant λ given by equation 3.37 and simplifying yields

$$\lambda = \frac{\Delta\bar{r}_0 \cdot \Delta\bar{v}_0}{\Delta r_0^2} = e \sin(\nu) \sqrt{\frac{\alpha}{1 + e \cos(\nu)}} \quad (3.44)$$

Substituting various values of true anomaly and eccentricity into equation 3.44 allows us to conclude the following:

- * When $e = 0$ (circular orbit), $\lambda = 0$.
- * When $e = 1$ (parabolic orbit), $\lambda = \sqrt{\alpha[1 - \cos(\nu)]}$.
- * When $\nu = 0^\circ$ or 180° , $\lambda = 0$.
- * When $\nu = 90^\circ$ or 270° , $\lambda = e\sqrt{\alpha}$.

Additionally, the expression for eccentricity given by equation 3.6 can be rewritten in terms of fundamental invariants.

$$e = \frac{\sqrt{(\beta - \alpha)^2 + \lambda^2(2\alpha - \beta)}}{\alpha} \quad (3.45)$$

Lagrange Coefficients and Recursion Relationships

By rearranging equation 3.41, it can be shown that the relative position vector of any point particle whose motion is described by the two-body problem can be expressed in terms of its initial position and velocity with respect to a primary body given an initial time such that

$$\Delta\bar{r}(t) = F\Delta\bar{r}_0 + G\Delta\bar{v}_0 \quad (3.46)$$

where the functions F and G are known as Lagrange coefficients. Further research of these time dependent Lagrange coefficients has lead to the development of recursion relationships that allow a trajectory designer to evaluate higher order derivatives of equation 3.46 in an efficient manner [71-72]. These recursion relationships are given by

$$(k+1)(k+2)f_{k+2} = -(\alpha_0 f_k + \alpha_1 f_{k-1} + \dots + \alpha_k f_0) \quad (3.47)$$

$$(k+1)(k+2)g_{k+2} = -(\alpha_0 g_k + \alpha_1 g_{k-1} + \dots + \alpha_k g_0) \quad (3.48)$$

$$(k+1)\alpha_{k+1} = -3(\alpha_0 \lambda_k + \alpha_1 \lambda_{k-1} + \dots + \alpha_k \lambda_0) \quad (3.49)$$

$$(k+1)\beta_{k+1} = -2[\lambda_0(\alpha_k + \beta_k) + \lambda_1(\alpha_{k-1} + \beta_{k-1}) + \dots + \lambda_k(\alpha_0 + \beta_0)] \quad (3.50)$$

$$(k+1)\lambda_{k+1} = \beta_k - \alpha_k - 2(\lambda_0 \lambda_k + \lambda_1 \lambda_{k-1} + \dots + \lambda_k \lambda_0) \quad (3.51)$$

where k is an integer such that;

$$k = 0, 1, 2, \dots \quad (3.52)$$

and the values of the zero and first order terms, respectively, are

$$f_0 = 1 \quad (3.53)$$

$$f_1 = 0 \quad (3.54)$$

$$g_0 = 0 \quad (3.55)$$

$$g_1 = 1 \quad (3.56)$$

With these definitions, the time dependent Lagrange coefficients are then found by summing their respective components,

$$F_{\xi} = \sum_{k=0}^{\xi} \frac{1}{k!} f_k t^k \quad (3.57)$$

$$G_{\xi} = \sum_{k=0}^{\xi} \frac{1}{k!} g_k t^k \quad (3.58)$$

where ξ is the desired order of the Lagrange coefficients. Using these definitions, the first seven terms of each time dependent Lagrange coefficient can be stated as

$$\begin{aligned} F = & 1 - \frac{1}{2}\alpha t^2 + \frac{1}{2}\alpha\lambda t^3 - \frac{1}{24}\alpha(2\alpha - 3\beta + 15\lambda^2)t^4 + \frac{1}{8}\alpha\lambda(2\alpha - 3\beta + 7\lambda^2)t^5 \\ & - \frac{1}{720}\alpha[22\alpha^2 - 66\alpha\beta + 45\beta^2 + 105\lambda^2(4\alpha - 6\beta + 9\lambda^2)]t^6 \\ & + \frac{1}{80}\alpha\lambda[12\alpha^2 - 36\alpha\beta + 25\beta^2 + 5\lambda^2(20\alpha - 30\beta + 33\lambda^2)]t^7 - \dots \end{aligned} \quad (3.59)$$

$$\begin{aligned} G = & t - \frac{1}{6}\alpha t^3 + \frac{1}{4}\alpha\lambda t^4 - \frac{1}{120}\alpha(8\alpha - 9\beta + 45\lambda^2)t^5 \\ & + \frac{1}{24}\alpha\lambda(5\alpha - 6\beta + 14\lambda^2)t^6 \\ & - \frac{1}{5040}\alpha[172\alpha^2 - 396\alpha\beta + 225\beta^2 + 315\lambda^2(8\alpha - 10\beta + 15\lambda^2)]t^7 + \dots \end{aligned} \quad (3.60)$$

Equations 3.59-3.60 apply to all types of orbits governed by the relative two-body problem. For the case of a circular orbit, where $\alpha = \beta$ and $\lambda = 0$, the time dependent Lagrange coefficients reduce to the terms of a Taylor series expansion for the cosine and sine trigonometric functions, respectively,

$$F = 1 - \frac{1}{2}\alpha t^2 + \frac{1}{24}\alpha^2 t^4 - \frac{1}{720}\alpha^3 t^6 + \dots = \sum_{k=0}^{\infty} \frac{(-\alpha t^2)^k}{(2k)!} = \cos(t\sqrt{\alpha}) \quad (3.61)$$

$$G = t - \frac{1}{6}\alpha t^3 + \frac{1}{120}\alpha^2 t^5 - \frac{1}{5040}\alpha^3 t^7 + \dots = \sum_{k=0}^{\infty} \frac{t(-\alpha t^2)^k}{(2k+1)!} = \frac{1}{\sqrt{\alpha}} \sin(t\sqrt{\alpha}) \quad (3.62)$$

These circular orbit results agree with the analytic solution given by equation 3.12. For the case of an elliptical or hyperbolic orbit, where the initial state is given at periapsis so that $v = 0$ and $\lambda = 0$, the time dependent Lagrange coefficients reduce to

$$F = 1 - \frac{1}{2}\alpha t^2 - \frac{1}{24}\alpha(2\alpha - 3\beta)t^4 - \frac{1}{720}\alpha(22\alpha^2 - 66\alpha\beta + 45\beta^2)t^6 - \dots \quad (3.63)$$

$$G = t - \frac{1}{6}\alpha t^3 - \frac{1}{120}\alpha(8\alpha - 9\beta)t^5 - \frac{1}{5040}\alpha(172\alpha^2 - 396\alpha\beta + 225\beta^2)t^7 - \dots \quad (3.64)$$

Finally, for the case of a parabolic orbit, where the initial state is given at periapsis so that $v = 0$, $\lambda = 0$, and $\beta = 2\alpha$; the time dependent Lagrange coefficients reduce to

$$F = 1 - \frac{1}{2}\alpha t^2 + \frac{1}{6}\alpha^2 t^4 - \frac{7}{72}\alpha^3 t^6 + \dots \quad (3.65)$$

$$G = t - \frac{1}{6}\alpha t^3 + \frac{1}{12}\alpha^2 t^5 - \frac{1}{18}\alpha^3 t^7 + \dots \quad (3.66)$$

Radius of Convergence

Implementing higher orders of the time dependent Lagrange coefficients will allow the outcomes of equation 3.46 to agree more closely with the results produced when the relative two-body problem is solved using the classical orbital element method or numerically integrated. However, there is a time interval beyond which the power series solution will diverge from the exact solution, regardless of the number of terms that are included when the Lagrange coefficients are calculated. This time interval is

called the Taylor series' radius of convergence. Fortunately, expressions for the radius of convergence have been developed. For elliptical orbits, the radius of convergence is given by

$$\tau_e = \sqrt{\frac{a^3}{\mu} \left\{ M_e^2 + \left[\ln \left(\frac{1 + \sqrt{1 - e^2}}{e} \right) - \sqrt{1 - e^2} \right]^2 \right\}} \quad (3.67)$$

where M_e is the elliptical orbit's mean anomaly,

$$M_e = E_0 - e \sin(E_0) \quad (3.68)$$

and E_0 is the eccentric anomaly corresponding to the initial state given by equation 3.22.

For parabolic orbits, the radius of convergence is given by

$$\tau_p = \sqrt{\frac{p^3}{3\mu} \left\{ 1 + 9 \left[\frac{1}{6} \tan^3 \left(\frac{v_0}{2} \right) + \frac{1}{2} \tan \left(\frac{v_0}{2} \right) \right]^2 \right\}} \quad (3.69)$$

Finally, for hyperbolic orbits, the radius of convergence is given by

$$\tau_h = \sqrt{\frac{-a^3}{\mu} \left\{ M_h^2 + \left[\sqrt{e^2 - 1} - \cos^{-1} \left(\frac{1}{e} \right) \right]^2 \right\}} \quad (3.70)$$

where the hyperbolic orbit's mean anomaly M_h is given by

$$M_h = e \sinh(E_h) - E_h \quad (3.71)$$

and the hyperbolic anomaly is defined as

$$E_h = 2 \tanh^{-1} \left[\sqrt{\frac{e-1}{e+1}} \tan\left(\frac{v_0}{2}\right) \right] \quad (3.72)$$

Using Power Series Solutions Iteratively

Even though the power series solution of the relative two-body problem has a finite radius of convergence, it can still be used iteratively to describe a complete trajectory. The author proposes the following algorithm to achieve this result for an elliptical trajectory with respect to the Earth. The same process can be used for parabolic and hyperbolic orbits. Given the period of the elliptical orbit, τ ; an initial relative position, $\Delta \bar{r}_0$; an initial relative velocity, $\Delta \bar{v}_0$; and a constant time step, Δt :

- ✱ The fundamental invariants (α , β , and λ) corresponding to the current state are computed using equations 3.35 and 3.37.
- ✱ The seventh-order Lagrange coefficients (F and G) are computed using equations 3.59 and 3.60.
- ✱ The seventh-order Lagrange coefficient rates (\dot{F} and \dot{G}) are evaluated by differentiating equations 3.59 and 3.60 with respect to time.
- ✱ The new position is evaluated using

$$\Delta \bar{r}_1 = F \Delta \bar{r}_0 + G \Delta \bar{v}_0 \quad (3.73)$$

- ✱ The new velocity is evaluated using

$$\Delta \bar{v}_1 = \dot{F} \Delta \bar{r}_0 + \dot{G} \Delta \bar{v}_0 \quad (3.74)$$

- ✱ The process is repeated for each new state for the remainder of the orbit's period.

Seventh-order Lagrange coefficients are being implemented in this algorithm because they return adequate results while maintaining a manageable polynomial size. Working

in the perifocal coordinate system shown in Figure 3.6, equations 3.27 and 3.28 illustrate that the relative position and velocity vectors are a function of the orbit's semi-parameter, true anomaly, and eccentricity,

$$\Delta \bar{r}_0 = \frac{p}{1 + e \cos(v)} [\cos(v) \hat{P} + \sin(v) \hat{Q}] \quad (3.75)$$

$$\Delta \bar{v}_0 = \sqrt{\frac{\mu}{p}} \{-\sin(v) \hat{P} + [e + \cos(v)] \hat{Q}\} \quad (3.76)$$

These two equations will be used to evaluate initial conditions for a numerical experiment involving the iterative algorithm just described. The test will analyze an elliptical orbit for a duration equaling the period τ using different time step sizes. The time steps are varied by 15-second intervals up to a maximum size of five minutes.

The experiment investigates an elliptical orbit with respect to the Earth ($\mu = 398,600 \text{ km}^3/\text{s}^2$) and assumes that the secondary body's gravitational parameter is equal to zero (a restricted two-body problem). The orbit's semi-parameter is ($p = 13,128 \text{ km}$) and its eccentricity is ($e = 0.966$). Its radius of periapsis is ($r_p = 6,678 \text{ km}$) and its radius of apoapsis is ($r_a = 384,400 \text{ km}$). This is equivalent to placing a satellite on a Hohmann transfer from low Earth orbit to the Moon and is shown in Figure 3.7. The blue sphere representing the Earth is drawn to scale.

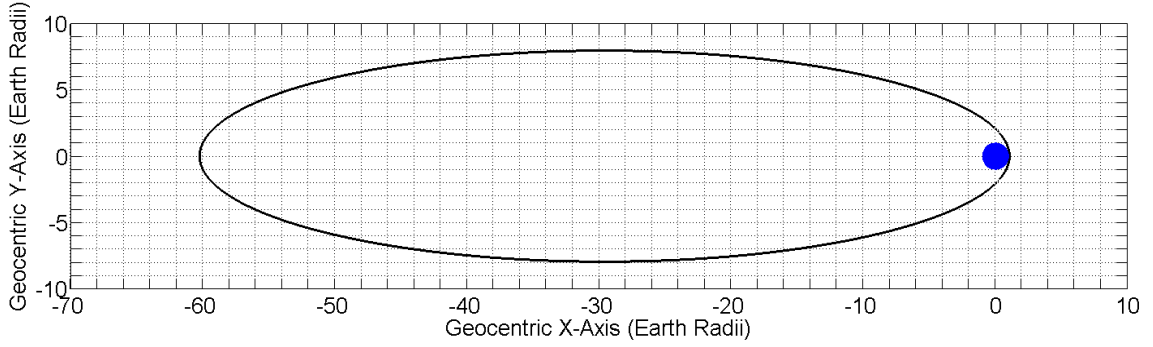


Figure 3.7: An Elliptical Orbit with Respect to the Earth

The satellite's initial position is at periaapsis $v = 0$, so it's initial conditions are

$$\Delta\bar{\mathbf{r}}_0 = r_p \hat{\mathbf{P}} \quad (3.77)$$

$$\Delta\bar{\mathbf{v}}_0 = (1+e) \sqrt{\frac{\mu}{p}} \hat{\mathbf{Q}} \quad (3.78)$$

Since the algorithm is evaluated for exactly the entire period of the elliptical orbit,

$$\tau = 2\pi \sqrt{\frac{a^3}{\mu}} \quad (3.79)$$

the correct final position should be equal to the initial position. However, the truncated Taylor series will produce a small amount of error after each time step. With this in mind, the final absolute error for each orbit analyzed is evaluated using

$$\text{Error} = \|\Delta\bar{\mathbf{r}}_0 - \Delta\bar{\mathbf{r}}_{\text{rk}}\| \quad (3.80)$$

where $\Delta\bar{\mathbf{r}}_{\text{rk}}$ is the final relative position vector returned by the seventh-order algorithm. Figure 3.8 shows the absolute error results (in Earth radii) obtained by this first

experiment and the computer time (in seconds) needed to integrate the orbit for each time step size.

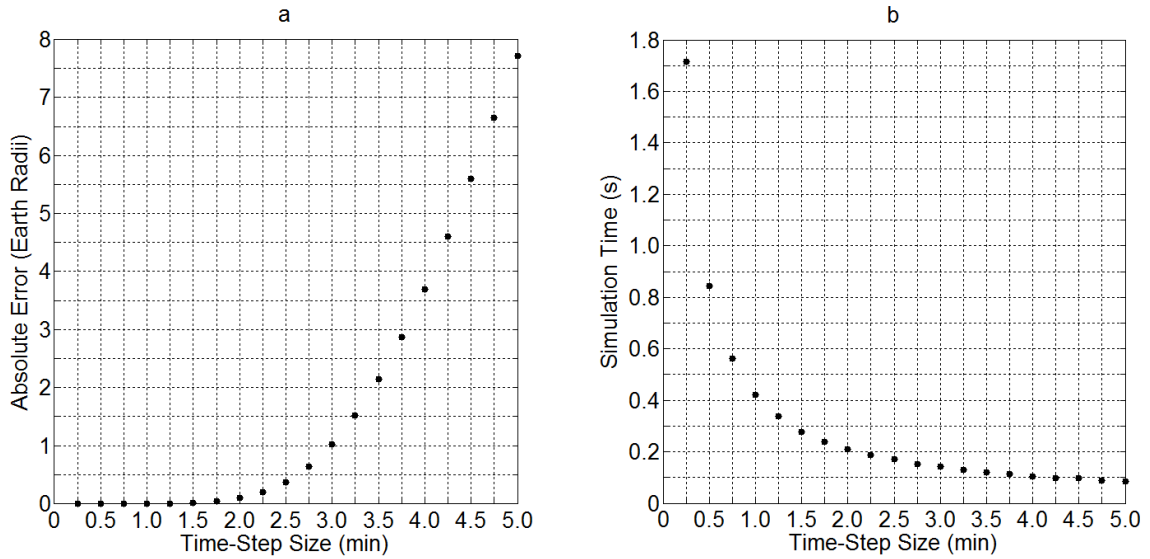


Figure 3.8: Absolute Error Results Using a Seventh-Order Iterative Power Series
a) Absolute Error, b) Simulation Time

Figure 3.8 shows that the power series solution of the relative two-body problem can be used iteratively to accurately describe an elliptical trajectory with a small computer time. As will be shown in the following chapters, this iterative procedure can be extended to the problem of N-bodies while maintaining the short computer time requirements.

NUMERICAL INTEGRATION SOLUTIONS

A useful solution alternative that can also be extended to the problem of N-bodies is to numerically integrate the equations of motion. As was stated earlier, the relative two-body problem is a nonlinear, coupled, space dependent system of ordinary differential equations. This nonlinear characteristic is the principle reason why it is difficult to derive an explicit, time dependent, analytic solution. Several approximation

techniques have been developed over the years to numerically integrate nonlinear, initial value problems such as the relative two-body problem and the N-body problem. For the purpose of this dissertation, the fourth-order and fifth-order Runge-Kutta numerical integration algorithms (RK4 and RK5, respectively) will be used as a benchmark to develop accurate orbital trajectories in both the relative two-body problem and the N-body problem [73-74]. These two numerical integration algorithms can achieve the accuracy of a Taylor series expansion without requiring the calculation of derivatives beyond the first.

Runge-Kutta 4

Beginning with the relative two-body problem given by equation 3.3,

$$\ddot{\vec{r}}_2 - \ddot{\vec{r}}_1 = -\frac{(\mu_1 + \mu_2)(\vec{r}_2 - \vec{r}_1)}{\|\vec{r}_2 - \vec{r}_1\|^3} \rightarrow \Delta\ddot{\vec{r}} = -\frac{\mu\Delta\vec{r}}{\Delta r^3} \quad (3.81)$$

its numerical integration using RK4 with step-size Δt is represented as

$$\Delta\vec{r}_1 = \Delta\vec{r}_0 + \vec{f} \quad (3.82)$$

$$\Delta\vec{v}_1 = \Delta\vec{v}_0 + \vec{g} \quad (3.83)$$

where the increment functions \vec{f} and \vec{g} are defined as

$$\vec{f} = \frac{1}{6}(\vec{f}_1 + 2\vec{f}_2 + 2\vec{f}_3 + \vec{f}_4) \quad (3.84)$$

$$\vec{g} = \frac{1}{6}(\vec{g}_1 + 2\vec{g}_2 + 2\vec{g}_3 + \vec{g}_4) \quad (3.85)$$

The vectors \bar{f}_1 through \bar{f}_4 and \bar{g}_1 through \bar{g}_4 are known as:

- * The initial estimate of the new position, \bar{f}_1 ;
- * The initial estimate of the new velocity, \bar{g}_1 ;
- * The first midpoint estimate of the new position, \bar{f}_2 ;
- * The first midpoint estimate of the new velocity, \bar{g}_2 ;
- * The second midpoint estimate of the new position, \bar{f}_3 ;
- * The second midpoint estimate of the new velocity, \bar{g}_3 ;
- * The endpoint estimate of the new position, \bar{f}_4 ;
- * The endpoint estimate of the new velocity, \bar{g}_4 ;

and are respectively defined as (where curly brackets imply “a function of”)

$$\bar{f}_1 = \Delta t \cdot \Delta \bar{v}_0 \quad (3.86)$$

$$\bar{g}_1 = \Delta t \cdot \Delta \ddot{\bar{r}} \{ \Delta \bar{r}_0 \} \quad (3.87)$$

$$\bar{f}_2 = \Delta t \cdot \left(\Delta \bar{v}_0 + \frac{1}{2} \bar{g}_1 \right) \quad (3.88)$$

$$\bar{g}_2 = \Delta t \cdot \Delta \ddot{\bar{r}} \left\{ \Delta \bar{r}_0 + \frac{1}{2} \bar{f}_1 \right\} \quad (3.89)$$

$$\bar{f}_3 = \Delta t \cdot \left(\Delta \bar{v}_0 + \frac{1}{2} \bar{g}_2 \right) \quad (3.90)$$

$$\bar{g}_3 = \Delta t \cdot \Delta \ddot{\bar{r}} \left\{ \Delta \bar{r}_0 + \frac{1}{2} \bar{f}_2 \right\} \quad (3.91)$$

$$\bar{f}_4 = \Delta t \cdot (\Delta \bar{v}_0 + \bar{g}_3) \quad (3.92)$$

$$\bar{g}_4 = \Delta t \cdot \Delta \bar{r} \{ \Delta \bar{r}_0 + \bar{f}_3 \} \quad (3.93)$$

The elliptical orbit numerical experiment performed earlier using the iterative power series solution of the relative two-body problem is now repeated using RK4. Figure 3.9 shows the absolute error results returned by this investigation.

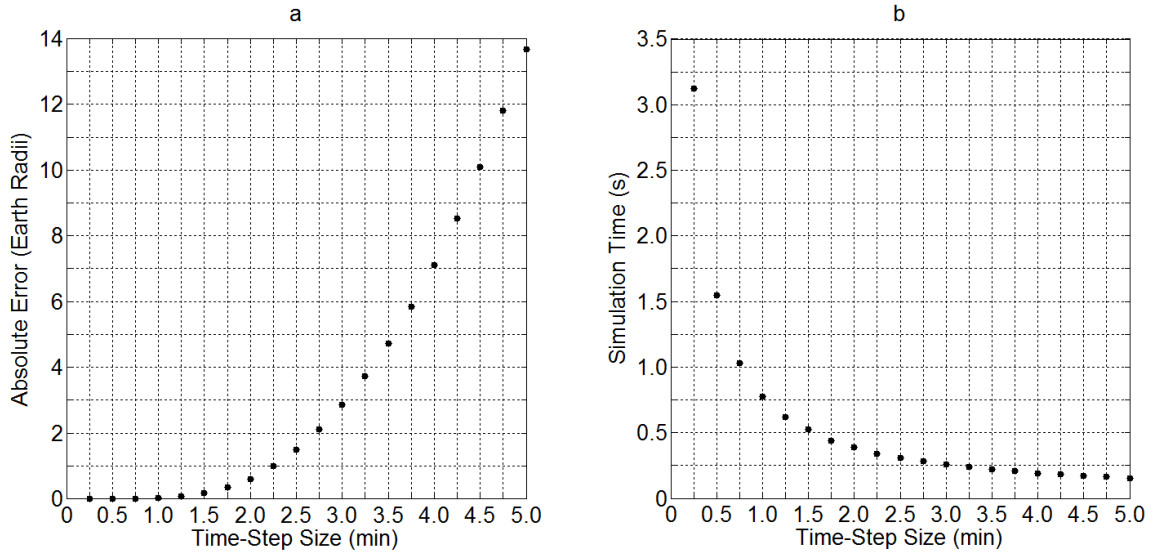


Figure 3.9: Absolute Error Results Using RK4
a) Absolute Error, b) Simulation Time

Runge-Kutta 5

Beginning with the relative two-body problem given by equation (3.81), its numerical integration using RK5 with step-size Δt is represented as

$$\Delta \bar{r}_1 = \Delta \bar{r}_0 + \bar{f} \quad (3.94)$$

$$\Delta \bar{v}_1 = \Delta \bar{v}_0 + \bar{g} \quad (3.95)$$

where the increment functions \bar{f} and \bar{g} are defined as

$$\bar{f} = \frac{1}{90} (7\bar{f}_1 + 32\bar{f}_3 + 12\bar{f}_4 + 32\bar{f}_5 + 7\bar{f}_6) \quad (3.96)$$

$$\bar{g} = \frac{1}{90} (7\bar{g}_1 + 32\bar{g}_3 + 12\bar{g}_4 + 32\bar{g}_5 + 7\bar{g}_6) \quad (3.97)$$

The vectors \bar{f}_1 through \bar{f}_6 and \bar{g}_1 through \bar{g}_6 are known as:

- * The initial estimate of the new position, \bar{f}_1 ;
- * The initial estimate of the new velocity, \bar{g}_1 ;
- * The first midpoint estimate of the new position, \bar{f}_2 ;
- * The first midpoint estimate of the new velocity, \bar{g}_2 ;
- * The second midpoint estimate of the new position, \bar{f}_3 ;
- * The second midpoint estimate of the new velocity, \bar{g}_3 ;
- * The third midpoint estimate of the new position, \bar{f}_4 ;
- * The third midpoint estimate of the new velocity, \bar{g}_4 ;
- * The fourth midpoint estimate of the new position, \bar{f}_5 ;
- * The fourth midpoint estimate of the new velocity, \bar{g}_5 ;
- * The endpoint estimate of the new position, \bar{f}_6 ;
- * The endpoint estimate of the new velocity, \bar{g}_6 ;

and are respectively defined as (where curly brackets imply “a function of”)

$$\bar{f}_1 = \Delta t \cdot \Delta \bar{v}_0 \quad (3.98)$$

$$\bar{g}_1 = \Delta t \cdot \Delta \ddot{r} \{ \Delta \bar{r}_0 \} \quad (3.99)$$

$$\bar{\mathbf{f}}_2 = \Delta t \cdot \left(\Delta \bar{\mathbf{v}}_0 + \frac{1}{4} \bar{\mathbf{g}}_1 \right) \quad (3.100)$$

$$\bar{\mathbf{g}}_2 = \Delta t \cdot \Delta \bar{\mathbf{r}} \ddot{\left\{ \Delta \bar{\mathbf{r}}_0 + \frac{1}{4} \bar{\mathbf{f}}_1 \right\}} \quad (3.101)$$

$$\bar{\mathbf{f}}_3 = \Delta t \cdot \left(\Delta \bar{\mathbf{v}}_0 + \frac{1}{8} \bar{\mathbf{g}}_1 + \frac{1}{8} \bar{\mathbf{g}}_2 \right) \quad (3.102)$$

$$\bar{\mathbf{g}}_3 = \Delta t \cdot \Delta \bar{\mathbf{r}} \ddot{\left\{ \Delta \bar{\mathbf{r}}_0 + \frac{1}{8} \bar{\mathbf{f}}_1 + \frac{1}{8} \bar{\mathbf{f}}_2 \right\}} \quad (3.103)$$

$$\bar{\mathbf{f}}_4 = \Delta t \cdot \left(\Delta \bar{\mathbf{v}}_0 - \frac{1}{2} \bar{\mathbf{g}}_2 + \bar{\mathbf{g}}_3 \right) \quad (3.104)$$

$$\bar{\mathbf{g}}_4 = \Delta t \cdot \Delta \bar{\mathbf{r}} \ddot{\left\{ \Delta \bar{\mathbf{r}}_0 - \frac{1}{2} \bar{\mathbf{f}}_2 + \bar{\mathbf{f}}_3 \right\}} \quad (3.105)$$

$$\bar{\mathbf{f}}_5 = \Delta t \cdot \left(\Delta \bar{\mathbf{v}}_0 + \frac{3}{16} \bar{\mathbf{g}}_1 + \frac{9}{16} \bar{\mathbf{g}}_4 \right) \quad (3.106)$$

$$\bar{\mathbf{g}}_5 = \Delta t \cdot \Delta \bar{\mathbf{r}} \ddot{\left\{ \Delta \bar{\mathbf{r}}_0 + \frac{3}{16} \bar{\mathbf{f}}_1 + \frac{9}{16} \bar{\mathbf{f}}_4 \right\}} \quad (3.107)$$

$$\bar{\mathbf{f}}_6 = \Delta t \cdot \left(\Delta \bar{\mathbf{v}}_0 - \frac{3}{7} \bar{\mathbf{g}}_1 + \frac{2}{7} \bar{\mathbf{g}}_2 + \frac{12}{7} \bar{\mathbf{g}}_3 - \frac{12}{7} \bar{\mathbf{g}}_4 + \frac{8}{7} \bar{\mathbf{g}}_5 \right) \quad (3.108)$$

$$\bar{\mathbf{g}}_6 = \Delta t \cdot \Delta \bar{\mathbf{r}} \ddot{\left\{ \Delta \bar{\mathbf{r}}_0 - \frac{3}{7} \bar{\mathbf{f}}_1 + \frac{2}{7} \bar{\mathbf{f}}_2 + \frac{12}{7} \bar{\mathbf{f}}_3 - \frac{12}{7} \bar{\mathbf{f}}_4 + \frac{8}{7} \bar{\mathbf{f}}_5 \right\}} \quad (3.109)$$

The elliptical orbit numerical experiment performed earlier using the iterative power series solution of the relative two-body problem and RK4 is now repeated a second time using RK5. Figure 3.10 shows the absolute error results returned by this investigation.

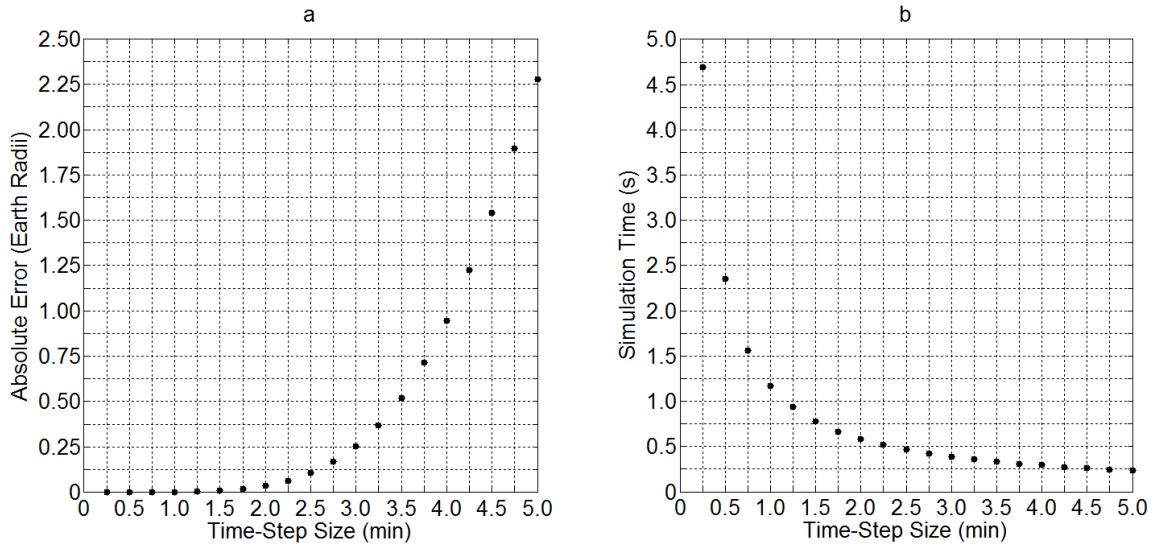


Figure 3.10: Absolute Error Results Using RK5
a) Absolute Error, b) Simulation Time

A Variable Time Step Runge-Kutta Algorithm

The fourth-order and fifth-order Runge-Kutta numerical integration algorithms (RK4 and RK5, respectively) described above can be used to develop a numerical integrator that automatically adjusts the time step size being used during the course of a computation. This process allows the integrator’s accuracy to increase by focusing its full computational power on portions of the satellite trajectory where significant changes occur (small time steps) and reducing this focus when the satellite experiences little change in its motion (large time steps). What results is a highly efficient procedure that gives the trajectory designer the ability to analyze an N-body problem scenario with much less computer time than is required by a constant time step integrator while maintaining a considerable amount of accuracy. Many variable time step integrators have been developed over the years because they are more reliable than their constant time step counterparts. The author proposes the following variable time step numerical

integration algorithm. Given a simulation time, τ , an initial relative position, $\Delta\bar{r}_0$, and initial relative velocity, $\Delta\bar{v}_0$, an initial time step size, Δt , and a tolerance, T:

- * Evaluate a new state using RK4.
- * Evaluate a new state using RK5.
- * Determine the deviation between RK4 and RK5 using

$$\text{Deviation} = \|\Delta\bar{r}_{\text{RK5}} - \Delta\bar{r}_{\text{RK4}}\| \quad (3.110)$$

- * If the deviation is greater than the tolerance, decrease the size of the current time step by dividing it by two and return to the first step of the algorithm.
- * If the deviation is less than the tolerance, the state returned by RK5 is the new relative position and velocity,

$$\Delta\bar{r}_1 = \Delta\bar{r}_{\text{RK5}} \quad (3.111)$$

$$\Delta\bar{v}_1 = \Delta\bar{v}_{\text{RK5}} \quad (3.112)$$

- * Increase the size of the current time step by multiplying it by two.
- * Repeat the entire process for the next state until the simulation time, τ , has been reached.

This algorithm will be used for the remainder of this dissertation to make a direct comparison between the capabilities of the Runge-Kutta methods and the processes that will be developed by the author. To see how well this variable time step algorithm actually performs, the highly elliptical trajectory is revisited. However, because the amount of computer time needed to analyze the entire trajectory is greatly diminished by the variable time step procedure, the following analysis will investigate the absolute error

obtained in intervals of time equal to the orbit's period. Since the satellite's relative position after each orbital period should be equal to the initial position, the absolute error after each period is once again evaluated using equation 3.80. Figures 3.11 and 3.12 show these absolute error results and the computer time needed to analyze the multiple orbital periods when tolerances of 10^{-6} km and 10^{-7} km are used.

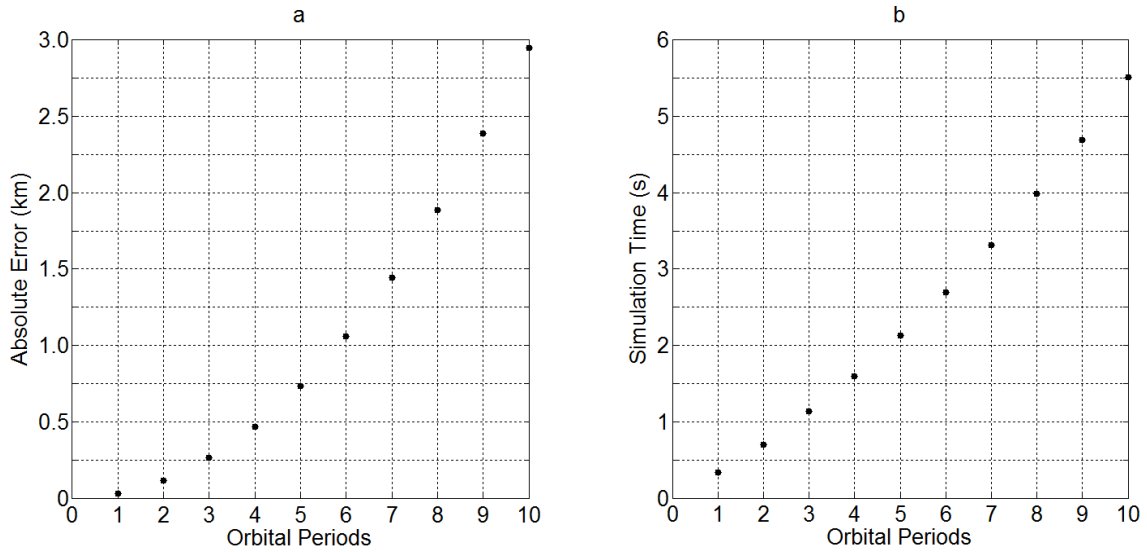


Figure 3.11: Absolute Error Results Using RK45 with a 10^{-6} Tolerance
a) Absolute Error, b) Simulation Time

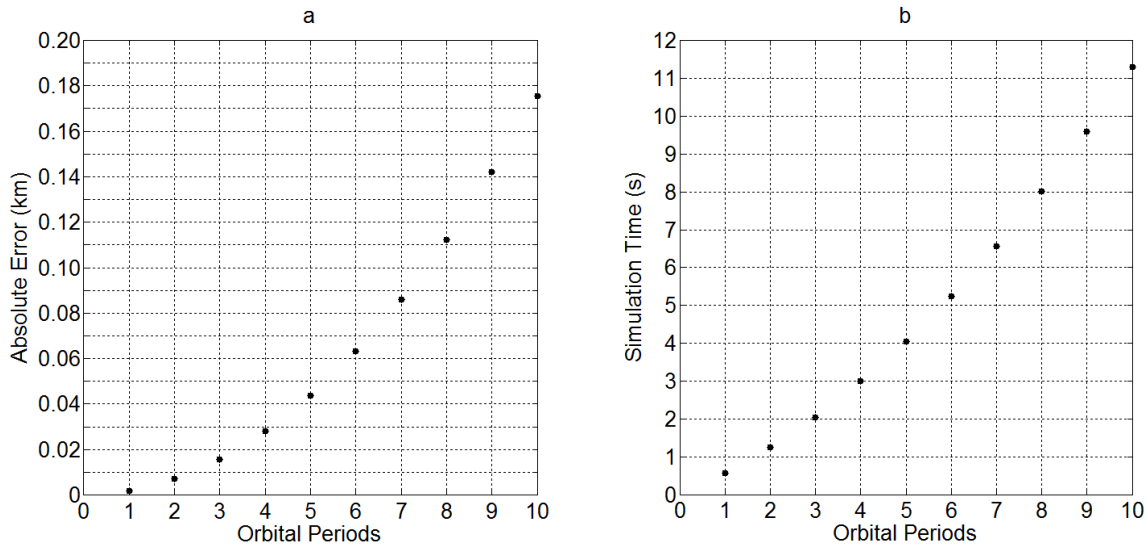


Figure 3.12: Absolute Error Results Using RK45 with a 10^{-7} Tolerance
a) Absolute Error, b) Simulation Time

These two figures demonstrate that the variable time step RK45 numerical integrator is both very accurate and very efficient. However, the author will derive two new methods that are both more accurate and much more efficient than RK45 in the following chapter.

DISCUSSION

As can be seen from the radius of convergence expressions given by equations 3.67-3.72, the accuracy of the power series solution derived for the relative two-body problem is extremely limited. For example, the radius of convergence of the power series solution for the elliptical orbit analyzed in this chapter is approximately 2,266 seconds. This is only 0.26% of the actual orbital period. However, Figures 3.8-3.10 demonstrate that the power series solution of the relative two-body problem can be used iteratively to determine future states for any type of orbit with results that are more accurate than RK4 and slightly less accurate than RK5. The results show that as time step size increases, the absolute error returned by any of the three processes also increases. The computer time needed to propagate the orbit decreases as time step size increases. This is an expected outcome. The important result obtained from this investigation is that the iterative power series process has the benefit of being able to predict a future state with less computer time than is required by either RK4 or RK5.

CHAPTER 4

NEW SOLUTIONS OF THE TWO-BODY PROBLEM

In this chapter, the relative two-body problem is transformed into a time dependent system using the power series solutions derived in Chapter 3. A fourth-order, analytic solution is derived for the transformed system and the result is shown to be a useful alternative to the universal form of Kepler's equation when working in any coordinate system. A fifth order solution is derived for the case when a vehicle is initially located at the periapsis of a parabolic orbit. Two methods are proposed to solve the transformed problem when higher-order coefficients are implemented. Finally, all of these results are used to develop two new variable time step propagators that are more accurate and more efficient than the variable time step Runge-Kutta numerical integrator.

A NEW TIME TRANSFORMATION

The relative two-body problem described by equation 3.3 is a function of the second body's position with respect to the first. Additionally, equation 3.46 shows how the solution of the relative two-body problem can be stated in terms of a time dependent Taylor series expansion whose radius of convergence is finite. Substituting equation 3.46 into equation 3.3 and simplifying yields

$$\begin{aligned}
\Delta \ddot{\vec{r}} &= -\frac{\mu \Delta \vec{r}}{\Delta r^3} \\
&= -\frac{\mu(F\Delta \vec{r}_0 + G\Delta \vec{v}_0)}{\|F\Delta \vec{r}_0 + G\Delta \vec{v}_0\|^3} \\
&= -\frac{\mu(F\Delta \vec{r}_0 + G\Delta \vec{v}_0)}{\left[F^2 \Delta r_0^2 + 2FG(\Delta \vec{r}_0 \cdot \Delta \vec{v}_0) + G^2 \Delta v_0^2\right]^{3/2}} \\
&= -\frac{\mu(F\Delta \vec{r}_0 + G\Delta \vec{v}_0)}{\Delta r_0^3 (F^2 + 2\lambda FG + \beta G^2)^{3/2}} \\
&= -\frac{\alpha(F\Delta \vec{r}_0 + G\Delta \vec{v}_0)}{(F^2 + 2\lambda FG + \beta G^2)^{3/2}}
\end{aligned} \tag{4.1}$$

This process transforms the relative two-body problem from a nonlinear, coupled, space dependent vector differential equation to a linear, uncoupled, time dependent vector differential equation whose solution can be stated as

$$\Delta \vec{r} = -\alpha \iint \frac{F\Delta \vec{r}_0 + G\Delta \vec{v}_0}{(F^2 + 2\lambda FG + \beta G^2)^{3/2}} dt^2 + t\bar{c}_1 + \bar{c}_2 \tag{4.2}$$

$$\Delta \vec{v} = -\alpha \int \frac{F\Delta \vec{r}_0 + G\Delta \vec{v}_0}{(F^2 + 2\lambda FG + \beta G^2)^{3/2}} dt + \bar{c}_1 \tag{4.3}$$

where \bar{c}_1 and \bar{c}_2 are vector constants of integration.

A FOURTH ORDER SOLUTION OF THE TWO BODY PROBLEM

Equation 4.1 can be solved analytically if first-order Lagrange coefficients are used. For this case, equation 3.46 can be written as the sum of the secondary body's initial position and the product of time with its initial velocity,

$$\Delta \vec{r} = F\Delta \vec{r}_0 + G\Delta \vec{v}_0 = \Delta \vec{r}_0 + t\Delta \vec{v}_0 \tag{4.4}$$

Substituting equation 4.4 into equation 4.1 yields

$$\Delta\ddot{\mathbf{r}} = -\frac{\alpha(F\Delta\bar{\mathbf{r}}_0 + G\Delta\bar{\mathbf{v}}_0)}{(F^2 + 2\lambda FG + \beta G^2)^{3/2}} = -\frac{\alpha(\Delta\bar{\mathbf{r}}_0 + t\Delta\bar{\mathbf{v}}_0)}{(1 + 2\lambda t + \beta t^2)^{3/2}} \quad (4.5)$$

This is a linear, uncoupled vector differential equation that is dependent on time and independent of space. Defining the lower-case gamma polynomial, γ , as the cube root of the denominator in equation 4.5 such that

$$\gamma(t) = \sqrt[3]{F^2 + 2\lambda FG + \beta G^2} = \sqrt[3]{1 + 2\lambda t + \beta t^2} \quad (4.6)$$

equation 4.5 can be rewritten as

$$\Delta\ddot{\mathbf{r}} = -\frac{\alpha(\Delta\bar{\mathbf{r}}_0 + t\Delta\bar{\mathbf{v}}_0)}{\gamma^3} \quad (4.7)$$

and the secondary body's velocity can be found by integrating both sides of equation 4.7,

$$\Delta\bar{\mathbf{v}}(t) = \frac{\alpha}{\gamma} \left[\frac{(\lambda + \beta t)\Delta\bar{\mathbf{r}}_0 - (1 + \lambda t)\Delta\bar{\mathbf{v}}_0}{\lambda^2 - \beta} \right] + \bar{\mathbf{c}}_1 \quad (4.8)$$

where $\bar{\mathbf{c}}_1$ is the first vector constant of integration. The value of this constant of integration is determined by substituting the initial conditions given by equation 3.8 into equation 4.8 and then simplifying,

$$\bar{\mathbf{c}}_1 = -\left(\frac{\alpha\lambda}{\lambda^2 - \beta} \right) \Delta\bar{\mathbf{r}}_0 + \left(\frac{\alpha + \lambda^2 - \beta}{\lambda^2 - \beta} \right) \Delta\bar{\mathbf{v}}_0 \quad (4.9)$$

Substituting equation 4.9 into equation 4.8 and then simplifying yields the unique relative velocity as a function of time,

$$\Delta\bar{v}(t) = \frac{\alpha}{\gamma} \left[\frac{\beta t + \lambda(1-\gamma)}{\lambda^2 - \beta} \right] \Delta\bar{r}_0 + \left[1 - \frac{\alpha}{\gamma} \left(\frac{\lambda t + 1 - \gamma}{\lambda^2 - \beta} \right) \right] \Delta\bar{v}_0 \quad (4.10)$$

The relative position can now be determined by integrating both sides of equation 4.10,

$$\Delta\bar{r}(t) = \alpha \left(\frac{\gamma - \lambda t}{\lambda^2 - \beta} \right) \Delta\bar{r}_0 + \left[\left(\frac{\alpha + \lambda^2 - \beta}{\lambda^2 - \beta} \right) t - \frac{\alpha\lambda}{\beta} \left(\frac{\gamma}{\lambda^2 - \beta} \right) + \frac{\alpha}{\beta^{3/2}} \ln(\lambda + \beta t + \sqrt{\beta}\gamma) \right] \Delta\bar{v}_0 + \bar{c}_2 \quad (4.11)$$

where \bar{c}_2 is the second vector constant of integration. The value of this constant of integration is determined by substituting the initial conditions given by equation 3.8 into equation 4.11 and then simplifying,

$$\bar{c}_2 = \left(1 - \frac{\alpha}{\lambda^2 - \beta} \right) \Delta\bar{r}_0 + \left[\frac{\alpha}{\beta} \left(\frac{\lambda}{\lambda^2 - \beta} \right) - \frac{\alpha}{\beta^{3/2}} \ln(\lambda + \sqrt{\beta}) \right] \Delta\bar{v}_0 \quad (4.12)$$

Substituting equation 4.12 into equation 4.11 and then simplifying yields the unique relative position as a function of time,

$$\Delta\bar{r}(t) = \left[1 - \frac{\alpha(\lambda t + 1 - \gamma)}{\lambda^2 - \beta} \right] \Delta\bar{r}_0 + \left[\frac{\alpha\lambda}{\beta} \left(\frac{1 - \gamma}{\lambda^2 - \beta} \right) + \left(1 + \frac{\alpha}{\lambda^2 - \beta} \right) t + \frac{\alpha}{\beta^{3/2}} \ln \left(\frac{\lambda + \beta t + \sqrt{\beta}\gamma}{\lambda + \sqrt{\beta}} \right) \right] \Delta\bar{v}_0 \quad (4.13)$$

With these results, the first-order state of the secondary body's relative motion can be written as

$$\Delta\bar{s}(t) = \Phi \Delta\bar{s}_0 \rightarrow \begin{Bmatrix} \Delta\bar{r} \\ \Delta\bar{v} \end{Bmatrix} = \begin{bmatrix} \tilde{\mathbf{F}}_{3 \times 3} & \tilde{\mathbf{G}}_{3 \times 3} \\ \tilde{\mathbf{F}}_{3 \times 3} & \tilde{\mathbf{G}}_{3 \times 3} \end{bmatrix} \begin{Bmatrix} \Delta\bar{r}_0 \\ \Delta\bar{v}_0 \end{Bmatrix} \quad (4.14)$$

where $\mathbf{I}_{3 \times 3}$ is a 3x3 identity matrix and the modified Lagrange coefficients $\tilde{\mathbf{F}}$, $\tilde{\mathbf{G}}$, and their respective derivatives are defined as

$$\tilde{F} = 1 - \frac{\alpha(\lambda t + 1 - \gamma)}{\lambda^2 - \beta} \quad (4.15)$$

$$\tilde{G} = \frac{\alpha\lambda}{\beta} \left(\frac{1-\gamma}{\lambda^2 - \beta} \right) + \left(1 + \frac{\alpha}{\lambda^2 - \beta} \right) t + \frac{\alpha}{\beta^{3/2}} \ln \left(\frac{\lambda + \beta t + \sqrt{\beta\gamma}}{\lambda + \sqrt{\beta}} \right) \quad (4.16)$$

$$\dot{\tilde{F}} = \frac{\alpha}{\gamma} \left[\frac{\beta t + \lambda(1-\gamma)}{\lambda^2 - \beta} \right] \quad (4.17)$$

$$\dot{\tilde{G}} = 1 - \frac{\alpha}{\gamma} \left(\frac{\lambda t + 1 - \gamma}{\lambda^2 - \beta} \right) \quad (4.18)$$

Equation 4.14 and its components given by equations 4.15-4.18 can be looked at as a universal substitute to Kepler's equation. A future state can be determined by using this expression in a recursive manner similar to the process outlined for the power series solution of the relative two-body problem in the previous chapter. The term universal is used to imply that it applies to any type of orbit that is governed by the relative two-body problem. Although a universal variable formulation has been developed for Kepler's equation, its results correspond to the perifocal coordinate system [75]. If a future state is desired with respect to an inertial coordinate system, the classical orbital element procedure also outlined in the previous chapter must be used after the universal variable Kepler's equation has been solved iteratively. Equation 4.14 bypasses all of these requirements and returns a future state in inertial coordinates in a couple of iterations, depending on the size of the time interval.

The accuracy of the results returned by equation 4.14 approaches the accuracy of a fourth-order power series solution of the relative two-body problem. This can be seen by finding the Taylor series expansion of equation 4.13,

$$\sum_{k=0}^{\infty} \frac{t^k}{k!} \frac{\partial^k \Delta r(t)}{\partial t^k} \Big|_{t=0} = \left[1 - \frac{1}{2} \alpha t^2 + \frac{1}{2} \alpha \lambda t^3 + \frac{1}{8} \alpha (\beta - 5\lambda^2) t^4 + \dots \right] \Delta \bar{r}_0 + \left(t - \frac{1}{6} \alpha t^3 + \frac{1}{4} \alpha \lambda t^4 + \dots \right) \Delta \bar{v}_0 \quad (4.19)$$

Comparing this result to the Lagrange coefficient terms of equations 3.59 and 3.60, a fourth-order accurate iteration time can be derived by subtracting equation 4.19 from the fourth-order form of equation 3.46,

$$\Delta t = \sqrt[4]{\frac{12T}{\alpha^2 \Delta r_0}} \quad (4.20)$$

where T is a user defined tolerance with units of length. In other words, if equation 4.14 is to be used as a substitute to Kepler's equation, a new state should be computed every Δt time given by equation 4.20 until the final state corresponding to the propagation time required is obtained.

A FIFTH ORDER SOLUTION FOR PARABOLIC ORBITS

Equation 4.1 can also be solved analytically if second order Lagrange coefficients are used and the secondary body is assumed to be initially located at the periapsis of a parabolic orbit with respect to the primary. With these assumptions, equation 3.46 can be written as,

$$\Delta\bar{r} = F\Delta\bar{r}_0 + G\Delta\bar{v}_0 = \left(1 - \frac{1}{2}\alpha t^2\right)\Delta\bar{r}_0 + t\Delta\bar{v}_0 \quad (4.21)$$

Substituting equation 4.21 into equation 4.1 yields

$$\Delta\ddot{\bar{r}} = -\frac{\alpha(F\Delta\bar{r}_0 + G\Delta\bar{v}_0)}{(F^2 + 2\lambda FG + \beta G^2)^{3/2}} = -\frac{\alpha\left[\left(1 - \frac{1}{2}\alpha t^2\right)\Delta\bar{r}_0 + t\Delta\bar{v}_0\right]}{\left[\left(1 - \frac{1}{2}\alpha t^2\right)^2 + 2\lambda\left(1 - \frac{1}{2}\alpha t^2\right)t + \beta t^2\right]^{3/2}} \quad (4.22)$$

Recall that for a parabolic orbit, $\beta = 2\alpha$, and $\lambda = 0$ at periapsis. With these definitions, equation 4.22 reduces to

$$\Delta\ddot{\bar{r}} = -\frac{\alpha\left[\left(1 - \frac{1}{2}\alpha t^2\right)\Delta\bar{r}_0 + t\Delta\bar{v}_0\right]}{\left[\left(1 - \frac{1}{2}\alpha t^2\right)^2 + 2\alpha t^2\right]^{3/2}} \quad (4.23)$$

which can be simplified to

$$\Delta\ddot{\bar{r}} = -\frac{4\alpha\left[(2 - \alpha t^2)\Delta\bar{r}_0 + 2t\Delta\bar{v}_0\right]}{(2 + \alpha t^2)^3} \quad (4.24)$$

Integrating both sides of equation 4.24 with respect to time yields the relative velocity,

$$\Delta\bar{v} = -\frac{1}{4}\alpha\left[\frac{2t(6 + \alpha t^2)}{(2 + \alpha t^2)^2} + \sqrt{\frac{2}{\alpha}}\tan^{-1}\left(t\sqrt{\frac{\alpha}{2}}\right)\right]\Delta\bar{r}_0 + \frac{2\Delta\bar{v}_0}{(2 + \alpha t^2)^2} + \bar{c}_1 \quad (4.25)$$

Applying initial conditions to equation 4.25 and simplifying yields the value of the first constant of integration,

$$\bar{c}_1 = \frac{1}{2} \Delta \bar{v}_0 \quad (4.26)$$

Substituting equation 4.26 into equation 4.25 and simplifying yields the unique relative velocity

$$\Delta \bar{v} = -\frac{1}{4} \alpha \left[\frac{2t(6 + \alpha t^2)}{(2 + \alpha t^2)^2} + \sqrt{\frac{2}{\alpha}} \tan^{-1} \left(t \sqrt{\frac{\alpha}{2}} \right) \right] \Delta \bar{r}_0 + \left[\frac{(2 + \alpha t^2)^2 + 4}{2(2 + \alpha t^2)^2} \right] \Delta \bar{v}_0 \quad (4.27)$$

Integrating both sides of equation 4.27 with respect to time yields the relative position,

$$\Delta \bar{r} = \frac{1}{4} \alpha \left[\frac{4}{\alpha(2 + \alpha t^2)} - t \sqrt{\frac{2}{\alpha}} \tan^{-1} \left(t \sqrt{\frac{\alpha}{2}} \right) \right] \Delta \bar{r}_0 + \frac{1}{2} \left[\frac{t(3 + \alpha t^2)}{2 + \alpha t^2} + \frac{1}{\sqrt{2\alpha}} \tan^{-1} \left(t \sqrt{\frac{\alpha}{2}} \right) \right] \Delta \bar{v}_0 + \bar{c}_2 \quad (4.28)$$

Applying initial conditions to equation 4.28 and simplifying yields the value of the second constant of integration,

$$\bar{c}_2 = \frac{1}{2} \Delta \bar{r}_0 \quad (4.29)$$

Substituting equation 4.29 into equation 4.28 and simplifying yields the unique relative position,

$$\Delta \bar{r} = \frac{1}{2} \left[\frac{4 + \alpha t^2}{(2 + \alpha t^2)} - \frac{\alpha t}{2} \sqrt{\frac{2}{\alpha}} \tan^{-1} \left(t \sqrt{\frac{\alpha}{2}} \right) \right] \Delta \bar{r}_0 + \frac{1}{2} \left[\frac{t(3 + \alpha t^2)}{2 + \alpha t^2} + \frac{1}{\sqrt{2\alpha}} \tan^{-1} \left(t \sqrt{\frac{\alpha}{2}} \right) \right] \Delta \bar{v}_0 \quad (4.30)$$

With these results, the second order state of the secondary body's relative motion can be written as

$$\Delta\bar{s}(t) = \Phi\Delta\bar{s}_0 \rightarrow \begin{Bmatrix} \Delta\bar{r} \\ \Delta\bar{v} \end{Bmatrix} = \begin{bmatrix} \tilde{\mathbf{F}}_{3 \times 3} & \tilde{\mathbf{G}}_{3 \times 3} \\ \tilde{\dot{\mathbf{F}}}_{3 \times 3} & \tilde{\dot{\mathbf{G}}}_{3 \times 3} \end{bmatrix} \begin{Bmatrix} \Delta\bar{r}_0 \\ \Delta\bar{v}_0 \end{Bmatrix} \quad (4.31)$$

where the modified Lagrange coefficients $\tilde{\mathbf{F}}$, $\tilde{\mathbf{G}}$, and their respective derivatives are defined as

$$\tilde{\mathbf{F}} = \frac{1}{2} \left[\frac{4 + \alpha t^2}{(2 + \alpha t^2)} - \frac{\alpha t}{2} \sqrt{\frac{2}{\alpha}} \tan^{-1} \left(t \sqrt{\frac{\alpha}{2}} \right) \right] \quad (4.32)$$

$$\tilde{\mathbf{G}} = \frac{1}{2} \left[\frac{t(3 + \alpha t^2)}{2 + \alpha t^2} + \frac{1}{\sqrt{2\alpha}} \tan^{-1} \left(t \sqrt{\frac{\alpha}{2}} \right) \right] \quad (4.33)$$

$$\dot{\tilde{\mathbf{F}}} = -\frac{1}{4} \alpha \left[\frac{2t(6 + \alpha t^2)}{(2 + \alpha t^2)^2} + \sqrt{\frac{2}{\alpha}} \tan^{-1} \left(t \sqrt{\frac{\alpha}{2}} \right) \right] \quad (4.34)$$

$$\dot{\tilde{\mathbf{G}}} = \frac{(2 + \alpha t^2)^2 + 4}{2(2 + \alpha t^2)^2} \quad (4.35)$$

The accuracy of the results returned by equation 4.31 approaches the accuracy of a fifth order power series solution of the relative two-body problem. This can be seen by finding the Taylor series expansion of equation 4.30,

$$\begin{aligned} \sum_{k=0}^{\infty} \frac{t^k}{k!} \left. \frac{\partial^k \Delta\mathbf{r}(t)}{\partial t^k} \right|_{t=0} &= \left[1 - \frac{1}{2} \alpha t^2 + \frac{1}{6} \alpha^2 t^4 - \dots \right] \Delta\bar{r}_0 \\ &+ \left(t - \frac{1}{6} \alpha t^3 + \frac{3}{40} \alpha^2 t^5 - \dots \right) \Delta\bar{v}_0 \end{aligned} \quad (4.31)$$

Comparing this result to the Lagrange coefficient terms of equations 3.59 and 3.60 (with $\beta = 2\alpha$ and $\lambda = 0$), a fifth order accurate iteration time can be derived by subtracting equation 4.31 from the fifth order form of equation 3.46,

$$\Delta t = \sqrt[5]{\frac{12T}{\alpha^2 \Delta v_0}} \quad (4.32)$$

where T is a user defined tolerance with units of length. Just like the fourth order solution, a new state should be computed every Δt time given by equation 4.32 until the final state corresponding to the propagation time required is obtained.

HIGHER-ORDER SOLUTIONS OF THE TWO-BODY PROBLEM

The time-dependent function that results when higher orders of Lagrange coefficients are substituted into equation 4.1 cannot be integrated directly. This obstacle can be overcome in two different ways.

The Modified Power Series Approach

The first approach involves rewriting the transformed relative two-body problem given by equation 4.4 as a truncated, time dependent Taylor series expansion. Writing the relative acceleration in terms of Lagrange coefficients of order ξ ,

$$\Delta \ddot{\mathbf{r}} = -\frac{\alpha(F_\xi \Delta \bar{\mathbf{r}}_0 + G_\xi \Delta \bar{\mathbf{v}}_0)}{(F_\xi^2 + 2\lambda F_\xi G_\xi + \beta G_\xi^2)^{3/2}} \quad (4.24)$$

the series expansion becomes

$$\Delta\ddot{\mathbf{r}} = -\alpha \sum_{k=0}^{\chi} \frac{t^k}{k!} \frac{\partial^k \Delta\ddot{\mathbf{r}}}{\partial t^k} \Big|_{t=0} \quad (4.25)$$

where χ is the order of the truncated Taylor series. Integrating both sides of equation 4.25 with respect to time and then applying initial conditions yields the relative velocity,

$$\Delta\bar{\mathbf{v}}(t) = \Delta\bar{\mathbf{v}}_0 - \alpha \int \sum_{k=0}^{\chi} \frac{t^k}{k!} \frac{\partial^k \Delta\ddot{\mathbf{r}}}{\partial t^k} \Big|_{t=0} dt \quad (4.26)$$

Integrating both sides of equation 4.26 with respect to time and then applying initial conditions yields the relative position,

$$\Delta\bar{\mathbf{r}} = \Delta\bar{\mathbf{r}}_0 + t\Delta\bar{\mathbf{v}}_0 - \alpha \iint \sum_{k=0}^{\chi} \frac{t^k}{k!} \frac{\partial^k \Delta\ddot{\mathbf{r}}}{\partial t^k} \Big|_{t=0} dt^2 \quad (4.27)$$

It can easily be shown that when $\chi = \xi$, the modified Lagrange coefficients resulting from equation 4.27 will be exactly two orders higher than the original Lagrange coefficients used in equation 4.24. In other words, if $\chi = \xi$, then

$$\Delta\bar{\mathbf{r}} = \tilde{\mathbf{F}}_{\xi} \Delta\bar{\mathbf{r}}_0 + \tilde{\mathbf{G}}_{\xi} \Delta\bar{\mathbf{v}}_0 = \mathbf{F}_{\xi+2} \Delta\bar{\mathbf{r}}_0 + \mathbf{G}_{\xi+2} \Delta\bar{\mathbf{v}}_0. \quad (4.28)$$

An additional increase in accuracy is obtained by letting χ be greater than ξ ; however, the $\tilde{\mathbf{F}}$ and $\tilde{\mathbf{G}}$ polynomials generated when $\xi \geq 5$ become too cumbersome to implement. As an example, the modified Lagrange coefficients generated when $\xi = 5$ and $\chi = 6$ are given by

$$\begin{aligned} \tilde{\mathbf{F}}_5 = \mathbf{F}_7 - \frac{1}{13440} \alpha \left[\alpha^2 (180\alpha - 832\beta + 6590\lambda^2) \right. \\ \left. + 24\alpha(49\beta^2 - 830\beta\lambda^2 + 1435\lambda^4) - 105(5\beta^3 - 135\beta^2\lambda^2 + 495\beta\lambda^4 - 429\lambda^6) \right] t^8 + \dots \end{aligned} \quad (4.29)$$

$$\begin{aligned}\tilde{G}_5 = G_7 + \frac{1}{6720}\alpha\lambda[\alpha(1117\alpha - 2676\beta + 7420\lambda^2) \\ + 315(5\beta^2 - 30\beta\lambda^2 + 33\lambda^4)]t^8 - \dots\end{aligned}\quad (4.30)$$

where F_7 and G_7 are the original seventh order Lagrange coefficients given by equations 3.59 and 3.60.

The Gamma Polynomial Approach

The second approach used to solve equation 4.4 is to rewrite the ratio of one to the denominator in terms of a truncated Taylor series expansion. Recall the definition given by equation 4.9:

$$\gamma^3 = (F^2 + 2\lambda FG + \beta G^2)^{3/2}\quad (4.31)$$

The truncated Taylor series expansion Γ_0 is defined as

$$\Gamma_0 = \sum_{k=0}^{\xi} \frac{t^k}{k!} \frac{\partial^k}{\partial t^k} \left(\frac{1}{\gamma^3} \right)_{t=0}\quad (4.32)$$

where ξ represents the order of the time dependent Lagrange coefficients being used. With this definition of the upper-case Gamma polynomial, equation 4.4 can now be rewritten as

$$\Delta\ddot{\bar{r}} = -\alpha\Gamma_0(F\Delta\bar{r}_0 + G\Delta\bar{v}_0)\quad (4.33)$$

Since equation 4.33 defines the relative acceleration as the product of finite-termed polynomials, an elegant representation of the relative velocity can be found using integration by parts on the right hand side. Integrating both sides of equation 4.33 yields

$$\Delta\bar{v}(t) = -\alpha \sum_{k=0}^{\xi} (-1)^k \frac{\partial^k F}{\partial t^k} \Gamma_{k+1} \Delta\bar{r}_0 - \alpha \sum_{k=0}^{\xi} (-1)^k \frac{\partial^k G}{\partial t^k} \Gamma_{k+1} \Delta\bar{v}_0 + \bar{c}_1 \quad (4.34)$$

where \bar{c}_1 is a vector constant of integration and Γ_{k+1} is a repeated integral of the Gamma polynomial, such that

$$\Gamma_{0+1} = \int \Gamma_0 dt; \Gamma_{1+1} = \iint \Gamma_0 dt^2; \Gamma_{2+1} = \iiint \Gamma_0 dt^3; \text{ etc.} \quad (4.35)$$

The value of the constant of integration is determined by substituting the initial conditions given by equation 3.8 into equation 4.34 and then simplifying,

$$\bar{c}_1 = \Delta\bar{v}_0 \quad (4.36)$$

Substituting equation 4.36 into equation 4.34 and then simplifying yields the unique relative velocity as a function of time,

$$\Delta\bar{v}(t) = -\alpha \sum_{k=0}^{\xi} (-1)^k \frac{\partial^k F}{\partial t^k} \Gamma_{k+1} \Delta\bar{r}_0 + \left[1 - \alpha \sum_{k=0}^{\xi} (-1)^k \frac{\partial^k G}{\partial t^k} \Gamma_{k+1} \right] \Delta\bar{v}_0 \quad (4.37)$$

The same procedure can be used to find the satellite's position. Integrating both sides of equation 4.37, solving for the second vector constant of integration, and then simplifying yields

$$\begin{aligned} \Delta\bar{r}(t) = & \left\{ 1 - \alpha \left[\sum_{k=0}^{\xi} (-1)^k \frac{\partial^k F}{\partial t^k} \Gamma_{k+2} + \dots + \sum_{k=\xi}^{\xi} (-1)^k \frac{\partial^k F}{\partial t^k} \Gamma_{k+2} \right] \right\} \Delta\bar{r}_0 \\ & + \left\{ t - \alpha \left[\sum_{k=0}^{\xi} (-1)^k \frac{\partial^k G}{\partial t^k} \Gamma_{k+2} + \dots + \sum_{k=\xi}^{\xi} (-1)^k \frac{\partial^k G}{\partial t^k} \Gamma_{k+2} \right] \right\} \Delta\bar{v}_0 \end{aligned} \quad (4.38)$$

Equation 4.38 can be simplified by using a double summation,

$$\Delta\bar{\mathbf{r}}(t) = \left[1 - \alpha \sum_{m=0}^{\xi} \sum_{k=m}^{\xi} (-1)^k \frac{\partial^k \mathbf{F}}{\partial t^k} \Gamma_{k+2} \right] \Delta\bar{\mathbf{r}}_0 + \left[t - \alpha \sum_{m=0}^{\xi} \sum_{k=m}^{\xi} (-1)^k \frac{\partial^k \mathbf{G}}{\partial t^k} \Gamma_{k+2} \right] \Delta\bar{\mathbf{v}}_0 \quad (4.39)$$

With these results, the ξ -order state of the secondary body's motion relative to a primary body can be written as

$$\Delta\bar{\mathbf{s}}(t) = \mathbf{\Phi} \Delta\bar{\mathbf{s}}_0 \rightarrow \begin{Bmatrix} \Delta\bar{\mathbf{r}} \\ \Delta\bar{\mathbf{v}} \end{Bmatrix} = \begin{bmatrix} \tilde{\mathbf{F}} \mathbf{I}_{3 \times 3} & \tilde{\mathbf{G}} \mathbf{I}_{3 \times 3} \\ \tilde{\dot{\mathbf{F}}} \mathbf{I}_{3 \times 3} & \tilde{\dot{\mathbf{G}}} \mathbf{I}_{3 \times 3} \end{bmatrix} \begin{Bmatrix} \Delta\bar{\mathbf{r}}_0 \\ \Delta\bar{\mathbf{v}}_0 \end{Bmatrix} \quad (4.40)$$

where $\mathbf{I}_{3 \times 3}$ is a 3x3 identity matrix and the modified Lagrange coefficients $\tilde{\mathbf{F}}$, $\tilde{\mathbf{G}}$, and their respective derivatives are defined as

$$\tilde{\mathbf{F}} = 1 - \alpha \sum_{m=0}^{\xi} \sum_{k=m}^{\xi} (-1)^k \frac{\partial^k \mathbf{F}}{\partial t^k} \Gamma_{k+2} \quad (4.41)$$

$$\tilde{\mathbf{G}} = t - \alpha \sum_{m=0}^{\xi} \sum_{k=m}^{\xi} (-1)^k \frac{\partial^k \mathbf{G}}{\partial t^k} \Gamma_{k+2} \quad (4.42)$$

$$\tilde{\dot{\mathbf{F}}} = -\alpha \left[\sum_{k=0}^{\xi} (-1)^k \frac{\partial^k \mathbf{F}}{\partial t^k} \Gamma_{k+1} \right] \quad (4.43)$$

$$\tilde{\dot{\mathbf{G}}} = 1 - \alpha \sum_{k=0}^{\xi} (-1)^k \frac{\partial^k \mathbf{G}}{\partial t^k} \Gamma_{k+1} \quad (4.44)$$

While elegant, this second method of obtaining higher-order solutions of the relative two-body problem generates even larger expressions for the modified Lagrange coefficients than the truncated Taylor series approach.

NEW VARIABLE TIME STEP PROPAGATORS

Previous numerical work conducted by the author shows that a true analytic solution of equation 4.4 will yield results that are more accurate than RK5 for any time step size if third-order Lagrange coefficients are implemented [76-77]. However, an analytic solution of equation 4.4 which can be expressed in terms elementary functions cannot be obtained when Lagrange coefficients of order two or higher are used. Consequently, the methods shown in the previous section yield approximate solutions which unfortunately, at best, return comparable results to the ones obtained when the original Lagrange coefficients are used recursively. With this in mind, the remaining work in this dissertation will use the sixth-order and seventh-order version of equation 3.46 and the fourth-order solution given by equations 4.13 and 4.16 to investigate orbital trajectories.

The 47 Variable Time Step Propagator

The fourth-order solution of the relative two-body problem given by equations 4.13 and 4.16 can be used in conjunction with the seventh-order power series solution given by equations 3.46, 3.59, and 3.60 to develop a variable time step propagator that is both more accurate and more efficient than the variable time step RK45 numerical integrator derived earlier. This fourth-order, seventh-order propagator (47P) uses the same algorithm developed for RK45. The only difference lies in the algorithm's first two steps. Given a simulation time, τ , an initial relative position, $\Delta\vec{r}_0$, and initial relative velocity, $\Delta\vec{v}_0$, an initial time step size, Δt , and a tolerance, T:

- * Evaluate a new state using the fourth-order solution given by equations 4.13 and 4.16.

- * Evaluate a new state using the seventh-order solution given by equation 3.46.
- * Determine the deviation between the fourth-order and seventh-order results using

$$\text{Deviation} = \left\| \Delta \bar{\mathbf{r}}_{\xi=7} - \Delta \bar{\mathbf{r}}_{\xi=4} \right\| \quad (4.45)$$

- * If the deviation is greater than the tolerance, decrease the size of the current time step by dividing it by two and return to the first step of the algorithm.
- * If the deviation is less than the tolerance, the state returned by the seventh-order solution is the new relative position and velocity,

$$\Delta \bar{\mathbf{r}}_1 = \Delta \bar{\mathbf{r}}_{\xi=7} \quad (4.46)$$

$$\Delta \bar{\mathbf{v}}_1 = \Delta \bar{\mathbf{v}}_{\xi=7} \quad (4.47)$$

- * Increase the size of the current time step by multiplying it by two.
- * Repeat the entire process for the next state until the simulation time, τ , has been reached.

This procedure will yield results that are more accurate and much more efficient than those obtained by RK45. To demonstrate this, the elliptical orbit test conducted by the variable time step RK45 numerical integrator is repeated using the 47P algorithm just described. The results of this investigation using a tolerance of 10^{-3} km are shown in Figure 4.3. Figure 4.4 shows the results obtained when a tolerance of 10^{-4} km is used.

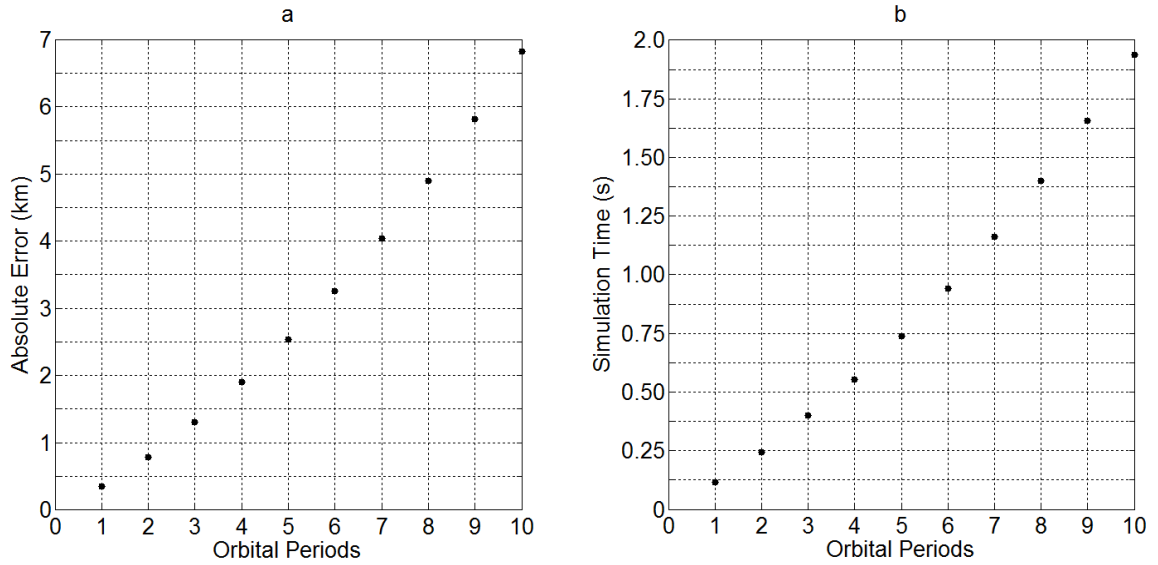


Figure 4.1: Absolute Error Results Using 47P with a 10^{-3} Tolerance
a) Absolute Error, b) Simulation Time

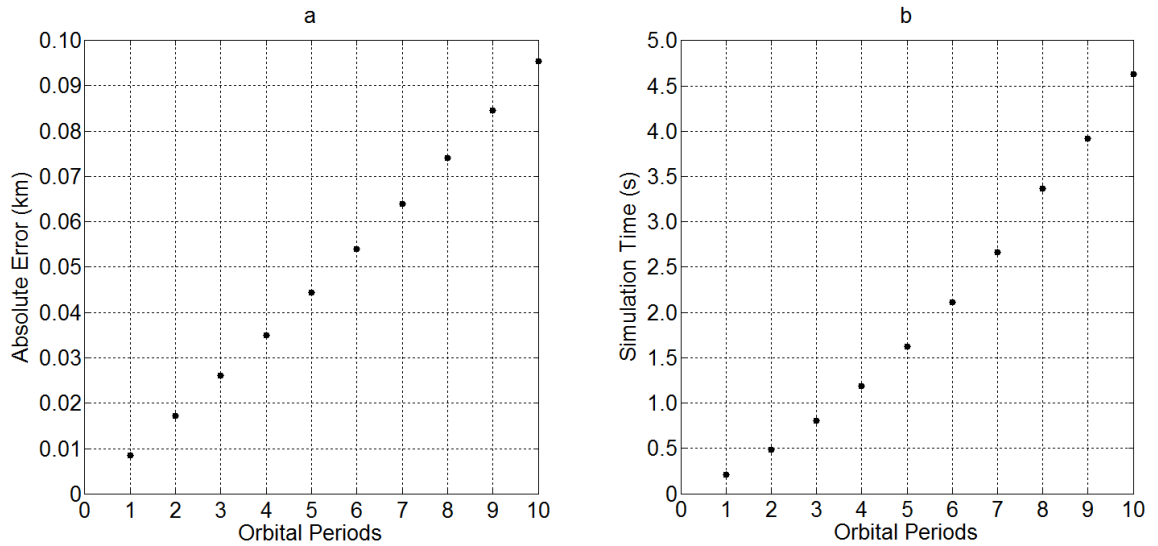


Figure 4.2: Absolute Error Results Using 47P with a 10^{-4} Tolerance
a) Absolute Error, b) Simulation Time

When the results of Figure 4.2 are compared directly to the results of Figure 4.4, it can be seen that the 47P algorithm returned outcomes that were 46% more accurate than RK5. The 47P algorithm was also 59% faster than RK5. Even better results can be obtained by 47P when the tolerance is set lower; however, based on further experimentation, the

author recommends that the tolerance of the 47P algorithm not exceed 10^{-5} . The use of tolerances smaller than this value will yield results that are much more accurate, but the cost required to achieve this in terms of computer time begins to increase exponentially.

The 67 Variable Time Step Propagator

The sixth-order and seventh-order power series solution given by equations 3.46, 3.59, and 3.60 can also be used to develop a variable time step propagator whose accuracy is comparable but more efficient than the variable time step RK45 numerical integrator derived earlier. This sixth-order, seventh-order propagator (67P) uses the same algorithm developed for RK45 and the 47P algorithm. Once again, the only difference lies in the algorithm's first two steps. Given a simulation time, τ , an initial relative position, $\Delta\bar{\mathbf{r}}_0$, and initial relative velocity, $\Delta\bar{\mathbf{v}}_0$, an initial time step size, Δt , and a tolerance, T:

- ✱ Evaluate a new state using the sixth-order solution given by equation 3.46.
- ✱ Evaluate a new state using the seventh-order solution given by equation 3.46.
- ✱ Determine the deviation between the sixth-order and seventh-order results using

$$\text{Deviation} = \left\| \Delta\bar{\mathbf{r}}_{\xi=7} - \Delta\bar{\mathbf{r}}_{\xi=6} \right\| \quad (4.48)$$

- ✱ If the deviation is greater than the tolerance, decrease the size of the current time step by dividing it by two and return to the first step of the algorithm.
- ✱ If the deviation is less than the tolerance, the state returned by the seventh-order solution is the new relative position and velocity,

$$\Delta\bar{\mathbf{r}}_1 = \Delta\bar{\mathbf{r}}_{\xi=7} \quad (4.49)$$

$$\Delta \bar{v}_1 = \Delta \bar{v}_{\xi=7} \quad (4.50)$$

- * Increase the size of the current time step by multiplying it by two.
- * Repeat the entire process for the next state until the simulation time, τ , has been reached.

As was stated above, this procedure will yield results whose accuracy is comparable, but much more efficient than the accuracy of RK45. To demonstrate this, the elliptical orbit test conducted by the variable time step RK45 numerical integrator is repeated using the 67P algorithm just described. The results of this investigation using a tolerance of 10^{-7} km are shown in Figure 4.5. Figure 4.6 shows the results obtained when a tolerance of 10^{-8} km is used.

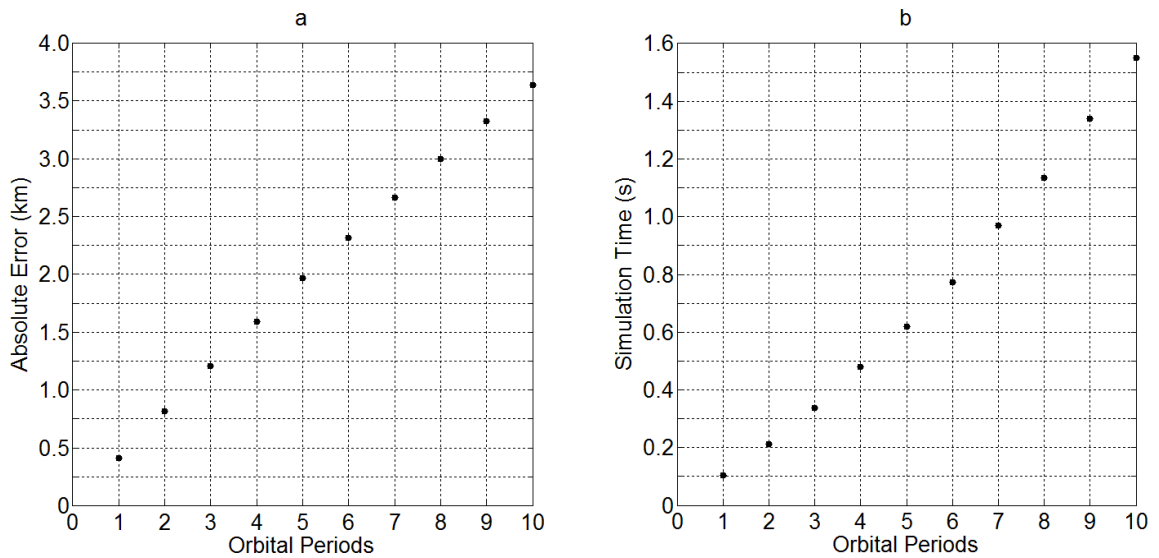


Figure 4.3: Absolute Error Results Using 67P with a 10^{-7} Tolerance
a) Absolute Error, b) Simulation Time

These two figures show that the 67P algorithm has an accuracy that is comparable to RK5 and is much more efficient than both RK5 and 47P. When the results of Figure 4.2

and 4.4 are compared directly to the results of Figure 4.6, it can be seen that the 67P algorithm was 77% faster than RK5, and 43% faster than 47P. The tolerances used by 67P were higher than those used by both RK5 and 47P. Further numerical analysis reveals that increasing the 67P tolerance to 10^{-9} km will yield results that are slightly less accurate, but still more efficient than 47P.

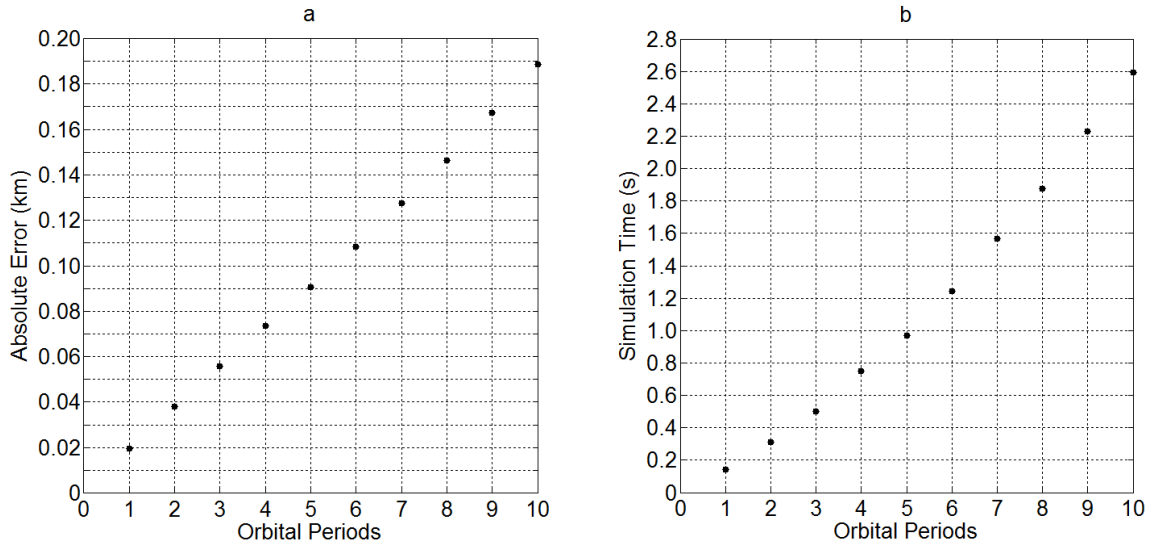


Figure 4.4: Absolute Error Results Using 67P with a 10^{-8} Tolerance
a) Absolute Error, b) Simulation Time

DISCUSSION

Obviously, a large array of variable time step propagators can be developed using the power series solution of the relative two-body problem. However, extensive numerical investigation conducted by the author has revealed that the 47P and 67P algorithms continuously produce results that are superior to any other order combination. This holds true for any type of orbit described by the relative two-body problem. Even more important than this, as will be shown in the next chapter, is the fact that these two variable time step propagators (47P and 67P) can be used to solve the N-body problem

more efficiently than RK45 while maintaining the same levels of accuracy observed when the algorithms were used to solve the two-body problem.

CHAPTER 5

NEW SOLUTIONS OF THE N-BODY PROBLEM

In this chapter, a new power series solution, a fourth-order solution, and a higher-order solution are derived for the N-body problem. A variable time step numerical integration algorithm that extends the RK45, 47P, and 67P capabilities derived in the previous chapter to the solution of the N-body problem is introduced. The algorithm is then used to solve periodic central configuration scenarios and non-periodic scenarios in the three-body and restricted three-body problem, respectively.

POWER SERIES SOLUTIONS

In compact form, the N-body problem equations of motion with respect to the system's barycenter (center of mass) are

$$\ddot{\bar{\mathbf{r}}}_i = \sum_{\substack{j=1 \\ j \neq i}}^N \frac{\mu_j (\bar{\mathbf{r}}_j - \bar{\mathbf{r}}_i)}{\|\bar{\mathbf{r}}_j - \bar{\mathbf{r}}_i\|^3} = \sum_{\substack{j=1 \\ j \neq i}}^N \frac{\mu_j \Delta \bar{\mathbf{r}}_{ji}}{\Delta r_{ji}^3} \quad (5.1)$$

In this expression, i is the index of the current body, j is an index that represents the effect of other bodies on the current object, $\ddot{\bar{\mathbf{r}}}$ and $\bar{\mathbf{r}}$ are the current body's acceleration and position vectors, respectively;

$$\ddot{\bar{\mathbf{r}}} = \{\ddot{x} \quad \ddot{y} \quad \ddot{z}\}^T \quad (5.2)$$

$$\bar{\mathbf{r}} = \{x \quad y \quad z\}^T \quad (5.3)$$

μ_j is the gravitational parameter of each respective body, and N represents the number of bodies being analyzed. The N-body problem can be seen as a sum of relative two-body

problems; therefore, the fundamental invariants pertaining to the various relative two-body accelerations are defined as

$$\alpha_{ji} = \frac{\mu_j}{\Delta r_{ji,0}^3} \quad (5.4)$$

$$\beta_{ji} = \left(\frac{\Delta v_{ji,0}}{\Delta r_{ji,0}} \right)^2 \quad (5.5)$$

$$\lambda_{ji} = \frac{\Delta \vec{r}_{ji,0} \cdot \Delta \vec{v}_{ji,0}}{\Delta r_{ji,0}^2} \quad (5.6)$$

In general, $3N(N - 1)$ fundamental invariants must be evaluated to transform the N -body problem into a time dependent system of equations, while only $3(N - 1)^2$ are required to transform the restricted N -body problem. Recall that the term “restricted” indicates that the mass of one of the particles being analyzed is negligible, causing it to have no gravitational influence on the motion of the remaining particles. With these definitions, an approximate solution of equation 5.1 can be written as

$$\vec{r}_i(t) = \vec{r}_{i,0} + t\vec{v}_{i,0} + \sum_{\substack{j=1 \\ j \neq i}}^N \left(F_{ji} \Delta \vec{r}_{ji,0} + G_{ji} \Delta \vec{v}_{ji,0} \right) \quad (5.7)$$

$$\vec{v}_i(t) = \vec{v}_{i,0} + \sum_{\substack{j=1 \\ j \neq i}}^N \left(\dot{F}_{ji} \Delta \vec{r}_{ji,0} + \dot{G}_{ji} \Delta \vec{v}_{ji,0} \right) \quad (5.8)$$

where F_{ji} , G_{ji} , and their derivatives are based on the Lagrange coefficients of each respective two-body acceleration.

$$\begin{aligned}
F_{ji} &= \frac{1}{2} \alpha_{ji} t^2 - \frac{1}{2} \alpha_{ji} \lambda_{ji} t^3 \\
&+ \frac{1}{24} \alpha_{ji} (2\alpha_{ji} - 3\beta_{ji} + 15\lambda_{ji}^2) t^4 - \frac{1}{8} \alpha_{ji} \lambda_{ji} (2\alpha_{ji} - 3\beta_{ji} + 7\lambda_{ji}^2) t^5 \\
&+ \frac{1}{720} \alpha_{ji} [22\alpha_{ji}^2 - 66\alpha_{ji}\beta_{ji} + 45\beta_{ji}^2 + 105\lambda_{ji}^2 (4\alpha_{ji} - 6\beta_{ji} + 9\lambda_{ji}^2)] t^6 \\
&- \frac{1}{80} \alpha_{ji} \lambda_{ji} [12\alpha_{ji}^2 - 36\alpha_{ji}\beta_{ji} + 25\beta_{ji}^2 + 5\lambda_{ji}^2 (20\alpha_{ji} - 30\beta_{ji} + 33\lambda_{ji}^2)] t^7 + \dots
\end{aligned} \tag{5.9}$$

$$\begin{aligned}
G &= \frac{1}{6} \alpha_{ji} t^3 - \frac{1}{4} \alpha_{ji} \lambda_{ji} t^4 \\
&+ \frac{1}{120} \alpha_{ji} (8\alpha_{ji} - 9\beta_{ji} + 45\lambda_{ji}^2) t^5 - \frac{1}{24} \alpha_{ji} \lambda_{ji} (5\alpha_{ji} - 6\beta_{ji} + 14\lambda_{ji}^2) t^6 \\
&+ \frac{1}{5040} \alpha_{ji} [172\alpha_{ji}^2 - 396\alpha_{ji}\beta_{ji} + 225\beta_{ji}^2 + 315\lambda_{ji}^2 (8\alpha_{ji} - 10\beta_{ji} + 15\lambda_{ji}^2)] t^7 - \dots
\end{aligned} \tag{5.10}$$

$$\begin{aligned}
\dot{F}_{ji} &= \alpha_{ji} t - \frac{3}{2} \alpha_{ji} \lambda_{ji} t^2 \\
&+ \frac{1}{6} \alpha_{ji} (2\alpha_{ji} - 3\beta_{ji} + 15\lambda_{ji}^2) t^3 - \frac{5}{8} \alpha_{ji} \lambda_{ji} (2\alpha_{ji} - 3\beta_{ji} + 7\lambda_{ji}^2) t^4 \\
&+ \frac{1}{120} \alpha_{ji} [22\alpha_{ji}^2 - 66\alpha_{ji}\beta_{ji} + 45\beta_{ji}^2 + 105\lambda_{ji}^2 (4\alpha_{ji} - 6\beta_{ji} + 9\lambda_{ji}^2)] t^5 \\
&- \frac{7}{80} \alpha_{ji} \lambda_{ji} [12\alpha_{ji}^2 - 36\alpha_{ji}\beta_{ji} + 25\beta_{ji}^2 + 5\lambda_{ji}^2 (20\alpha_{ji} - 30\beta_{ji} + 33\lambda_{ji}^2)] t^6 + \dots
\end{aligned} \tag{5.11}$$

$$\begin{aligned}
\dot{G}_{ji} &= \frac{1}{2} \alpha_{ji} t^2 - \alpha_{ji} \lambda_{ji} t^3 \\
&+ \frac{1}{24} \alpha_{ji} (8\alpha_{ji} - 9\beta_{ji} + 45\lambda_{ji}^2) t^4 - \frac{1}{4} \alpha_{ji} \lambda_{ji} (5\alpha_{ji} - 6\beta_{ji} + 14\lambda_{ji}^2) t^5 \\
&+ \frac{1}{720} \alpha_{ji} [172\alpha_{ji}^2 - 396\alpha_{ji}\beta_{ji} + 225\beta_{ji}^2 + 315\lambda_{ji}^2 (8\alpha_{ji} - 10\beta_{ji} + 15\lambda_{ji}^2)] t^6 - \dots
\end{aligned} \tag{5.12}$$

These expressions will be used by the 47P and the 67P algorithms when solving various scenarios pertaining to the N-body problem.

FOURTH-ORDER SOLUTIONS

The N-body problem can be transformed into a linear, uncoupled, time dependent system of equations in the same manner as was done with the relative two-body problem,

$$\ddot{\bar{\mathbf{r}}}_i = \sum_{\substack{j=1 \\ j \neq i}}^N \frac{\mu_j (\bar{\mathbf{r}}_j - \bar{\mathbf{r}}_i)}{\|\bar{\mathbf{r}}_j - \bar{\mathbf{r}}_i\|^3} = \sum_{\substack{j=1 \\ j \neq i}}^N \frac{\mu_j \Delta \bar{\mathbf{r}}_{ji}}{\Delta r_{ji}^3} \rightarrow \ddot{\bar{\mathbf{r}}}_i = \sum_{\substack{j=1 \\ j \neq i}}^N \frac{\alpha_{ji} (\mathbf{F}_{ji} \Delta \bar{\mathbf{r}}_{ji,0} + \mathbf{G}_{ji} \Delta \bar{\mathbf{v}}_{ji,0})}{(\mathbf{F}_{ji}^2 + 2\lambda_{ji} \mathbf{F}_{ji} \mathbf{G}_{ji} + \beta_{ji} \mathbf{G}_{ji}^2)^{3/2}} \quad (5.13)$$

When first order Lagrange coefficients are used, equation 5.13 reduces to

$$\ddot{\bar{\mathbf{r}}}_i = \sum_{\substack{j=1 \\ j \neq i}}^N \frac{\alpha_{ji} (\Delta \bar{\mathbf{r}}_{ji,0} + t \Delta \bar{\mathbf{v}}_{ji,0})}{(1 + 2\lambda_{ji} t + \beta_{ji} t^2)^{3/2}} \quad (5.14)$$

Using the following definition,

$$\gamma_{ji} = \sqrt{1 + 2\lambda_{ji} t + \beta_{ji} t^2} \quad (5.15)$$

a fourth-order, time dependent solution of the N-body problem can be stated as

$$\begin{aligned} \bar{\mathbf{r}}_i(t) &= \bar{\mathbf{r}}_{i,0} + t \bar{\mathbf{v}}_{i,0} \\ &+ \sum_{\substack{j=1 \\ j \neq i}}^N \alpha_{ji} \left(\frac{\lambda_{ji} t + 1 - \gamma_{ji}}{\lambda_{ji}^2 - \beta_{ji}} \right) \Delta \bar{\mathbf{r}}_{ji,0} \\ &- \sum_{\substack{j=1 \\ j \neq i}}^N \left[\frac{\alpha_{ji} \lambda_{ji}}{\beta_{ji}} \left(\frac{1 - \gamma_{ji}}{\lambda_{ji}^2 - \beta_{ji}} \right) + \left(\frac{\alpha_{ji}}{\lambda_{ji}^2 - \beta_{ji}} \right) t + \frac{\alpha_{ji}}{\beta_{ji}^{3/2}} \ln \left(\frac{\lambda_{ji} + \beta_{ji} t + \sqrt{\beta_{ji} \gamma_{ji}}}{\lambda_{ji} + \sqrt{\beta_{ji}}} \right) \right] \Delta \bar{\mathbf{v}}_{ji,0} \end{aligned} \quad (5.16)$$

$$\bar{\mathbf{v}}_i(t) = \bar{\mathbf{v}}_{i,0} - \sum_{\substack{j=1 \\ j \neq i}}^N \frac{\alpha_{ji}}{\gamma_{ji}} \left[\frac{\beta_{ji} t + \lambda_{ji} (1 - \gamma_{ji})}{\lambda_{ji}^2 - \beta_{ji}} \right] \Delta \bar{\mathbf{r}}_{ji,0} - \sum_{\substack{j=1 \\ j \neq i}}^N \frac{\alpha_{ji}}{\gamma_{ji}} \left(\frac{\lambda_{ji} t + 1 - \gamma_{ji}}{\lambda_{ji}^2 - \beta_{ji}} \right) \Delta \bar{\mathbf{v}}_{ji,0} \quad (5.17)$$

This expression will be used by the 47P algorithm when solving various scenarios pertaining to the N-body problem.

HIGHER ORDER SOLUTIONS

As occurred with the relative two-body problem, when higher orders of the Lagrange coefficients given by equations 5.9 and 5.10 are substituted into equation 5.13, the time dependent function that results cannot be integrated directly. Defining the denominator of equation 5.13 as

$$\gamma_{ji}^3 = \left(F_{ji}^2 + 2\lambda_{ji} F_{ji} G_{ji} + \beta_{ji} G_{ji}^2 \right)^{3/2} \quad (5.18)$$

its truncated Taylor series expansion, $\Gamma_{ji,0}$, is defined as

$$\Gamma_{ji,0} = \sum_{k=0}^{\xi} \frac{t^k}{k!} \frac{\partial^k}{\partial t^k} \left(\frac{1}{\gamma_{ji}^3} \right)_{t=0} \quad (5.19)$$

where ξ represents the order of the time dependent Lagrange coefficients being used.

With this definition of the upper-case Gamma polynomial, equation 5.13 is now rewritten as

$$\ddot{\mathbf{r}}_i = \sum_{\substack{j=1 \\ j \neq i}}^N \alpha_{ji} \Gamma_{ji,0} \left(F_{ji} \Delta \bar{\mathbf{r}}_{ji,0} + G_{ji} \Delta \bar{\mathbf{v}}_{ji,0} \right) \quad (5.20)$$

Since equation 5.20 defines the acceleration as the product of finite-termed polynomials, an elegant representation of the position and velocity for each point particle being analyzed can be found using integration by parts on the right hand side. After initial conditions have been applied to the velocity and position outcomes and all expressions have been simplified, a higher-order solution of the N-body problem can then be stated as

$$\begin{aligned} \bar{\mathbf{r}}_i(t) = & \bar{\mathbf{r}}_{i,0} + t\bar{\mathbf{v}}_{i,0} \\ & + \sum_{\substack{j=1 \\ j \neq i}}^N \alpha_{ji} \left(\sum_{m=0}^{\xi} \sum_{k=m}^{\xi} (-1)^k \frac{\partial^k \mathbf{F}_{ji}}{\partial t^k} \Gamma_{ji,k+2} \right) \Delta \bar{\mathbf{r}}_{ji,0} + \sum_{\substack{j=1 \\ j \neq i}}^N \alpha_{ji} \left(\sum_{m=0}^{\xi} \sum_{k=m}^{\xi} (-1)^k \frac{\partial^k \mathbf{G}_{ji}}{\partial t^k} \Gamma_{ji,k+2} \right) \Delta \bar{\mathbf{v}}_{ji,0} \end{aligned} \quad (5.21)$$

$$\bar{\mathbf{v}}_i(t) = \bar{\mathbf{v}}_{i,0} + \sum_{\substack{j=1 \\ j \neq i}}^N \alpha_{ji} \left(\sum_{k=0}^{\xi} (-1)^k \frac{\partial^k \mathbf{F}_{ji}}{\partial t^k} \Gamma_{ji,k+1} \right) \Delta \bar{\mathbf{r}}_{ji,0} + \sum_{\substack{j=1 \\ j \neq i}}^N \alpha_{ji} \left(\sum_{k=0}^{\xi} (-1)^k \frac{\partial^k \mathbf{G}_{ji}}{\partial t^k} \Gamma_{ji,k+1} \right) \Delta \bar{\mathbf{v}}_{ji,0} \quad (5.22)$$

where $\Gamma_{ji,k+1}$ is a repeated integral of the Gamma polynomial, such that

$$\Gamma_{ji,0+1} = \int \Gamma_{ji,0} dt; \quad \Gamma_{ji,1+1} = \iint \Gamma_{ji,0} dt^2; \quad \Gamma_{ji,2+1} = \iiint \Gamma_{ji,0} dt^3; \quad \text{etc.} \quad (5.23)$$

This approximate, higher-order solution has been derived for completeness, but will not be used to solve the N-body problem iteratively because it produces polynomial expressions that are too cumbersome to implement.

VARIABLE TIME STEP ALGORITHM FOR THE N-BODY PROBLEM

The following variable time step algorithm will be used by RK5, 47P, and 67P to solve various scenarios pertaining to the N-body problem. The algorithm assumes that the particles being analyzed are ordered in terms of decreasing gravitational parameter. Given a simulation time, τ , the initial position of each particle, \mathbf{R}_0 , (a matrix whose column vectors correspond to the position of each body being analyzed),

$$\mathbf{R}_0 = \{ \bar{\mathbf{r}}_{1,0} \quad \bar{\mathbf{r}}_{2,0} \quad \cdots \quad \bar{\mathbf{r}}_{N,0} \} \quad (5.24)$$

the initial velocity of each particle, \mathbf{V}_0 , (a matrix whose column vectors correspond to the velocity of each body being analyzed),

$$\mathbf{V}_0 = \{ \bar{\mathbf{v}}_{1,0} \quad \bar{\mathbf{v}}_{2,0} \quad \cdots \quad \bar{\mathbf{v}}_{N,0} \} \quad (5.25)$$

an initial time step size, Δt , and a tolerance, T :

- * A new state is evaluated using the lower-order integrator (RK4 in the case of RK45, the fourth-order solution in the case of 47P, or the sixth-order power series solution in the case of 67P).
- * A new state is evaluated using the higher-order integrator (RK5 in the case of RK45 or the seventh-order power series solution in the case of 47P and 67P).
- * Determine the deviation between the lower-order and higher-order results by evaluating the change in position corresponding to the body with the smallest gravitational parameter,

$$\text{Deviation} = \left\| \Delta \vec{r}_{\text{high}} - \Delta \vec{r}_{\text{low}} \right\| \quad (5.24)$$

- * If the deviation is greater than the tolerance, decrease the size of the current time step by dividing it by two and return to the first step of the algorithm.
- * If the deviation is less than the tolerance, the state returned by the higher-order solution is the new relative position and velocity,

$$\mathbf{R}_1 = \mathbf{R}_{\text{high}} \quad (5.25)$$

$$\mathbf{V}_1 = \mathbf{V}_{\text{high}} \quad (5.26)$$

- * Increase the size of the current time step by multiplying it by two.
- * Repeat the entire process for the next state until the simulation time, τ , has been reached.

The algorithm will now be used to solve periodic and non-periodic scenarios of the three-body and restricted three-body problem.

CENTRAL CONFIGURATION TRAJECTORIES

Beginning with equation 5.1, the equations of motion for the three-body problem are given by

$$\ddot{\bar{\mathbf{r}}}_1 = \frac{\mu_2(\bar{\mathbf{r}}_2 - \bar{\mathbf{r}}_1)}{\|\bar{\mathbf{r}}_2 - \bar{\mathbf{r}}_1\|^3} + \frac{\mu_3(\bar{\mathbf{r}}_3 - \bar{\mathbf{r}}_1)}{\|\bar{\mathbf{r}}_3 - \bar{\mathbf{r}}_1\|^3} \quad (5.27)$$

$$\ddot{\bar{\mathbf{r}}}_2 = \frac{\mu_1(\bar{\mathbf{r}}_1 - \bar{\mathbf{r}}_2)}{\|\bar{\mathbf{r}}_1 - \bar{\mathbf{r}}_2\|^3} + \frac{\mu_3(\bar{\mathbf{r}}_3 - \bar{\mathbf{r}}_2)}{\|\bar{\mathbf{r}}_3 - \bar{\mathbf{r}}_2\|^3} \quad (5.28)$$

$$\ddot{\bar{\mathbf{r}}}_3 = \frac{\mu_1(\bar{\mathbf{r}}_1 - \bar{\mathbf{r}}_3)}{\|\bar{\mathbf{r}}_1 - \bar{\mathbf{r}}_3\|^3} + \frac{\mu_2(\bar{\mathbf{r}}_2 - \bar{\mathbf{r}}_3)}{\|\bar{\mathbf{r}}_2 - \bar{\mathbf{r}}_3\|^3} \quad (5.29)$$

Lagrange derived analytic solutions for many special cases of the three-body problem, including a family of solutions known as central configurations which lie at the vertices of a rotating equilateral triangle that can shrink and expand periodically. One such central configuration solution involves three point particles with equal gravitational parameters orbiting their common center of mass in a circular orbit. A second type of central configuration solution involves three point particles with different gravitational parameters orbiting their common center of mass. The geometry of these two scenarios was shown in Figures 2.8 and 2.9.

In order to derive a solution for any three-body central configuration setting, equations 5.27-5.29 are rewritten as

$$\ddot{\bar{\mathbf{r}}}_1 - \omega_2^2(\bar{\mathbf{r}}_2 - \bar{\mathbf{r}}_1) - \omega_3^2(\bar{\mathbf{r}}_3 - \bar{\mathbf{r}}_1) = 0 \quad (5.30)$$

$$\ddot{\bar{\mathbf{r}}}_2 - \omega_1^2(\bar{\mathbf{r}}_1 - \bar{\mathbf{r}}_2) - \omega_3^2(\bar{\mathbf{r}}_3 - \bar{\mathbf{r}}_2) = 0 \quad (5.31)$$

$$\ddot{\bar{\mathbf{r}}}_3 - \omega_1^2(\bar{\mathbf{r}}_1 - \bar{\mathbf{r}}_3) - \omega_2^2(\bar{\mathbf{r}}_2 - \bar{\mathbf{r}}_3) = 0 \quad (5.32)$$

The angular velocities ω_1 , ω_2 , and ω_3 are defined as

$$\omega_1 = \sqrt{\frac{\mu_1}{d^3}} \quad (5.33)$$

$$\omega_2 = \sqrt{\frac{\mu_2}{d^3}} \quad (5.34)$$

$$\omega_3 = \sqrt{\frac{\mu_3}{d^3}} \quad (5.35)$$

where μ_1 , μ_2 , μ_3 are the gravitational parameters of the three point particles, respectively, and d is the constant distance between each body, such that

$$d = \|\bar{\mathbf{r}}_1 - \bar{\mathbf{r}}_2\| = \|\bar{\mathbf{r}}_2 - \bar{\mathbf{r}}_3\| = \|\bar{\mathbf{r}}_3 - \bar{\mathbf{r}}_1\| \quad (5.36)$$

Using differential operator notation, equations 5.30-5.32 can be rewritten as a single system of equations,

$$\begin{bmatrix} D^2 + \omega_2^2 + \omega_3^2 & -\omega_2^2 & -\omega_3^2 \\ -\omega_1^2 & D^2 + \omega_1^2 + \omega_3^2 & -\omega_3^2 \\ -\omega_1^2 & -\omega_2^2 & D^2 + \omega_1^2 + \omega_2^2 \end{bmatrix} \begin{Bmatrix} \bar{\mathbf{r}}_1 \\ \bar{\mathbf{r}}_2 \\ \bar{\mathbf{r}}_3 \end{Bmatrix} = 0 \quad (5.37)$$

where D^2 is a differential operator defined as

$$D^2 = \frac{\partial^2}{\partial t^2} \quad (5.38)$$

The characteristic equation of this system is found by evaluating the determinant of the matrix on the left hand side and simplifying,

$$D^2(D^2 + \omega_1^2 + \omega_2^2 + \omega_3^2)^2 = 0 \quad (5.39)$$

The solution of equation 5.39 that corresponds to a periodic outcome is given by

$$D = \pm i\sqrt{\omega_1^2 + \omega_2^2 + \omega_3^2} \quad (5.40)$$

where i is the imaginary unit. The final, periodic solution of the three-body central configuration in state form can now be written as

$$\bar{\mathbf{s}}(t) = \mathbf{\Phi} \bar{\mathbf{s}}_0 \rightarrow \begin{Bmatrix} \bar{\mathbf{r}}_1 \\ \bar{\mathbf{r}}_2 \\ \bar{\mathbf{r}}_3 \\ \bar{\mathbf{v}}_1 \\ \bar{\mathbf{v}}_2 \\ \bar{\mathbf{v}}_3 \end{Bmatrix} = \begin{bmatrix} \cos(\omega t) \mathbf{I}_{6 \times 6} & \frac{1}{\omega} \sin(\omega t) \mathbf{I}_{6 \times 6} \\ -\omega \sin(\omega t) \mathbf{I}_{6 \times 6} & \cos(\omega t) \mathbf{I}_{6 \times 6} \end{bmatrix} \begin{Bmatrix} \bar{\mathbf{r}}_{1,0} \\ \bar{\mathbf{r}}_{2,0} \\ \bar{\mathbf{r}}_{3,0} \\ \bar{\mathbf{v}}_{1,0} \\ \bar{\mathbf{v}}_{2,0} \\ \bar{\mathbf{v}}_{3,0} \end{Bmatrix} \quad (5.41)$$

where the angular speed of the system, ω , is defined as

$$\omega = \sqrt{\frac{\mu_1 + \mu_2 + \mu_3}{d^3}} \quad (5.42)$$

The initial conditions used in conjunction with equation 5.41 can be computed using equation 5.36 and the gravitational parameters of each point particle:

$$\bar{\mathbf{r}}_{1,0} = -\frac{d}{2\mu} \left[(2\mu_2 + \mu_3) \hat{\mathbf{i}} + \sqrt{3}\mu_3 \hat{\mathbf{j}} \right] \quad (5.43)$$

$$\bar{\mathbf{r}}_{2,0} = \frac{d}{2\mu} \left[(2\mu_1 + \mu_3) \hat{\mathbf{i}} - \sqrt{3}\mu_3 \hat{\mathbf{j}} \right] \quad (5.44)$$

$$\bar{\mathbf{r}}_{3,0} = \frac{d}{2\mu} [(\mu_1 - \mu_2)\hat{\mathbf{i}} + \sqrt{3}(\mu_1 + \mu_2)\hat{\mathbf{j}}] \quad (5.45)$$

$$\bar{\mathbf{v}}_{1,0} = \frac{1}{2\sqrt{d\mu}} [\sqrt{3}\mu_3\hat{\mathbf{i}} - (2\mu_2 + \mu_3)\hat{\mathbf{j}}] \quad (5.46)$$

$$\bar{\mathbf{v}}_{2,0} = \frac{1}{2\sqrt{d\mu}} [\sqrt{3}\mu_3\hat{\mathbf{i}} + (2\mu_1 + \mu_3)\hat{\mathbf{j}}] \quad (5.47)$$

$$\bar{\mathbf{v}}_{3,0} = \frac{1}{2\sqrt{d\mu}} [-\sqrt{3}(\mu_1 + \mu_2)\hat{\mathbf{i}} + (\mu_1 - \mu_2)\hat{\mathbf{j}}] \quad (5.48)$$

In order to compare the performance of RK45, 47P, and 67P to the exact results provided by the central configuration results just discussed, consider a case in which the motions of three fictitious point particles with equal gravitational parameters are governed by the central configuration expressions given by equations 5.41-5.48. The gravitational parameters of the three particles are set equal to 30,000 km³/s² and the constant distance between each particle was assumed to be 25,000 km. Figure 5.1 shows a portion of the exact trajectories just described.

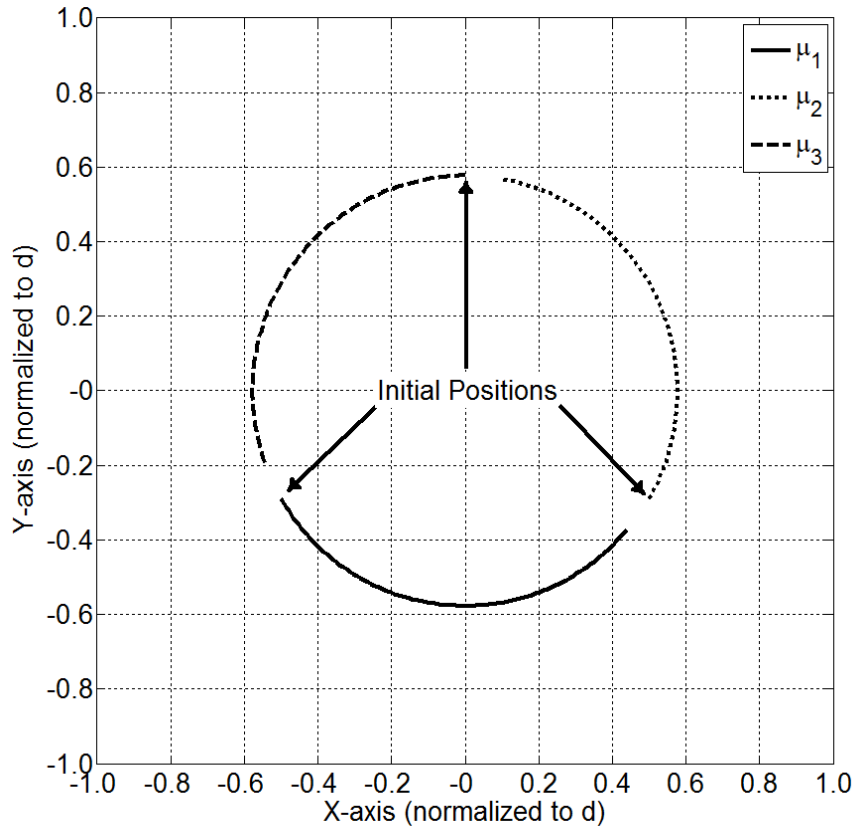


Figure 5.1: Three-Body Equal Mass Central Configuration

The RK45, 47P, and 67P algorithms are now evaluated for the first five periods of this central configuration. The orbital period of the entire system is approximately 23 hours. For each algorithm, the absolute error is evaluated after each orbital period along with the amount of computer time needed to reach that outcome. Figures 5.2-5.4 show the results of this investigation using different tolerances for each algorithm.

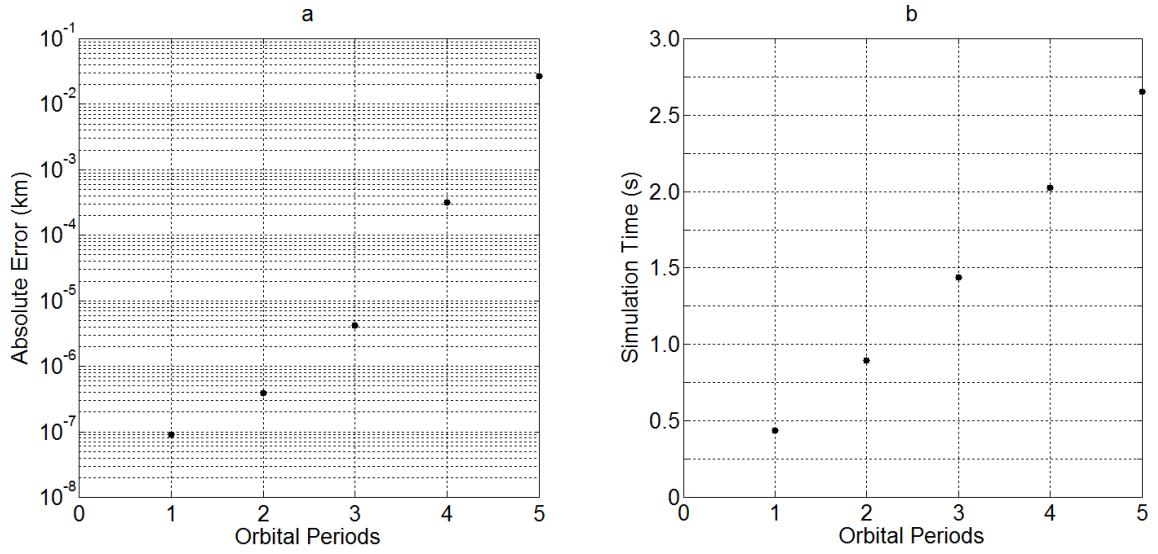


Figure 5.2: Equal Mass Central Configuration Using RK45 with a 10^{-7} Tolerance
 a) Absolute Error, b) Simulation Time

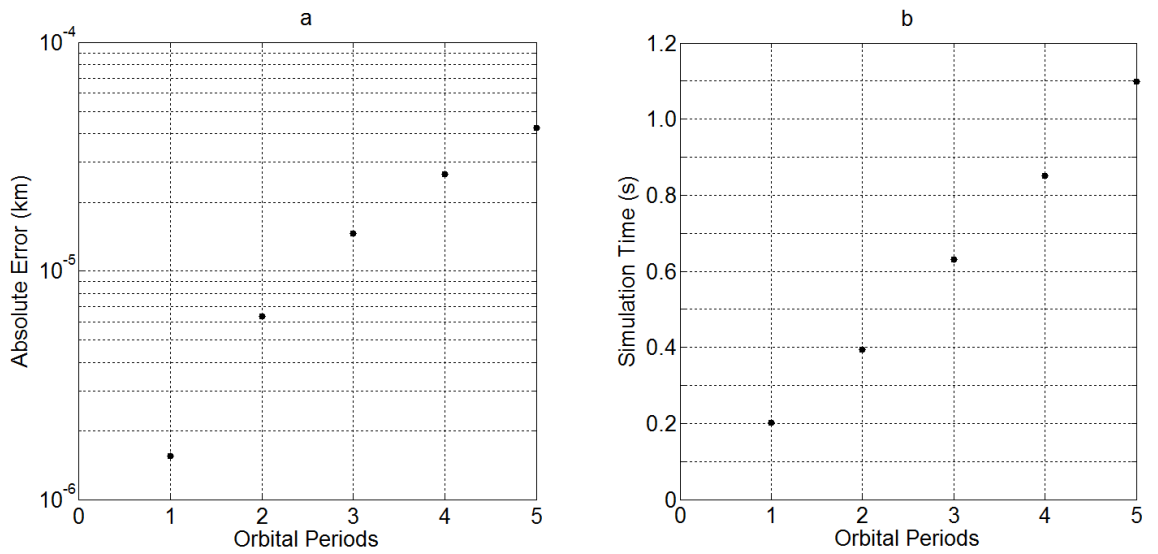


Figure 5.3: Equal Mass Central Configuration Using 47P with a 10^{-4} Tolerance
 a) Absolute Error, b) Simulation Time

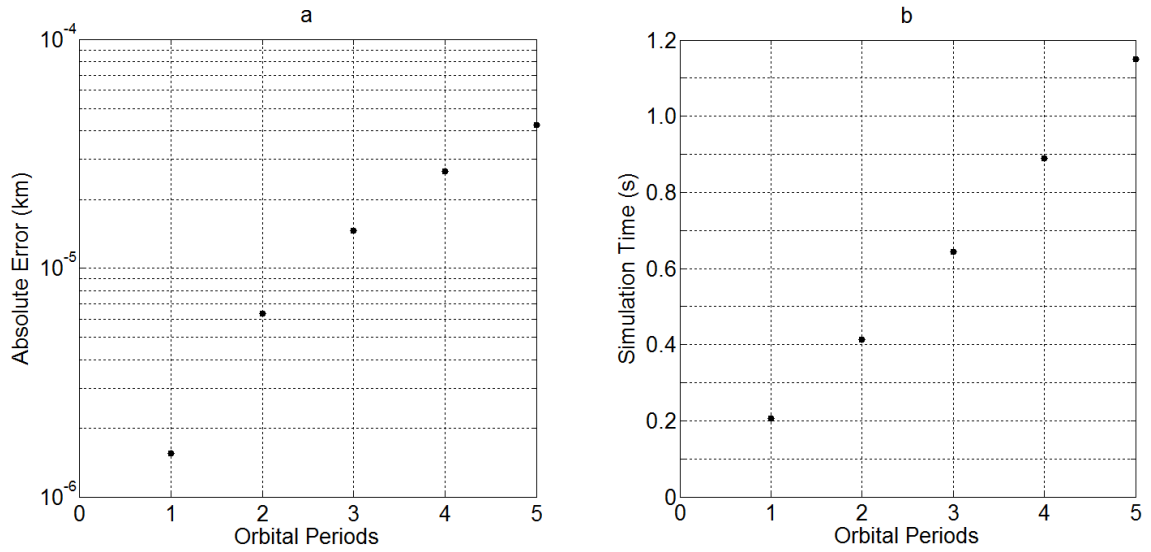


Figure 5.4: Equal Mass Central Configuration Using 67P with a 10^{-8} Tolerance
 a) Absolute Error, b) Simulation Time

The experiment is repeated for the case of three unequal masses, whose gravitational parameters are equal to $30,000 \text{ km}^3/\text{s}^2$, $20,000 \text{ km}^3/\text{s}^2$, and $10,000 \text{ km}^3/\text{s}^2$, respectively. The constant distance between the three particles is assumed to be $25,000 \text{ km}$. Figure 5.5 shows a portion of the exact trajectories just described.

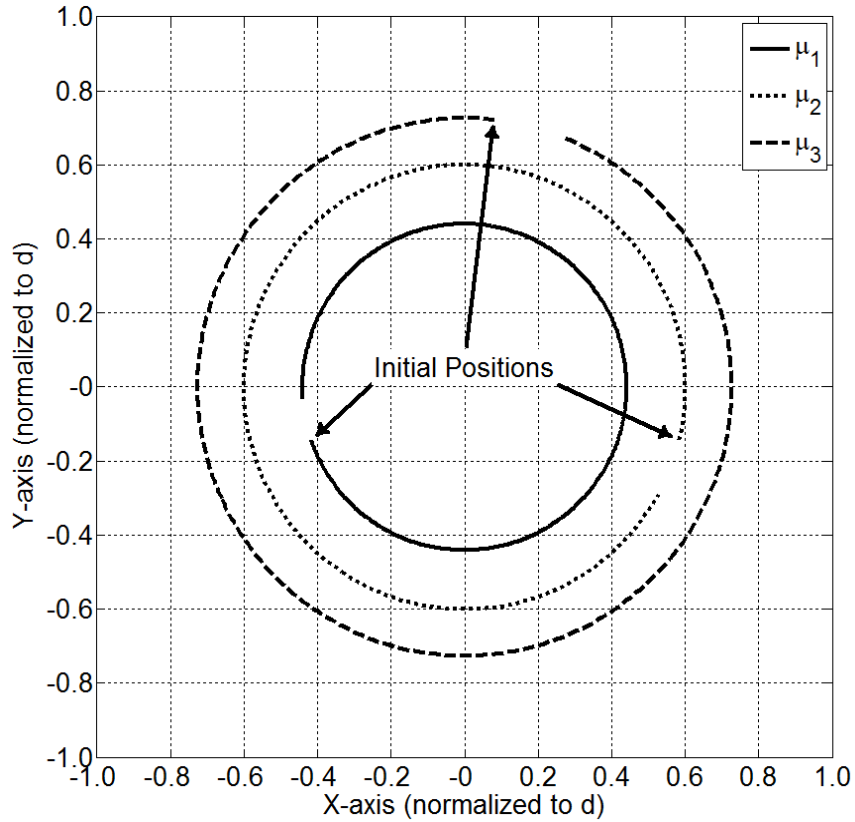


Figure 5.5: Three-Body Unequal Mass Central Configuration

The RK45, 47P, and 67P algorithms are now evaluated for the first five periods of this central configuration. The orbital period of the entire system is approximately 28 hours. As with the equal mass system, the absolute error is evaluated after each orbital period along with the amount of computer time needed to reach that outcome for each algorithm. Figures 5.6-5.8 show the results of this investigation using different tolerances for each algorithm.

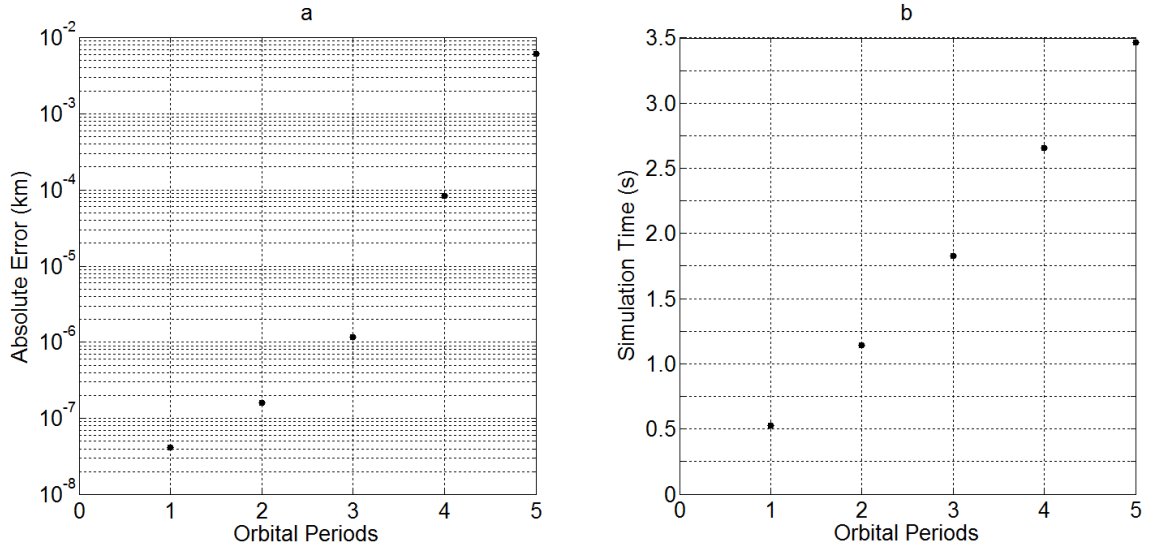


Figure 5.6: Unequal Mass Central Configuration Using RK45 with a 10^{-7} Tolerance
 a) Absolute Error, b) Simulation Time

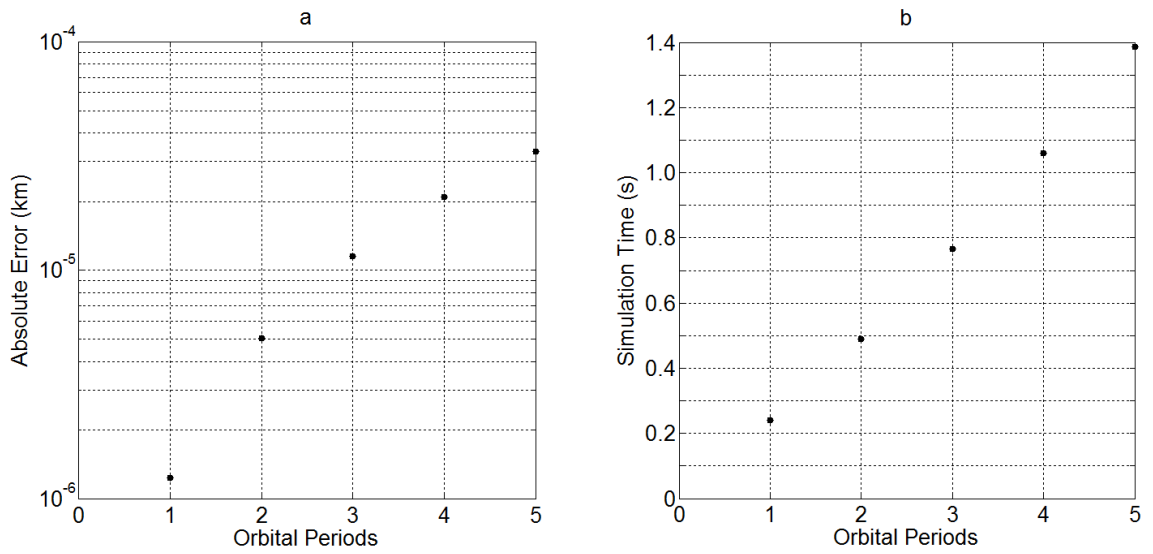


Figure 5.7: Unequal Mass Central Configuration Using 47P with a 10^{-4} Tolerance
 a) Absolute Error, b) Simulation Time

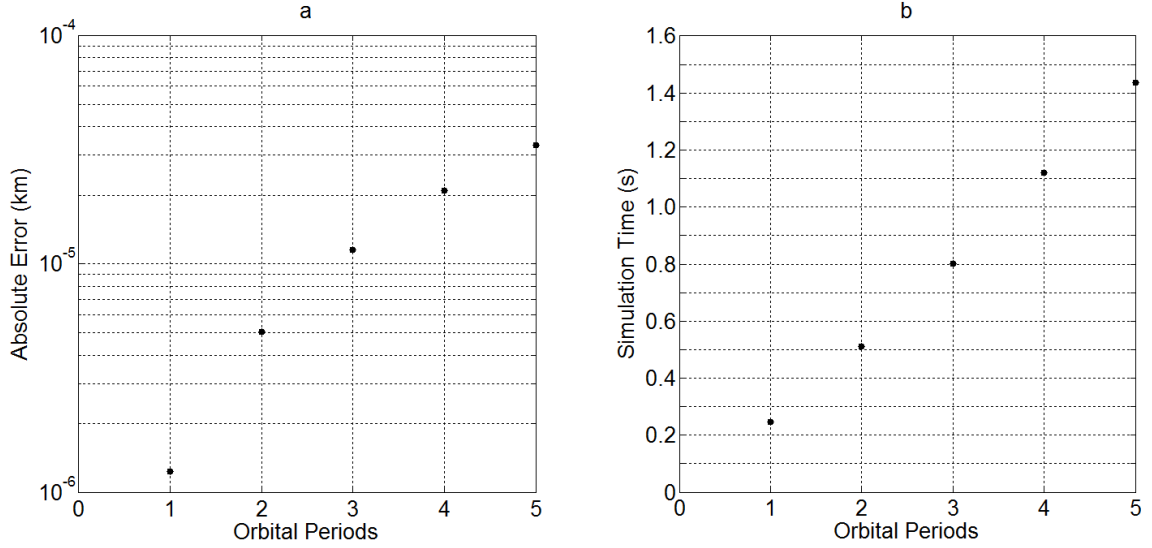


Figure 5.8: Unequal Mass Central Configuration Using 67P with a 10^{-8} Tolerance
a) Absolute Error, b) Simulation Time

A HOHMANN TRANSFER IN THE RESTRICTED THREE-BODY PROBLEM

Consider a two-dimensional, restricted three-body application, consisting of the Earth, the Moon, and a satellite on a translunar trajectory. The gravitational parameters of the Earth and Moon are set equal to $398,600 \text{ km}^3/\text{s}^2$ and $4,903 \text{ km}^3/\text{s}^2$, respectively. The Earth and the Moon are initially on the X-axis and in counter-clockwise, elliptical orbits with respect to each other. The semimajor axis and eccentricity of the Moon with respect to the Earth are assumed to be $384,400 \text{ km}$ and 0.0549 , respectively. The initial conditions of these two bodies are given by

$$\bar{\mathbf{r}}_{1,0} = -\frac{\mu_2 \Delta \bar{\mathbf{r}}_m}{\mu_1 + \mu_2} \quad (5.49)$$

$$\bar{\mathbf{r}}_{2,0} = \frac{\mu_1 \Delta \bar{\mathbf{r}}_m}{\mu_1 + \mu_2} \quad (5.50)$$

$$\bar{\mathbf{v}}_{1,0} = -\frac{\mu_2 \Delta \bar{\mathbf{v}}_m}{\mu_1 + \mu_2} \quad (5.51)$$

$$\bar{v}_{2,0} = \frac{\mu_1 \Delta \bar{v}_m}{\mu_1 + \mu_2} \quad (5.52)$$

where μ_1 and μ_2 are the gravitational parameters of the Earth and the Moon, respectively,

$\Delta \bar{r}_m$ is the initial position of the moon relative to the Earth,

$$\Delta \bar{r}_m = a_m (1 - e_m) \hat{\mathbf{i}} \quad (5.53)$$

$\Delta \bar{v}_m$ is the initial velocity of the moon relative to the Earth,

$$\Delta \bar{v}_m = \sqrt{\frac{(\mu_1 + \mu_2)(1 + e_m)}{a_m(1 - e_m)}} \hat{\mathbf{j}} \quad (5.54)$$

a_m is the semimajor axis of the moon with respect to the Earth and e_m is the eccentricity of the moon with respect to the Earth. The initial positions of each body can be seen Figure 5.9.

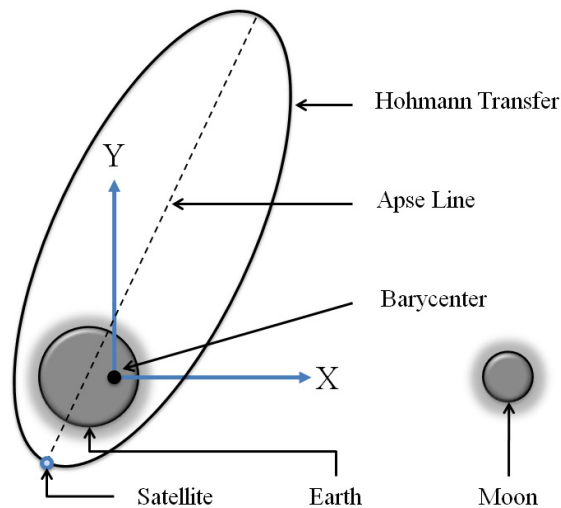


Figure 5.9: Hohmann Transfer in the Restricted Three-Body Problem

A satellite with a negligible gravitational parameter that is initially in a 300 km altitude low Earth orbit ($r_p = 6678$ km) is placed on a Hohmann transfer towards the Moon. The Hohmann transfer's apse line initially makes a $\theta = 65^\circ$ angle with the X-axis and the transfer's apoapsis is on the orbit of the Moon. The initial state of the satellite is given by

$$\bar{\mathbf{r}}_{3,0} = \bar{\mathbf{r}}_{1,0} - r_p \{ \cos(\theta)\hat{\mathbf{I}} + \sin(\theta)\hat{\mathbf{J}} \} \quad (5.55)$$

$$\bar{\mathbf{v}}_{3,0} = \bar{\mathbf{v}}_{1,0} + v \{ \sin(\theta)\hat{\mathbf{I}} - \cos(\theta)\hat{\mathbf{J}} \} \quad (5.56)$$

where v is the Hohmann transfer speed with respect to the Earth,

$$v = \sqrt{\frac{\mu_1(2a - r_p)}{ar_p}} \quad (5.57)$$

and a is the Hohmann transfer's semimajor axis ($a = 195539$ km). Figure 5.10 shows the orbit of the moon and the satellite with respect to the Earth and the trajectory of the satellite with respect to the Moon during the course of one lunar period (approximately 27.3 days).

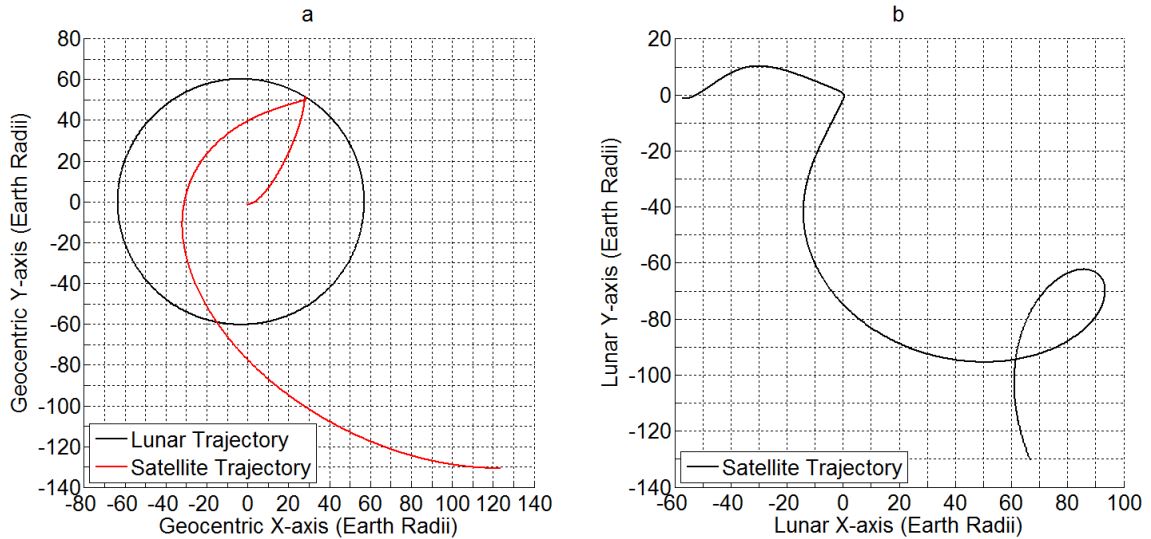


Figure 5.10: Hohmann Transfer in the Earth-Moon System
 a) Satellite Trajectory with Respect to the Earth, b) Satellite Trajectory with Respect to the Moon

As expected, Figure 5.10 reveals that the satellite remains on its Hohmann transfer trajectory until it reaches the Moon's sphere of influence, which has a radius of 66,200 km or 10.3 Earth radii, approximately 4.9 days into the mission. At this point, a gravity assist provided by the Moon causes the satellite's trajectory to become retrograde and non-periodic with respect to the Earth-Moon system's barycenter until it leaves the lunar sphere of influence approximately 1.4 days later (6.3 days into the mission). This can be seen in Figure 5.11.

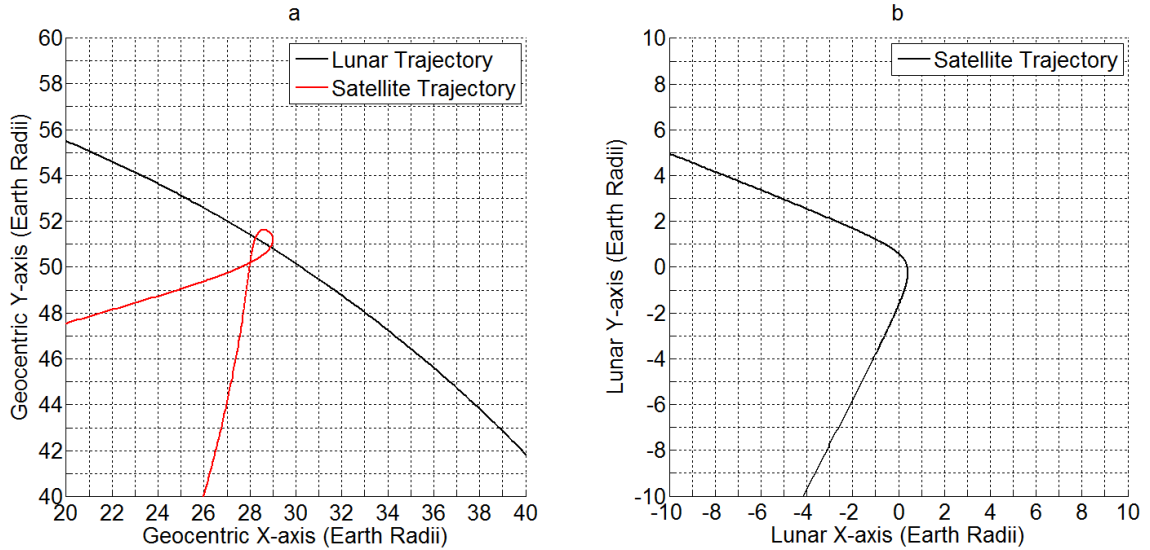


Figure 5.11: Satellite Transit through Lunar Sphere of Influence
a) Satellite Trajectory with Respect to the Earth, b) Satellite Trajectory with Respect to the Moon

This non-periodic satellite trajectory provides an ideal environment in which to test the accuracy and efficiency of a variable time step numerical integrator. The RK45, 47P, and 67P algorithms are now evaluated for a period equal to five lunar periods. The orbital period of the Moon is approximately 27.3 days. The correct orbital positions of each body after five periods were determined by numerically integrating the restricted three-body problem with a constant time step, fifth order Runge-Kutta algorithm. For each variable time step algorithm, the absolute error is evaluated after each orbital period along with the amount of computer time needed to reach that outcome. Figures 5.12-5.14 show the results of this investigation using different tolerances for each algorithm.

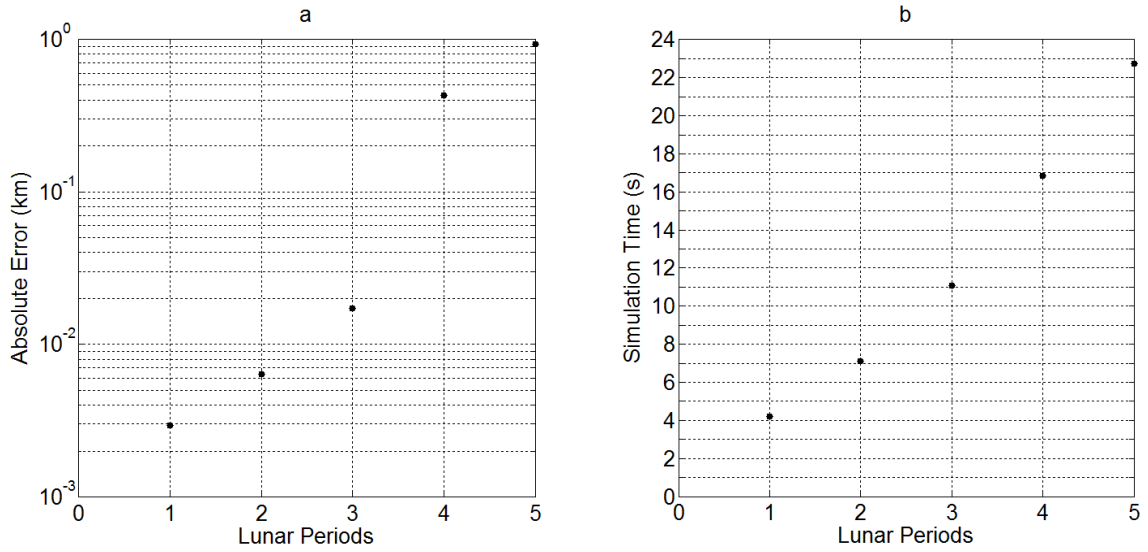


Figure 5.12: Three-Body Hohmann Transfer Using RK45 with a 10^{-8} Tolerance
 a) Absolute Error, b) Simulation Time

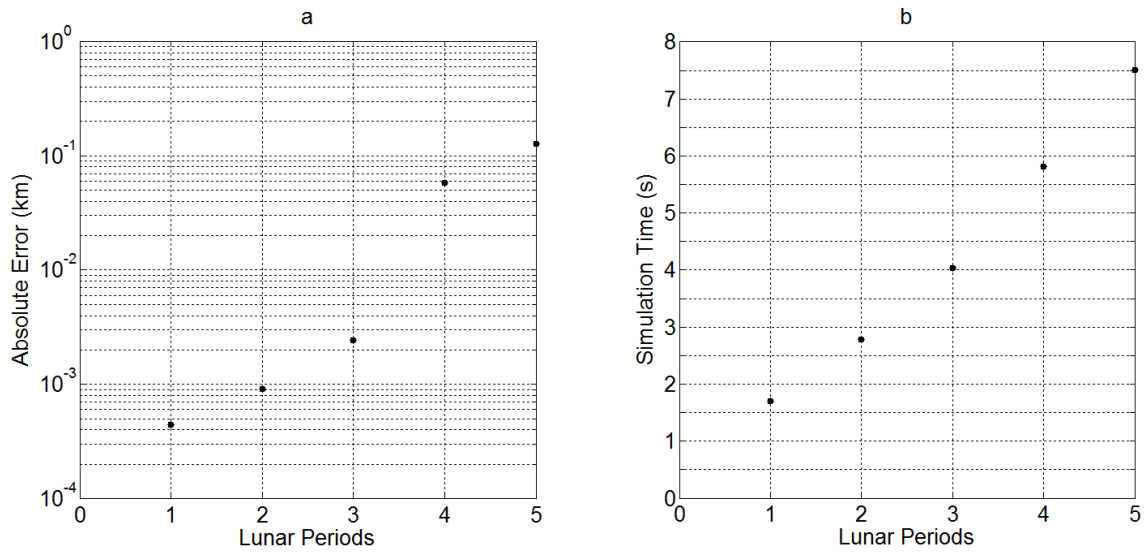


Figure 5.13: Three-Body Hohmann Transfer Using 47P with a 10^{-5} Tolerance
 a) Absolute Error, b) Simulation Time

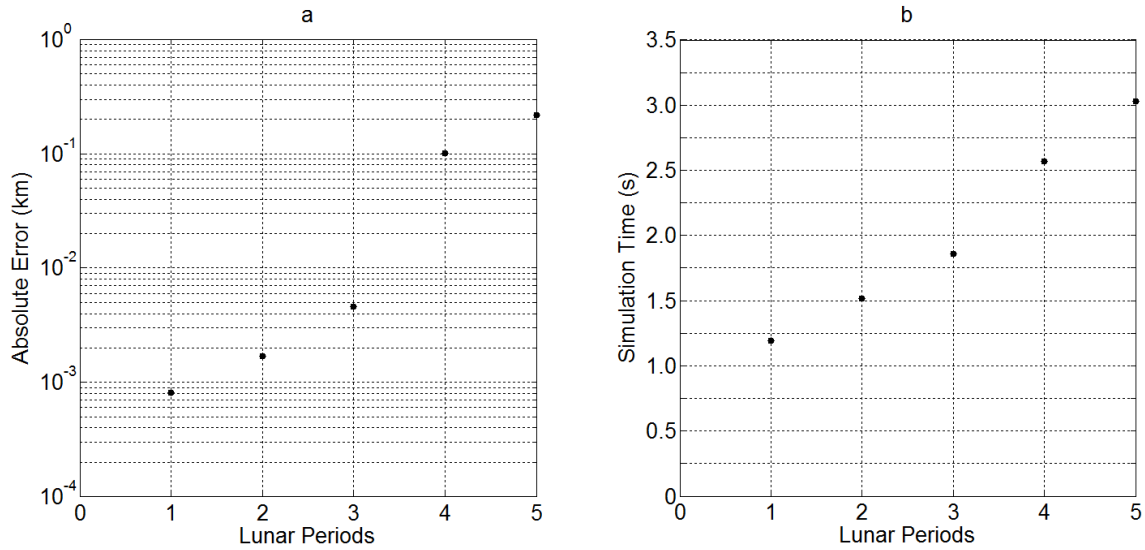


Figure 5.14: Three-Body Hohmann Transfer Using 67P with a 10^{-9} Tolerance
a) Absolute Error, b) Simulation Time

DISCUSSION

The absolute error graphs produced for the central configuration and restricted three-body problem scenarios were plotted using a logarithmic scale. This was done because it was observed that absolute error increased approximately by an order of magnitude with each orbital period. This outcome can be attributed to the chaotic nature of the three-body problem. The central configuration solution derived earlier in this chapter is only marginally stable. As a result, small changes in the objects' state over time will eventually result in disordered motion. No matter how accurate a numerical propagator may be, round-off error will always accumulate as propagation time increases. In the case of the restricted three-body problem, this can result in orbits whose evolution is so sensitive to minor changes, that they essentially become unpredictable.

These details explain why the tolerances used by the author to solve the periodic and non-periodic three-body problem were higher than the tolerances used to solve the relative two-body problem. The goal was to maintain an adequate level of accuracy that

was comparable to the accuracy obtained when the relative two-body problem as analyzed. In the end, the results obtained for the three-body problem were not as accurate, but when one considers the large amount of time that each scenario was propagated, this is an expected outcome.

For all the situations analyzed in this chapter, the 47P and 67P algorithms returned results that were at least slightly more accurate than their RK45 counterpart. But more importantly is the amount of computer time that 47P and 67P needed to obtain these outcomes. This computer time was consistently much shorter than RK45. From these observations, it can be concluded that the 47P and 67P algorithms are more accurate and much more efficient than the variable time step RK45 numerical integrator when various N-body problem scenarios are investigated.

CHAPTER 6

CONCLUSIONS AND FUTURE WORK

SUMMARY

A brief history of the N-body problem has been given and a list of technical sources has been provided that will help the reader navigate through the various theoretical aspects of this problem. The equations of motion of the two-body problem were presented and discussed in detail. An analytic, time dependent solution for the case of circular orbits was derived. The classical orbital element method used to determine future states for elliptical, parabolic, and hyperbolic orbits was also outlined and discussed.

Time dependent, power series solutions of the relative two-body problem were presented and analyzed. The fundamental invariants corresponding to these power series were introduced and their characteristics were analyzed in detail. Recursion relationships for the time dependent Lagrange coefficients were presented and their radius of convergence was discussed for the various types of orbits predicted by the relative two-body problem. A seventh order series solution was used iteratively to propagate a highly elliptical trajectory with respect to the Earth with very good results. The process was repeated using a fourth-order and fifth-order constant time step Runge-Kutta (RK4 and RK5, respectively) numerical integration algorithm. The results returned by the iterative use of the seventh-order power series were more accurate than the outcomes returned by RK4 and slightly less accurate than the results returned by RK5. More importantly, the power series solution required much less computer time to reach a solution. A variable time step algorithm was introduced and used to achieve accurate trajectory design results in conjunction with RK4 and RK5 in an efficient manner (RK45). The capabilities of

RK45 were used as a comparison benchmark to evaluate the capabilities of the algorithms introduced by the author.

The relative two-body problem was then transformed into a time dependent system using the power series solutions derived earlier. A fourth-order, analytic solution was derived for the transformed system and the result was shown to be a useful alternative to the universal form of Kepler's equation when working in inertial coordinates. The fourth-order solution and the seventh-order power series solution of the relative two-body problem were substituted into the RK45 variable time step algorithm as a replacement to RK4 and RK5. This new algorithm (47P) returned trajectory design results that were much more accurate and much more efficient than RK45. A second variable time step algorithm was developed by substituting the fourth-order solution with a sixth-order power series expression (67P). While this second algorithm returned results that were only slightly more accurate than RK45, its efficiency exceeded the performance of both RK45 and 47P considerably. These outcomes remained consistent when periodic scenarios were analyzed in the two-body problem and three-body problem and a non-periodic scenario was analyzed in the restricted three-body problem.

CONCLUSIONS

The performance of the 47P and 67P algorithms has been shown to exceed the performance capabilities of RK45. This can be attributed to the way these procedures were derived. The various Runge-Kutta integrators that have been developed over the years are intended to be robust. That is, they can be applied to a wide array of problems and still maintain an acceptable level of accuracy and efficiency. The 47P and 67P algorithms, on the other hand, were derived from the actual equations of motion that are

specifically being solved in this work. This causes them to be more accurate than a generic, robust integrator. More importantly, the increase in accuracy comes with a considerable increase in efficiency as the methods developed by the author require fewer function evaluations per time step than RK45. Based on additional numerical work, the author recommends that the 47P algorithm be used when short simulation times are needed and the 67P algorithm be used for larger time scales. Larger simulation times require that the tolerance of the 47P algorithm be lowered beyond 10^{-5} . Although the accuracy returned will be greater than the accuracy obtained when larger tolerances are used, the efficiency of 47P begins to degrade drastically as tolerance decreases beyond 10^{-5} . This phenomenon is not observed with 67P.

RELEVANCE

This work is relevant because it provides a useful trajectory design alternative to the methods that have been developed in the past. The time dependent equations derived in this dissertation are based on fundamental invariants of the two-body problem. Because of this, they can be applied to any coordinate system. As was shown in Chapter 3, propagating an orbit given an initial state in an inertial coordinate system requires a considerable number of steps, which includes solving Kepler's equation iteratively for the respective type of orbit that is being analyzed. On the other hand, the methods proposed by the author require only one step to find a time dependent outcome. Furthermore, Kepler's equation cannot be extended to the problem of N-bodies. The equations derived by the author can. Moreover, as will be shown in the next section, the fourth-order solution of the relative two-body problem along with the 47P and 67P procedures can also be extended to include other types of perturbations that are encountered by trajectory

designers in everyday orbit determination. The results of this future work will be able to be viewed as new time dependent Kepler equations that cover a larger range of perturbations than the original.

FUTURE WORK

Higher Order Solutions

The transformed relative two-body problem given by equation 4.4 (restated here for convenience)

$$\Delta\ddot{\bar{\mathbf{r}}} = -\frac{\alpha(F\Delta\bar{\mathbf{r}}_0 + G\Delta\bar{\mathbf{v}}_0)}{(F^2 + 2\lambda FG + \beta G^2)^{3/2}} \quad (6.1)$$

was solved using first-order Lagrange coefficients,

$$\Delta\bar{\mathbf{s}}(t) = \Phi\Delta\bar{\mathbf{s}}_0 \rightarrow \begin{Bmatrix} \Delta\bar{\mathbf{r}} \\ \Delta\bar{\mathbf{v}} \end{Bmatrix} = \begin{bmatrix} \tilde{\mathbf{F}}\mathbf{I}_{3 \times 3} & \tilde{\mathbf{G}}\mathbf{I}_{3 \times 3} \\ \tilde{\mathbf{F}}\mathbf{I}_{3 \times 3} & \tilde{\mathbf{G}}\mathbf{I}_{3 \times 3} \end{bmatrix} \begin{Bmatrix} \Delta\bar{\mathbf{r}}_0 \\ \Delta\bar{\mathbf{v}}_0 \end{Bmatrix} \quad (6.2)$$

The time-dependent expressions that result when coefficients of order two or higher are implemented are known as Abelian integrals (also known as hyperelliptic integrals) [78]. A possible avenue of future research would be to try to develop expressions that analytically solve equation 6.1 when Lagrange coefficients of order two and three are used. Coefficients of order two will yield an analytic solution whose accuracy approaches fifth-order and a solution using coefficients of order three will yield an outcome whose accuracy approaches sixth-order. Extensive numerical work conducted by the author has shown that these two analytic solutions return results that are more accurate than RK4 and RK5, respectively, for any size time step. In addition to having two new time-dependent expressions that are more accurate than equation 6.2 and could

be used as alternatives to the universal formulation of Kepler's equation, the two solutions could also be used to form a 56P variable time step propagator whose efficiency would rival and maybe even possibly exceed the performance of 47P and 67P.

Linear Orbit Theory

The relative motion between two satellites (a target and a chaser) whose gravitational parameters are negligible when compared to the parameter of a primary body can be described by the Hill-Clohessy-Wiltshire (HCW) equations. These equations are well known in the orbital mechanics world, having been first introduced for natural bodies by Hill and applied by Clohessy and Wilshire for man-made satellites [79]. The reader is referred to any number of texts on Astrodynamics for the derivation of these equations [80-81]. The HCW expressions are only valid for scenarios where the ratio of the distance between the target and chase vehicle to the distance of the primary body to the chase vehicle is much less than one. This distance requirement could easily be alleviated by using equation 6.2 as a substitute for the HCW equations. By changing the constraining variable from distance to time, the target and chaser could be located anywhere with respect to the primary body. Future research into this would develop radius of convergence expressions that would allow the trajectory designer to determine when an update in initial conditions would be needed to continue using equation 6.2 accurately.

Thrust Applications

The transformed problem given by equation 6.1 can be modified to include both finite thrust and continuous thrust applications,

$$\Delta\ddot{\mathbf{r}} = -\frac{\alpha(F\Delta\bar{\mathbf{r}}_0 + G\Delta\bar{\mathbf{v}}_0)}{(F^2 + 2\lambda FG + \beta G^2)^{3/2}} + \frac{\bar{\mathbf{T}}(t)}{m(t)} \quad (6.3)$$

where $\bar{\mathbf{T}}(t)$ is the thrust vector and $m(t)$ is the vehicle's mass, both of which are functions of time. Future research into equation 6.3 would shed light into the accuracy of this expression and would also reveal the conditions and limitations of its application to real-world scenarios.

Perturbations Dependent on Position and Velocity

The methods introduced in this dissertation can be extended beyond the N-body problem to include any perturbation that relies on a satellite's relative position and velocity. Such perturbations include non-spherical mass distributions and atmospheric drag, which are dependent on satellite position and velocity, respectively. Research into this area would develop analytic expressions that could potentially be used iteratively much like 47P and 67P. It is predicted by the author that these new iterative solutions would be more accurate and much more efficient than RK45 making them a useful tool for trajectory design.

REFERENCES

- [1] Vallado, D. A. (2001): *Fundamentals of Astrodynamics and Applications*, 2nd Edition; Microcosm Press: El Segundo, CA; pp. 1-12.
- [2] Prussing, J. E.; Conway, B. A. (1993): *Orbital Mechanics*; Oxford University Press, Inc.: New York, NY; p. 3.
- [3] “Aristotle” (2004): *Encyclopedia Americana*, International Edition; Volume 2; Scholastic Library Publishing, Inc.: Danbury, CT; pp. 288-292.
- [4] “Aristotle” (2007): *The New Encyclopedia Britannica*, 15th Edition; Volume 1; Encyclopedia Britannica, Inc.: Chicago, IL; p. 556.
- [5] “Aristotle” (1999): From the School of Mathematics and Statistics, University of St. Andrews, Scotland; <http://www-history.mcs.st-andrews.ac.uk/Mathematicians/Aristotle.html>; First viewed January 8, 2001.
- [6] “Geocentric System” (2004): *Encyclopedia Americana*, International Edition; Volume 12; Scholastic Library Publishing, Inc.: Danbury, CT; p. 428.
- [7] “Geocentric System” (2007): *The New Encyclopedia Britannica*, 15th Edition; Volume 5; Encyclopedia Britannica, Inc.: Chicago, IL; p. 187.
- [8] “Ptolemy of Alexandria” (2004): *Encyclopedia Americana*, International Edition; Volume 22; Scholastic Library Publishing, Inc.: Danbury, CT; pp. 742-743.
- [9] “Ptolemy” (2007): *The New Encyclopedia Britannica*, 15th Edition; Volume 9; Encyclopedia Britannica, Inc.: Chicago, IL; pp. 775-776.
- [10] “Claudius Ptolemy” (1999): From the School of Mathematics and Statistics, University of St. Andrews, Scotland; <http://www-history.mcs.st-andrews.ac.uk/Mathematicians/Ptolemy.html>; First viewed June 24, 2009.
- [11] “Ptolemaic System” (2004): *Encyclopedia Americana*, International Edition; Volume 22; Scholastic Library Publishing, Inc.: Danbury, CT; pp. 741-742.
- [12] “Ptolemaic System” (2007): *The New Encyclopedia Britannica*, 15th Edition; Volume 9; Encyclopedia Britannica, Inc.: Chicago, IL; pp. 770-771.
- [13] Saari, D. G. (2005): *Collisions, Rings, and Other Newtonian N-Body Problems*; American Mathematical Society: Providence, RI; pp. 1-13.
- [14] “Copernicus, Nicolaus” (2004): *Encyclopedia Americana*, International Edition; Volume 7; Scholastic Library Publishing, Inc.: Danbury, CT; pp. 755-756.

- [15] “Nicolaus Copernicus” (2002): From the School of Mathematics and Statistics, University of St. Andrews, Scotland; <http://www-history.mcs.st-andrews.ac.uk/Mathematicians/Copernicus.html>; First viewed October 21, 2009.
- [16] “Copernicus, Nicolaus” (2007): *The New Encyclopedia Britannica*, 15th Edition; Volume 3; Encyclopedia Britannica, Inc.: Chicago, IL; p. 610.
- [17] “Copernican System” (2007): *The New Encyclopedia Britannica*, 15th Edition; Volume 3; Encyclopedia Britannica, Inc.: Chicago, IL; p. 610.
- [18] “Heliocentric System” (2004): *Encyclopedia Americana*, International Edition; Volume 14; Scholastic Library Publishing, Inc.: Danbury, CT; p. 65.
- [19] “Heliocentric System” (2007): *The New Encyclopedia Britannica*, 15th Edition; Volume 5; Encyclopedia Britannica, Inc.: Chicago, IL; p. 812.
- [20] “Galileo” (2004): *Encyclopedia Americana*, International Edition; Volume 12; Scholastic Library Publishing, Inc.: Danbury, CT; pp. 240-244.
- [21] “Galileo” (2007): *The New Encyclopedia Britannica*, 15th Edition; Volume 5; Encyclopedia Britannica, Inc.: Chicago, IL; p. 86.
- [22] “Galileo Galilei” (2002): From the School of Mathematics and Statistics, University of St. Andrews, Scotland; <http://www-history.mcs.st-andrews.ac.uk/Mathematicians/Galileo.html>; First viewed June 21, 2009.
- [23] “Brahe, Tycho” (2004): *Encyclopedia Americana*, International Edition; Volume 4; Scholastic Library Publishing, Inc.: Danbury, CT; p. 409.
- [24] “Brahe, Tycho” (2007): *The New Encyclopedia Britannica*, 15th Edition; Volume 2; Encyclopedia Britannica, Inc.: Chicago, IL; pp. 459-460.
- [25] “Tycho Brahe” (2003): From the School of Mathematics and Statistics, University of St. Andrews, Scotland; <http://www-history.mcs.st-andrews.ac.uk/Mathematicians/Brahe.html>; First viewed December 2, 2004.
- [26] “Tychonic System” (2007): *The New Encyclopedia Britannica*, 15th Edition; Volume 12; Encyclopedia Britannica, Inc.: Chicago, IL; pp. 82-83.
- [27] “Kepler, Johannes” (2004): *Encyclopedia Americana*, International Edition; Volume 16; Scholastic Library Publishing, Inc.: Danbury, CT; pp. 403-405.
- [28] “Kepler, Johannes” (2007): *The New Encyclopedia Britannica*, 15th Edition; Volume 6; Encyclopedia Britannica, Inc.: Chicago, IL; pp. 809-810.
- [29] “Johannes Kepler” (1999): From the School of Mathematics and Statistics, University of St. Andrews, Scotland; <http://www-history.mcs.st-andrews.ac.uk/Mathematicians/Kepler.html>; First viewed September 10, 2000.

- [30] Weisstein, E. W. (2009): "Platonic Solid" From *MathWorld*--A Wolfram Web Resource; <http://mathworld.wolfram.com/PlatonicSolid.html>; First viewed October, 19, 2009.
- [31] Smolin, L. (2006): *What's Wrong With Physics: The Rise of String Theory, the Fall of a Science, and What Comes Next*; Houghton Mifflin Company: Boston, MA; pp. 18-31.
- [32] "Kepler's Laws of Planetary Motion" (2007): *The New Encyclopedia Britannica*, 15th Edition; Volume 6; Encyclopedia Britannica, Inc.: Chicago, IL; p. 810.
- [33] Bate, R. R.; Mueller, D. D.; White, J. E. (1971): *Fundamentals of Astrodynamics*; Dover Publications, Inc.: New York, NY; pp. 177-181.
- [34] "Newton, Sir Isaac" (2004): *Encyclopedia Americana*, International Edition; Volume 20; Scholastic Library Publishing, Inc.: Danbury, CT; pp. 288-292.
- [35] "Newton" (2007): *The New Encyclopedia Britannica*, 15th Edition; Volume 24; Encyclopedia Britannica, Inc.: Chicago, IL; pp. 931-935.
- [36] "Sir Isaac Newton" (2000): From the School of Mathematics and Statistics, University of St. Andrews, Scotland; <http://www-history.mcs.st-andrews.ac.uk/Mathematicians/Newton.html>; First viewed May 9, 2001.
- [37] Stein, S. K. (1996): "Exactly How Did Newton Deal With His Planets?" *The Mathematical Intelligencer*, Volume 18, Number 2; pp. 6-11.
- [38] "Gravitation" (2007): *The New Encyclopedia Britannica*, 15th Edition; Volume 20; Encyclopedia Britannica, Inc.: Chicago, IL; pp. 169-177.
- [39] "Euler, Leonhard" (2004): *Encyclopedia Americana*, International Edition; Volume 10; Scholastic Library Publishing, Inc.: Danbury, CT; p. 660.
- [40] "Euler, Leonhard" (2007): *The New Encyclopedia Britannica*, 15th Edition; Volume 4; Encyclopedia Britannica, Inc.: Chicago, IL; p. 596.
- [41] "Leonhard Euler" (1998): From the School of Mathematics and Statistics, University of St. Andrews, Scotland; <http://www-history.mcs.st-andrews.ac.uk/Mathematicians/Euler.html>; First viewed May 11, 2000.
- [42] Curtis, H. D. (2005): *Orbital Mechanics for Engineering Students*; Elsevier, Butterworth, Heinemann: Boston, MA; pp. 89-92.
- [43] Havas, P. (1973): "Homographic Solutions of a Newtonian System of Point Masses" *Celestial Mechanics*, Volume 7; pp. 321-346.
- [44] "Lagrange, Joseph Louis" (2004): *Encyclopedia Americana*, International Edition; Volume 16; Scholastic Library Publishing, Inc.: Danbury, CT; p. 667.

- [45] “Lagrange, Joseph-Louis” (2007): *The New Encyclopedia Britannica*, 15th Edition; Volume 7; Encyclopedia Britannica, Inc.: Chicago, IL; pp. 101-102.
- [46] “Joseph-Louis Lagrange” (1999): From the School of Mathematics and Statistics, University of St. Andrews, Scotland; <http://www-history.mcs.st-andrews.ac.uk/Mathematicians/Lagrange.html>; First viewed May 24, 2006.
- [47] Curtis, H. D. (2005): *Orbital Mechanics for Engineering Students*; Elsevier, Butterworth, Heinemann: Boston, MA; pp. 92-96.
- [48] Lagrange, J. L. (1997): *Analytical Mechanics*; Kluwer Academic Publishers: Boston, MA; pp. 309-438. Translated and edited from *Mécanique Analytique*, Nouvelle Édition of 1811 by Auguste Boissonnade and Victor N. Vagliente.
- [49] Diacu, F. (1996): “The Solution of the N-Body Problem” *The Mathematical Intelligencer*, Volume 18, Number 3; pp. 66-70.
- [50] “Poincaré, Henri” (2004): *Encyclopedia Americana*, International Edition; Volume 22; Scholastic Library Publishing, Inc.: Danbury, CT; p. 288.
- [51] “Poincaré, Henri” (2007): *The New Encyclopedia Britannica*, 15th Edition; Volume 9; Encyclopedia Britannica, Inc.: Chicago, IL; pp. 544-545.
- [52] “Jules Henri Poincaré” (2003): From the School of Mathematics and Statistics, University of St. Andrews, Scotland; <http://www-history.mcs.st-andrews.ac.uk/Mathematicians/Poincare.html>; First viewed February 1, 2007.
- [53] Zak, M. (1986): “Chaotic Instability in the Three-Body Problem” *Acta Mechanica*, Volume 61, Numbers 1-4; pp. 203-208.
- [54] Gidea, M.; Deppe, F. (2006): “Chaotic Orbits in a Restricted Three-Body Problem: Numerical Experiments and Heuristics” *Communications in Nonlinear Science and Numerical Simulation*, Volume 11, Issue 2; pp. 161-171.
- [55] “Karl Frithiof Sundman” (2007): From the School of Mathematics and Statistics, University of St. Andrews, Scotland; <http://www-history.mcs.st-andrews.ac.uk/Mathematicians/Sundman.html>; First viewed June, 24, 2009.
- [56] Wang, Q. D. (1991): “The Global Solution of the N-Body Problem” *Celestial Mechanics and Dynamical Astronomy*; Volume 50, Number 1; pp. 73-88.
- [57] Curtis, H. D. (2005): *Orbital Mechanics for Engineering Students*; Elsevier, Butterworth, Heinemann: Boston, MA.
- [58] Vallado, D. A. (2001): *Fundamentals of Astrodynamics and Applications*, 2nd Edition; Microcosm Press: El Segundo, CA.

- [59] Newton, I. (1999): *The Principia: The Mathematical Principles of Natural Philosophy*; University of California Press: Berkeley, CA; Translated and edited from *Philosophiae Naturalis Principia Mathematica* of 1687 by I. Bernard Cohen and Anne Whitman.
- [60] Lagrange, J. L. (1997): *Analytical Mechanics*; Kluwer Academic Publishers: Boston, MA. Translated and edited from *Mécanique Analytique*, Nouvelle Édition of 1811 by Auguste Boissonnade and Victor N. Vagliente.
- [61] Szebehely, V. (1967): *Theory of Orbits: The Restricted Problem of Three Bodies*; Academic Press: New York, NY.
- [62] Polard, H. (1966): *Mathematical Introduction to Celestial Mechanics*; Prentice-Hall: Englewood, NJ.
- [63] Meyer, K. R. (1999): *Periodic Solutions of the N-Body Problem*; Springer-Verlag: Berlin, Germany.
- [64] Zill, D. G. (2001): *A First Course in Ordinary Differential Equations*, 5th Edition; Brooks/Cole: Pacific Grove, CA; pp. 375-398.
- [65] Curtis, H. D. (2005): *Orbital Mechanics for Engineering Students*; Elsevier, Butterworth, Heinemann: Boston, MA; pp. 107-133.
- [66] Vallado, D. A. (2001): *Fundamentals of Astrodynamics and Applications*, 2nd Edition; Microcosm Press: El Segundo, CA; pp. 49-130.
- [67] Curtis, H. D. (2005): *Orbital Mechanics for Engineering Students*; Elsevier, Butterworth, Heinemann: Boston, MA; pp. 172-176.
- [68] Curtis, H. D. (2005): *Orbital Mechanics for Engineering Students*; Elsevier, Butterworth, Heinemann: Boston, MA; pp. 78-89.
- [69] Bond, V. R. and Allman, M. C. (1996): *Modern Astrodynamics, Fundamentals and Perturbation Methods*; Princeton University Press: Princeton, NJ; pp. 78-80.
- [70] Battin, R. H. (1987): *An Introduction to the Mathematics and Methods of Astrodynamics*, AIAA Education Series; American Institute of Aeronautics and Astronautics, Inc.: New York, NY; pp. 110-114.
- [71] Bond, V. R. (1966): “Recursive Computation of the Coefficients of the Time dependent F and G Series Solution of Keplerian Motion and a Study of the convergence Properties of the Solution”; *NASA Manned Spacecraft Center Publication*; MSC Internal Note, TN D-3322; pp. 48-59.
- [72] Bond, V. R. (1966): “A Recursive Formulation for Computing the Coefficients of the Time dependent F and G Series Solution to the Two-Body Problem”; *Astronomical Journal*; Volume 71, Number 1; pp. 33-50.

- [73] Zill, D. G. (2001): *A First Course in Ordinary Differential Equations*, 5th Edition; Brooks/Cole: Pacific Grove, CA; pp. 448-451.
- [74] Boulet, D. (1991): *Methods of Orbit Determination for the Microcomputer*; Willmann-Bell, Inc.: Richmond, VA; pp. 102-105.
- [75] Curtis, H. D. (2005): *Orbital Mechanics for Engineering Students*; Elsevier, Butterworth, Heinemann: Boston, MA; pp. 134-144.
- [76] Benavides, J. C. and Spencer D. B. (2010): "Approximate Time-Dependent Solutions of the Two-Body Problem" AAS 10-182; AAS/AIAA Space Flight Mechanics Conference; San Diego, California; February, 2010.
- [77] Benavides, J. C. and Spencer D. B. (2010): "Approximate Time-Dependent Solutions of the N-Body Problem" AAS 10-186; AAS/AIAA Space Flight Mechanics Conference; San Diego, California; February, 2010.
- [78] Weisstein, E. W. (2009): "Abelian Integral" From *MathWorld*--A Wolfram Web Resource; <http://mathworld.wolfram.com/AbelianIntegral.html>; First viewed July, 1, 2007.
- [79] Clohessy, W. H. and Wilshire, R. S. (1960): "Terminal Guidance System for Satellite Rendezvous"; *Journal of Aerospace Sciences*, Volume 27, Number 9; pp. 653-674.
- [80] Vallado, D. A. (2001): *Fundamentals of Astrodynamics and Applications*, 2nd Edition; Microcosm Press: El Segundo, CA; pp. 372-395.
- [81] Curtis, H. D. (2005): *Orbital Mechanics for Engineering Students*; Elsevier, Butterworth, Heinemann: Boston, MA; pp. 407-411.

CURRICULUM VITAE

Julio César Benavides graduated from McAllen Memorial High School in May, 1993. He attended South Texas Community College in McAllen, Texas from 1999-2001 where he completed the requirements towards three Associate's degrees in Math, Physics, and Engineering. He transferred to Embry-Riddle Aeronautical University in Prescott, Arizona in January, 2002 and earned a Bachelor's degree in Aerospace Engineering in December, 2004.

During his time at Embry-Riddle, Julio participated in two Research Experience for Undergraduates (REU) programs at the Milwaukee School of Engineering (summer 2003) and the University of Missouri-Rolla (summer 2004). At the Milwaukee School of Engineering, he studied the capabilities of solid freeform fabrication and investigated the heat transfer capabilities of a newly developed heat fin whose geometry is known as TetralatticeTM. At the University of Missouri-Rolla, he conducted research in mechatronics and smart structures and developed a morphing aircraft wing design using a smart material known as Nickel-Titanium Alloy.

After spending the spring semester of 2005 at Cornell University, Julio transferred to the Graduate School at Penn State University in August, 2005 where he completed his Master's degree in Aerospace Engineering in May, 2007. He will be completing his Ph.D. in Aerospace Engineering in the fall of 2010. Julio is now an Assistant Professor in the Aerospace Engineering Department at Embry-Riddle Aeronautical University in Prescott, Arizona.